RTD-TDR-63-4190

HIGH-TEMPERATURE VAPOR-FILLED THERMIONIC CONVERTER

FINAL TECHNICAL REPORT

MARCH 15, 1962, THROUGH SEPTEMBER 15, 1963

TECHNICAL DOCUMENTARY REPORT No. RTD-TDR-63-4190

January 3, 1964

AF AERO PROPULSION LABORATORY

Research and Technology Division
Air Force Systems Command
Wright-Patterson Air Force Base, Ohio

Project No. 8173, Task No. 817305-5

(Prepared under Contract No. AF 33(657)-8563
by General Atomic Division, General Dynamics Corporation
San Diego, California
Author: R. Skoff)

DISCLAIMER

NOTICES

When Government drawings, specifications, or other data are used for any purpose other than in connection with a definitely related Government procurement operation, the United States Government thereby incurs no responsibility nor any obligation whatsoever; and the fact that the Government may have formulated, furnished, or in any way supplied the said drawings, specifications, or other data, is not to be regarded by implication or otherwise as in any manner licensing the holder or any other person or corporation, or conveying any rights or permission to manufacture, use, or sell any patented invention that may in any way be related thereto.

Qualified requesters may obtain copies of this report from the Defense Documentation Center (DDC) (formerly ASTIA), Cameron Station, Bldg. 5, 5010 Duke Street, Alexandria, Virginia, 22314.

This report has been released to the Office of Technical Services, U. S. Department of Commerce, Washington 25, D. C., for sale to the general public.

Copies of this report should not be returned to the Research and Technology Division, Wright-Patterson Air Force Base, Ohio, unless return is required by security considerations, contractual obligations, or notice on a specific document.

FOREWORD

This report was prepared by General Atomic Division of General Dynamics Corporation, San Diego, California, under Air Force Contract AF33(657)-8563, Project 8173. Robert W. Pidd was the General Atomic project manager for this contract. Capt. E. F. Redden of the Static Energy Conversion Section, Flight Vehicle Power Branch, Air Force Aero Propulsion Laboratory was the Research and Technology Division project engineer.

This final technical report describes a research and development program, "High-temperature Vapor-filled Thermionic Converter," which was initiated March 15, 1962, and concluded September 15, 1963. (This program was a continuation of research conducted under Contract AF33(616)-7422, Project 3145, during the period July 1, 1960, through January 31, 1962.)

The contractor's report number is GA-4012.

ABSTRACT

This document represents the final report on Contract AF33(657)-8563, Project No. 8173, for the period March 15, 1962, through September 15, 1963. Under this contract, the operating characteristics of plasma converters utilizing bare uranium–zirconium carbide as the emitting surface were determined as a function of operational lifetime. The emitter design was cylindrical in a size representative of that expected in a space thermionic reactor. The electrode spacing varied from 0.040 in. early in the program to 0.012 in.

The primary objective of the program was to evaluate the converter performance as a function of lifetime and to determine the failure mechanism on those converters which no longer demonstrated useful power levels. An operational lifetime of 3000 hr was considered a reasonable goal. Electrically heated, as opposed to fission-heated, converters were selected as the most economical method of fulfilling these objectives.

Six converters were operated for over 6000 hr at power levels of 10 to 40 watts (1 to 4 watts/cm^2) on a continuous-performance basis. A maximum power density of 6.8 watts/cm^2 was observed at an emitter temperature of 2245°K. The optimum cesium-reservoir temperature for all converters tested occurred at 605° to 630°K. Collector-temperature optimization was not clearly established within the temperature range investigated. The performance of bare-carbide converters increases almost exponentially with increasing emitter temperature. Performance observations were made in the emitter-temperature range 1900° to 2400°K.

Five of the six converters operated under this program failed during operation owing to envelope leakage, resulting in the complete loss of cesium to the surrounding vacuum chamber. Despite the depletion of uranium from the bulk of the emitter, vacuum-emission currents measured pre- and

post-test were nearly identical in magnitude. Both uranium and zirconium, evaporated from the emitter surface, were deposited on the collector.

CONTENTS

ILLUSTRATIONS

I. INTRODUCTION

The performance evaluation and life testing of thermionic converters described in this report were conducted for the Air Force by General Atomic Division of General Dynamics Corporation during the period March 15, 1962, through September 15, 1963. This program on bare-carbide thermionic converters was initiated in June, 1960. At that time UC-ZrC, a refractory form of uranium, appeared attractive for employment both as the nuclear fuel and the electron emitter in a low-specific-weight nuclear reactor system for space-power application. It was known that uranium-bearing compounds emit electrons copiously at the work function characteristic of metallic uranium.* From the refractory system UC-ZrC, usable electron emission is attainable at a temperature where relatively long operational life might be expected. The high thermal and electrical conductivity of UC-ZrC enhanced its value as both a fuel and an emitting surface.

The major limitation on lifetime appeared to be the vaporization rate of the emitter material. Material losses of 1 to 3 mils per year were selected as the maximum acceptable, since electrode spacings of 10 mils or less would be jeopardized from preferential deposition on the collector. At the time, only limited vacuum-vaporization data existed; the effect on the vaporization rate, if any, of cesium vapor at a few millimeters pressure was unknown. However, from existing data and a general knowledge of the physical properties of the UC-ZrC system, it was evident that at low UC concentrations the vaporization rates were within the arbitrary tolerances without accepting credit for an advantageous cesium effect.

The selection of electrically heated converters for evaluation of the merit of bare-carbide emitters was made in the interest of economy and to

*It has been shown during the last three years that UC-ZrC behaves as dispenser cathodes and emission characteristics are dependent only on the maintenance of a monolayer of uranium metal on the emitting surface.

Manuscript released by author in January 1963, for publication as an RTD Technical Documentary Report.

provide an easier approach to post-test failure analysis than would be available with highly radioactive components from a fission-heated generator. The converter design was tailored by the expected application to space power reactor systems. Consequently, cylindrical geometry was chosen as representative of a single module of a thermionic-reactor fuel element. Material selections were based on temperature requirements and fabricability. The converter simulated in temperature distribution the heat-rejection system most attractive to space application--liquid-metal coolant receiving heat from the collector at ~1000°K and dissipating this energy through a radiator.

After completion of the reference design of the test converter, fabrication development of the emitter and the converter envelope was undertaken. The manufacture of the emitter structure was an exceedingly difficult problem, since the requirements were stringent and unique only to laboratory converter operation. The emitter structure must be a hollow, leak-tight cylinder to accommodate filamentary heating. All UC-ZrC compositions and all densities less than 100% of theoretical exhibit some degree of porosity. Consequently, a carbide overlay on a refractory-metal vacuum tube, which did not react with the UC-ZrC, was required. After several trials and emitter design changes, a satisfactory compromise was achieved using tantalum as the substrate material. Tantalum was known to react with UC-ZrC, especially at high UC concentrations, at 2000°C. However, the reaction rate could be materially decreased by maintaining the emitter temperatures at 1800°C or below, and at this temperature it was predicted that relatively long life would ensue.

In the final eighteen months of the program, six converters were fabricated and operated for a total of over 6000 hr. One converter was operated for over 1700 hr at usable power levels. Interaction of the carbide and the tantalum substrate in all emitters decreased the bulk uranium content severely; however, the failure mechanism in all cases was the loss of cesium due to leakage of the cell envelope. The pre- and post-test

vacuum-emission data indicated in all cases that the emission capability of the UC-ZrC had not deteriorated during the operational life of the converter.

II. SUMMARY

The Mark V cells employed in this program were electrically heated thermionic diodes with cylindrical, bare UC–ZrC emitters and a nickel collector. All other components were of oxygen-free copper except the insulator, which was of high-purity alumina brazed to Kovar and Monel. All joints were either brazed or electron-beam-welded. Tantalum-sheathed W–W/26% Re thermocouples were used to monitor the emitter temperature. A Kovar ampoule containing the cesium was placed in the cell envelope during assembly.

The fabrication of the emitter consisted in hot-pressing 10 mol-% UC–90 mol-% ZrC powder into a tantalum slug, from which the emitter was machined. Fabrication of high-uranium-concentration (up to 90 mol-% UC–10 mol-% ZrC) emitters was attempted by various means. Tantalum was bonded successfully to the carbide, but the extensive tantalum-carbon reaction promoted the formation of free uranium, which then evaporated. In another approach (direct bonding to tungsten), the differential expansion of the tungsten and the carbide eliminated the former as a substrate material. Vapor-deposition of tungsten on the carbides was attempted, but lack of time and funds prevented further pursuit of this approach and others to the fabrication of high-uranium-content emitters.

In April, 1962, the first cell (E) was placed in operation under the present program. The only change from previous cells was the use of nickel for the collector, which permitted the desired higher collector temperatures to be achieved. Cell E was sealed off with a high-temperature, high-vacuum valve. This valve was eliminated in Cells F through K by pinching off the pumpout tube. Other changes were also made to improve the ultimate vacuum in the cell during bakeout.

Because the 0.040-in.-diameter emitter thermocouple of Cell E failed prematurely, all subsequent cells were fitted with two 0.062-in.-diameter thermocouples. The bodies of all cells were fitted with cooling coils to maintain the desired cell temperatures. It became apparent, however, during operation of Cell E that an acceptable thermal gradient existed throughout the cell body without cell cooling, and consequently all subsequent cells were operated without cooling.

To maintain desired collector temperatures, a radiator was mechanically attached to the collector. This method of heat reflection was found inadequate, and subsequently a cooling coil was clamped to the collector. The collector was also equipped with a heating coil which permitted a temperature control of about 150°.

Cell H differed from the previous cells in that it had two separate cesium vials to demonstrate the possibility of rejuvenating the cell by the introduction of an additional charge of cesium.

During the fabrication of Cell K, a large hydrogen furnace was used to braze all joints, thus eliminating two electron-beam welds which had proved to be unreliable.

Vacuum-emission measurements were made on all emitters to determine their characteristics before and during cell assembly. Upon initiation of cesium-cell operation, cesium-pressure optimization was conducted. The effect of cesium temperature was investigated between 475° and 650°K for emitter temperatures from 1900° to 2500°K. The optimum cesium-well temperature was about 610°K for most cases. No optimum collector temperature was found. The collector was operated between 800° and 1250°K.

All cells except E demonstrated a power capacity in excess of 50 watts. In one cell a maximum of 68 watts was observed. The continuous power output of the cells varied between 10 and 40 watts, except for Cell E, which produced only 2 to 8 watts during its operational period of 1034 hr. Cells G and J were operated for 1753 hr and 1427 hr, respectively. At the maximum power an efficiency of 6.2% was observed. During continuous operation, efficiencies of up to 4% were recorded.

Short-circuit-current measurements showed higher current values than were obtained during vacuum-emission studies. The short-circuit current was also found to be a function of cesium pressure, as was the open-circuit voltage and the voltage at maximum power. The cell voltage decreased with increasing cesium pressure but increased with increasing emitter temperature.

An average effective emissivity of 0.55 was observed; the time dependence of the emissivity was not determined.

On two occasions, cells were successfully operated when connected electrically in series and in parallel. The data obtained are in agreement with Ohm's law for direct current.

Cell failure could in all cases be traced to a loss of cesium, although heavy uranium and zirconium deposits on the collector, especially in Cell G, indicated that interelectrode shorting might become a problem in longer-term tests. Post-test analysis also revealed an extensive metallurgical reaction between the deposits and the nickel collector, and between the tantalum substrate and the carbide of the emitter. In spite of a severe depletion of uranium, the post-test vacuum-emission current exceeded the pre-lifetest values--in one case by a factor of 8.

The biggest problem experienced with emitter thermocouples was inadequate immersion depth, which permitted several of them to pull out of their cavity. Post-test recalibration agreed within 10° to 70°K with the pre-test calibration of other thermocouples in spite of the hundreds of hours of operation in excess of 2200°K. A reaction of the beryllium oxide insulation with the tantalum sheath may limit the operational life of these thermocouples.

A theoretical study of cell contamination by fission products revealed that they may have a wide variety of effects on cell performance. The noble gases krypton and xenon presumably will have the least detrimental effect in a vented system. The electronegative fission products tend to combine with the cesium to some extent. Since the cesium reservoir will

be at the lowest temperature in the cell, most of the condensates of the fission products should collect there. The remaining fission products will condense on the various components of the cell.

III. CELL FABRICATION

CELL-BODY FABRICATION

The components of the cells were fabricated in the machine shop according to engineering drawings (see Fig. 1 for a schematic diagram of the cell). Oxygen-free copper was used for all parts except the emitter, collector, and insulator. (The emitter fabrication is described later in this section.) The collector was machined from high-purity "A" nickel. The interelectrode spacing varied for the six cells tested from 0.040 in. for Cell E to 0.020 in. for Cell F to 0.012 to 0.015 in. for all other cells. These dimensions were measured with the component at room temperature.

The insulator was of high-purity, high-density alumina, copper-brazed to a Kovar ring which in turn was brazed to a Monel ring. The insulator assembly was purchased. The cooling coils were brazed in a hydrogen atmosphere to the copper emitter and collector bases. Then the insulator was electron-beam-welded to these two subassemblies.

A different assembly procedure was initiated with Cell K, which improved the envelope reliability. The electron-beam weld, which caused considerable difficulty during assembly and always leaked after cell operation, was eliminated, and the collector and emitter bases were simultaneously brazed with Inconel 10 to the Monel rings of the insulator in a hydrogen furnace. The hydrogen atmosphere cleaned up the cell to an extent not otherwise possible and minimized the stresses across the insulator joint.

The collector flange and the emitter support were machined after assembly to assure concentricity. After electron-beam welding of the emitter to the cell, the emitter thermocouples were installed, calibrated, and welded to the cell. Preliminary outgassing of the cell occurred at this stage. Finally, a collector, which had been outgassed previously

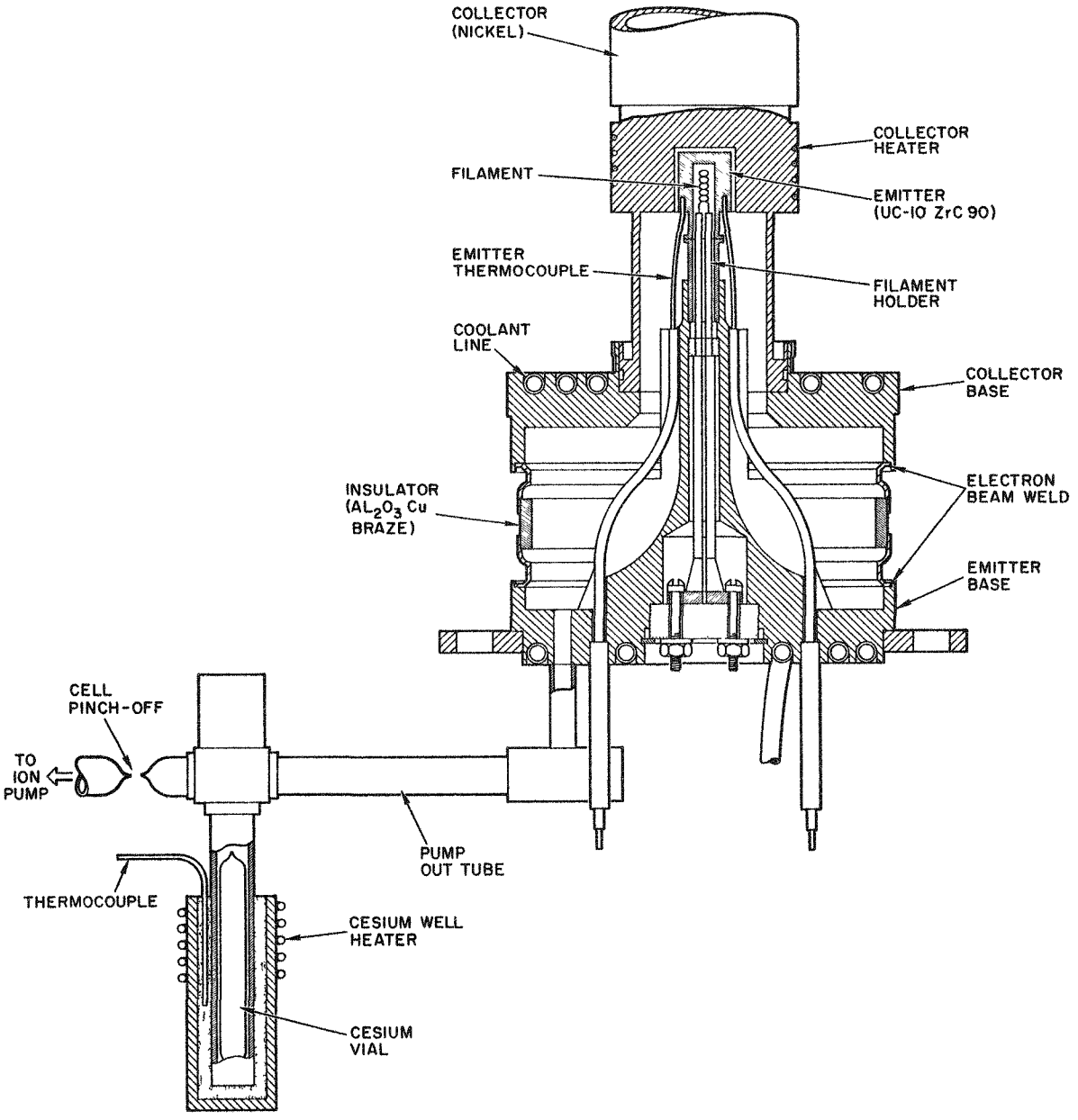

Fig. 1--Schematic diagram of Mark V cell

at 1100°K, was electron-beam-welded to the cell. The pumpout tube was prepared separately with a cesium vial in the well. This assembly was welded to the cell in the bell jar and then connected to the ion pump. Final bakeout of the cell was then undertaken.

Starting with Cell F, several improvements were made in design, fabrication, and assembly to obtain improved converter operation. Since a knowledge of the emitter temperature is essential, the emitter thermocouple was increased from 0.040 to 0.062 in. in diameter and a second thermocouple was added. The larger thermocouple not only had a thicker tantalum sheath, it also had larger tungsten and tungsten-rhenium sensor wires. This promised increased thermocouple life and reliability. During thermal-cycling, the thermocouples are put under severe stress, so to avoid failure the guide-tube diameter was increased to allow for independent expansion and contraction of the thermocouple within the cell. In addition, a 1-mil molybdenum sheet was placed around the hot junction of the thermocouple to prevent self-bonding or pressure-welding of the tantalum sheath to the tantalum substrate of the emitter.

During vacuum-brazing of the thermocouple to the cell envelope, frequent sheath failure in this specific region was observed. It was believed that during the brazing operation any nitrogen or oxygen trapped within the sheath would be gettered by the heated sheath. This would render it brittle and cause it to leak. Much greater reliability was achieved when the thermocouples were evacuated after the hot junction was made and then back-filled with argon, and the cold junction was sealed with a high-temperature, low-vapor-pressure epoxy.

In spite of the extensive bakeout of the cell, it was believed that residual gases might contaminate the emitter or become gettered in the tantalum of the emitter stem and the thermocouple sheath. To inhibit this reaction, a 0.020-in. titanium skirt was placed around the emitter stem. The titanium was in contact with both the very high- and very low-temperature regions of the stem, which assured that one area would be at the optimum gettering temperature for titanium for most gases.

To eliminate any possible contamination from the reaction of cesium with the glass ampoule, Kovar ampoules were used. The cesium was distilled into a clean Kovar ampoule under vacuum, and the Kovar tube was sealed by welding with electron bombardment.

Because the low density of bare carbide emitters is an inherent source of gases, extensive outgassing at elevated emitter temperatures was required. To assure the best ultimate vacuum in the cell, the oil diffusion pump used in Cell E was replaced by a 9-liter ion pump. The conductance of the tube connecting the cell with the pump was increased by eliminating all right angles, increasing its diameter, and eliminating the high-vacuum valve, which constituted a major restriction. This valve was used as the final closure of Cell E, but was found to be leaking after the test. All other cells were pinched off close to the cesium vial. This facilitated cell operation because less of the tubing had to be maintained above the cesium-well temperature. The knife edge of the pinchoff was welded over, producing a less fragile and more reliable seal. At the end of the 48-hr bakeout period, a pressure of 1×10^{-6} torr was recorded at a cell-body temperature of 820°K and a pressure of 1×10^{-9} torr at room temperature.

THERMIONIC-EMITTER FABRICATION

Fabrication techniques for the preparation of bare UC-ZrC emitters have been under development at General Atomic for the past three years.[1] Improvements in technique resulted in the evolution of the present emitter through four stages of development: (1) the three-piece emitter, (2) the two-piece emitter, (3) the one-piece brazed emitter, and (4) the one-piece hot-pressed emitter. In stages 1, 2, and 3, the emitter was zirconium-brazed to a tantalum sleeve, but in the fourth stage the braze was eliminated by successfully bonding a thin carbide layer directly to a serrated tantalum slug by hot-pressing. Since tantalum flows readily at hot-pressing temperatures, a solid slug was used to prevent severe distortion during

processing. After final vacuum-sintering of the carbide, the tantalum substrate was machined to provide a short stem and a filament cavity. The carbide overlay was ultrasonically machined to dimensions consistent with cell design. The emitters were hollow cylinders approximately 1-1/16 in. in diameter and 3/4 in. long. The total emitting area, neglecting the top, was 10 cm^2. Forty-three emitters composed of 10 mol-% UC–90 mol-% ZrC were manufactured during the course of the program. The first of these emitters was welded into Cell E.

The development of high-uranium-content (>10 mol-%) carbide emitters for bench-testing was undertaken early in this program for the following reasons:

1. A thermionic space reactor will require a higher uranium concentration than 10 mol-% UC–90 mol-% ZrC.
2. The vacuum-emission data available at the time indicated increasing emitter capability with increasing uranium content.
3. Since the emission capability of UC-ZrC compounds is dependent on a layer of uranium metal on the emitter surface, adequate emission could be sustained over longer periods if a greater supply of uranium were present in the bulk material to replenish the uranium evaporated from the surface.

The first approach to higher-UC emitter development was patterned after the successful technique employed in making 10 mol-% UC–90 mol-% ZrC emitters. Emitters with a 30 mol-% UC–70 mol-% ZrC composition were fabricated according to this procedure. After fabrication and rough machining, the emitters were thermal-cycled up to 20 hr. During this experiment, hair-line cracks opened up and uranium evaporation occurred at temperatures above 2000°K (Fig. 2). Investigation showed that the carbide powder used for the emitter fabrication was metal-rich. TaC formation occurred at the tantalum interface, which further increased the metal-to-carbon ratio. Liquid uranium then evaporated, leaving numerous voids. It was also noted that the density of the carbide on the

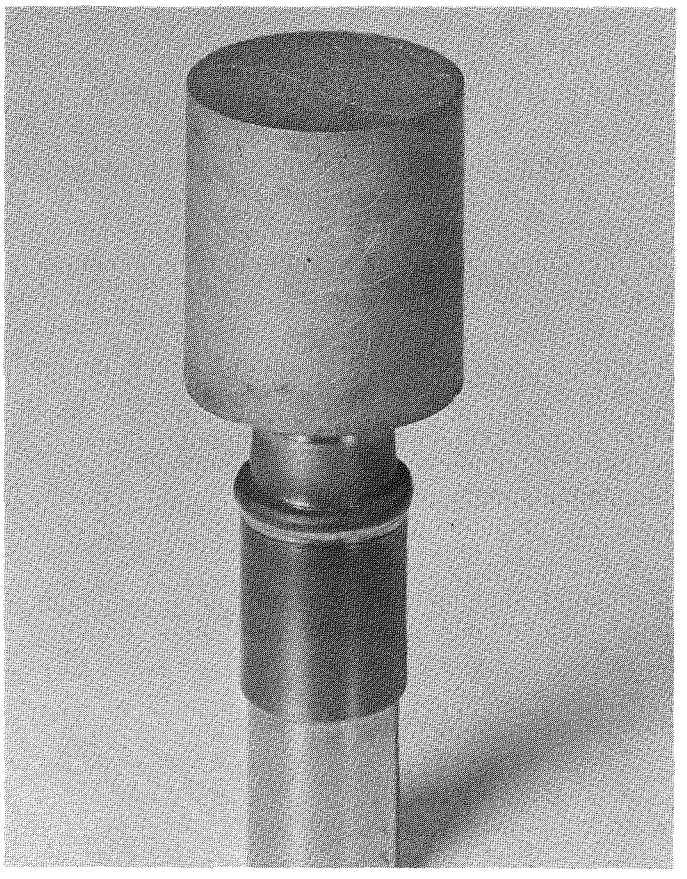

Fig. 2--30 mol-% UC–70 mol-% ZrC emitter on tantalum stem after 20 hr of thermal-cycling (note hair-line cracks in carbide)

surface of the emitter was quite low. It is possible that during the thermal-cycling and heat-treatment the lower-density material tended to densify by further sintering, resulting in decreased volume and enlarged cracks.

Two changes in fabrication procedure were pursued in order to overcome these problems:

1. Use of a carbon-rich carbide powder which allows a TaC layer to form at the metal-UC-ZrC interface and prevents further interaction.
2. Use of a higher pressing temperature (1850°C). At this temperature, the tantalum flows more readily and consequently will transmit more pressure to the radial surfaces of the die wall, thus increasing the density of the carbide.

Increased and more uniform density was obtained with the higher pressing temperature, but the use of carbon-rich carbide powder only delayed (for a matter of hours) the liquid-uranium formation owing to the large amount of tantalum present for subsequent reaction with carbon.

Another technique employed was to bond tungsten and ZrC at 2400°C, then bond 10 mol-% UC–90 mol-% ZrC and finally 90 mol-% UC–10 mol-% ZrC to the ZrC side at lower temperatures. This created a good bond with less cracking, but alpha-counting of the surface indicated a concentration of UC of only about 40 mol-%. Evidently the UC tended to diffuse at bonding temperatures toward the areas of lower UC concentrations.

Two other approaches were followed to develop a high-uranium-content emitter:

1. Vapor Deposition of Tungsten. This had been successfully done in industry, but it had not been conclusively demonstrated that a vacuum-tight deposit results, particularly in difficult geometries and after thermal-cycling. For this application, tungsten must be deposited on the inside of a hollow UC cylinder. Samples were made for studies of the permeability of various thicknesses and for thermal-cycling tests. Owing to lack of time and funds, this

approach was abandoned after difficulty was experienced with the first samples.

2. Tantalum Support with Tungsten Barrier. It was known from past experience in 10 mol-% UC–90 mol-% ZrC emitter fabrication that a tantalum support tube is almost essential to the hydrostatic hot-pressing operation. The possibility of using the same technique in 90 mol-% UC–10 mol-% ZrC processing with a thin tungsten barrier applied between the tantalum and the carbide to prevent massive carbon loss to the support tube appeared promising. Two methods of application were studied: (1) vapor-depositing a thin coating of tungsten on the outer surface of the tantalum tube, and (2) sandwiching a 0.005-in. sheet of tungsten between the tube and the carbide.

A preliminary test of method (2) was made using 30 mol-% UC–70 mol-% ZrC specimens. A visual examination of a cross section of such a joint revealed good bonding of the tantalum to the tungsten and the tungsten to the carbide. The carbide was slightly cracked but appeared well bonded. Thermal-cycling tests subsequently conducted on similar specimens revealed that the bond integrity could not be maintained owing to the large differences in thermal expansion of the three materials.

Concurrent with the development of high-uranium-content emitters, metallurgical investigation of carbides for thermionic cathodes under NASA sponsorship revealed new and interesting data on their saturated vacuum emission. The results of this investigation can be summarized as follows:[3]

1. For all compositions, the desired current density of 5 amp/cm^2 can be obtained at temperatures lower than 2000°K.
2. The emission behavior is not enhanced by increasing the uranium content of the bulk specimens.

As a result of these findings, the development effort on high-uranium-content emitters for bench-testing in this program was terminated.

Furthermore, it became apparent that the solution to high-UC emitter fabrication for eventual reactor application was not possible within the time and funding scope of this program. The major roadblock to success was the preparation of the carbide on a vacuum-tight refractory-metal substrate, which is unique to bench-testing. The ultimate use of bare carbides in a thermionic reactor does not present this requirement.

IV. CELL OPERATION

CELL E

The Mark V cells described in this report are thermionic diodes designed to permit evaluation of cell performance during bench-testing for up to 3000 hr. The maximum design output for these cells was 75 watts (Fig. 3). The emitter was heated by a tungsten filament and by electron bombardment up to 600 volts (dc). The cells were tested in a bell jar, under a vacuum in the 10^{-6}-torr range (Fig. 3). Electrical heaters were used to maintain the cell insulator and the cesium well at desired temperatures. The collector was cooled by means of a radiator plus a cooling ring through which Dowtherm oil flowed.

Cell E was in a partially completed state at the beginning of this program. During completion of the cell, a leak in the emitter thermocouple sheath within the cell envelope was detected. By sealing the cold junction of the thermocouple, a leaktight cell was achieved and Cell E was placed in operation on April 25, 1962. This cell was identical to Cell D[1] except that a nickel instead of copper collector was used. After bakeout, the cell was sealed off by closing the high-temperature, high-vacuum valve.

A systematic study of the cell current versus voltage characteristics was conducted for a wide cesium-temperature range and with the emitter temperatures set from 1900° to 2450°K. The maximum current, maximum power, and cell voltages were studied. The maximum power output recorded was 14 watts, which was obtained at an emitter temperature of 2413°K, a cesium-well temperature of 608°K, and a collector temperature of 998°K.

During the unattended periods of operation, the emitter temperature was maintained at approximately 2250°K, resulting in a power output of

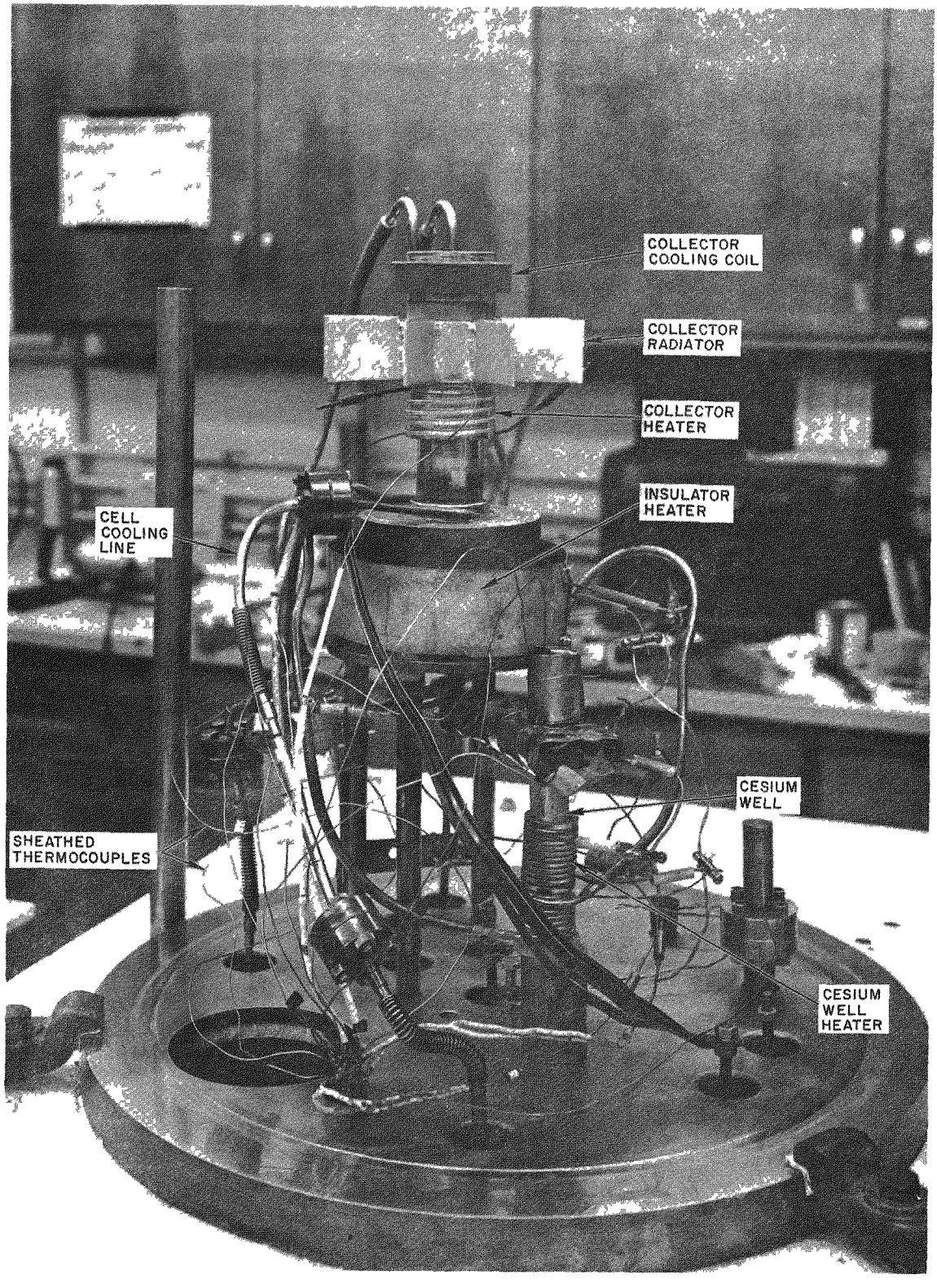

Fig. 3--Fully instrumented thermionic diode on vacuum stand

about 4 to 8 watts. Slight drifting of the temperature of the emitter occurred owing to line fluctuations of the input power.

On the morning of April 28, a decrease in the millivolt output of the emitter thermocouple was noted, with no apparent change in any other parameters. This was believed to be the result of cesium leakage through a microcrack of the sheath (noted above), which shorted the thermocouple leads in a colder region. The emitter temperature was henceforth related to previous power input data. Just prior to final failure of the cell, the thermocouple millivolt response increased drastically. It appeared that once the cesium had leaked out of the cell envelope, it also leaked out of the sheath, opening up the short.

Early in May, a leak in the collector cooling line was discovered. Since improved cell performance was observed at higher collector temperatures, the collector cooling line was removed completely and cell operation continued until 600 hr were logged, when a filament failure interrupted the operation. After replacement of the filament, the output of Cell E exhibited a 50% drop. Nevertheless, cell operation and the study of cell parameters was continued until 1000 hr were recorded. A short-term operation at emitter temperatures up to approximately 2500°K was conducted before the cell was dismantled for post-test analysis. A total of 1034 hr of operation were recorded for Cell E.

CELL F

After completion of all the modifications discussed in Section II, "Cell Fabrication," Cell F was mounted in the bell jar for vacuum-emission studies of the emitter. At various stages during cell assembly, these studies were repeated to assure that the emitter had not become contaminated during any particular operation. The final emission check was performed after cell isolation. This not only assured that the pinchoff was successful, but also proved that the thermocouples had maintained their calibration.

The vacuum-emission data are discussed in detail in Section V, "Performance Evaluation of Cells."

On November 7, cesium was introduced into the cell after all cooling lines, heating coils, and thermocouples had been properly installed and connected.

During the first 10 days of operation, the effect of cesium pressure was studied. Current-voltage characteristics of the cell were observed over a cesium-temperature range of 473° to 660°K and an emitter-temperature range of 1700° to 2200°K. Since the only collector cooling provision for this cell was a copper ring with fins, the collector temperature varied for the different operating conditions. The maximum collector temperature observed was 1250°K.

Because there was evidence in Cell E that the response to the change in cesium pressure was slow, Cell F was allowed to come to equilibrium for several hours. Data taken within an hour after the change in cesium pressure, however, were identical to data obtained after 24 hr of equilibration.

The maximum power produced in Cell F was 50 watts (72 amp at 0.7 volt) at the following cell conditions: $T_E = 2440^\circ K$, $T_{Cs} = 626^\circ K$, $T_{col} = 1250^\circ K$. The maximum cell current recorded at minimum external load was 120 amp.

On November 17, an electron-gun filament burned out after 181 hr of operation. While the filament was being replaced, a leak in a cooling-system line was repaired. On November 23, a second filament failure occurred. When the filament holder was removed, it was badly eroded 3/4 in. below the junction of the filament and the holder. Operation of Cell F continued for 215 hr on an intermittent basis owing to repeated filament burnout. Very little reliable performance data could be obtained during this period because the cell was rarely at equilibrium conditions. However, it was established that the cell power output had decreased on or about December 7, 1962. The current-voltage plots indicated a lack of cesium. Increasing the cesium-reservoir temperature improved the cell performance. It was

concluded that insufficient cesium was present in the cell to maintain a two-phase system owing to a leak in the cell envelope, probably in the emitter stem. Consequently, operation of Cell F was discontinued since any data obtained would be difficult to correlate with data on other carbide cells. Figure 4 is a plot of the power output of the cell as a function of operational time. It can be seen that the cell operated above 20 watts for about 140 hr.

CELL G

The operation of Cell G was initiated in mid-January of 1963. From the operating experience obtained on Cell F, it was possible to optimize cesium temperature within the first week of operation. Current range of voltage plots were obtained for emitter temperatures between 1800° and 2200°K for a 140° cesium-well temperature. The optimum power was computed from these plots. The maximum power from Cell G was 68 watts, obtained at an emitter temperature of 2250°K, a cesium-well temperature of 628°K, and a collector temperature of 953°K. During unattended operation, the cell was connected to an adjustable load. The recorded power output varied between 10 and 26 watts for emitter temperatures of 2075° to 2210°K (Fig. 5).

A filament failure occurred after 153 hr. While no degradation was observed after replacement of the filament, a 25% drop in output was noted after 300 hr of operation. The maximum power at 2285°K was only 48 watts. The cell continued to run without any degradation or operational interruptions until the second filament burned out at 1192 hr. After its replacement, an increase in power output for a given emitter temperature was observed relative to previous data. At an emitter temperature of 2195°K, a cesium-well temperature of 574°K, and a collector temperature of 879°K, the power output was 56 watts. A study of the input power revealed that the emitter thermocouple calibration was in doubt. Since the other emitter thermocouple had failed previously, the emitter temperature was estimated from power

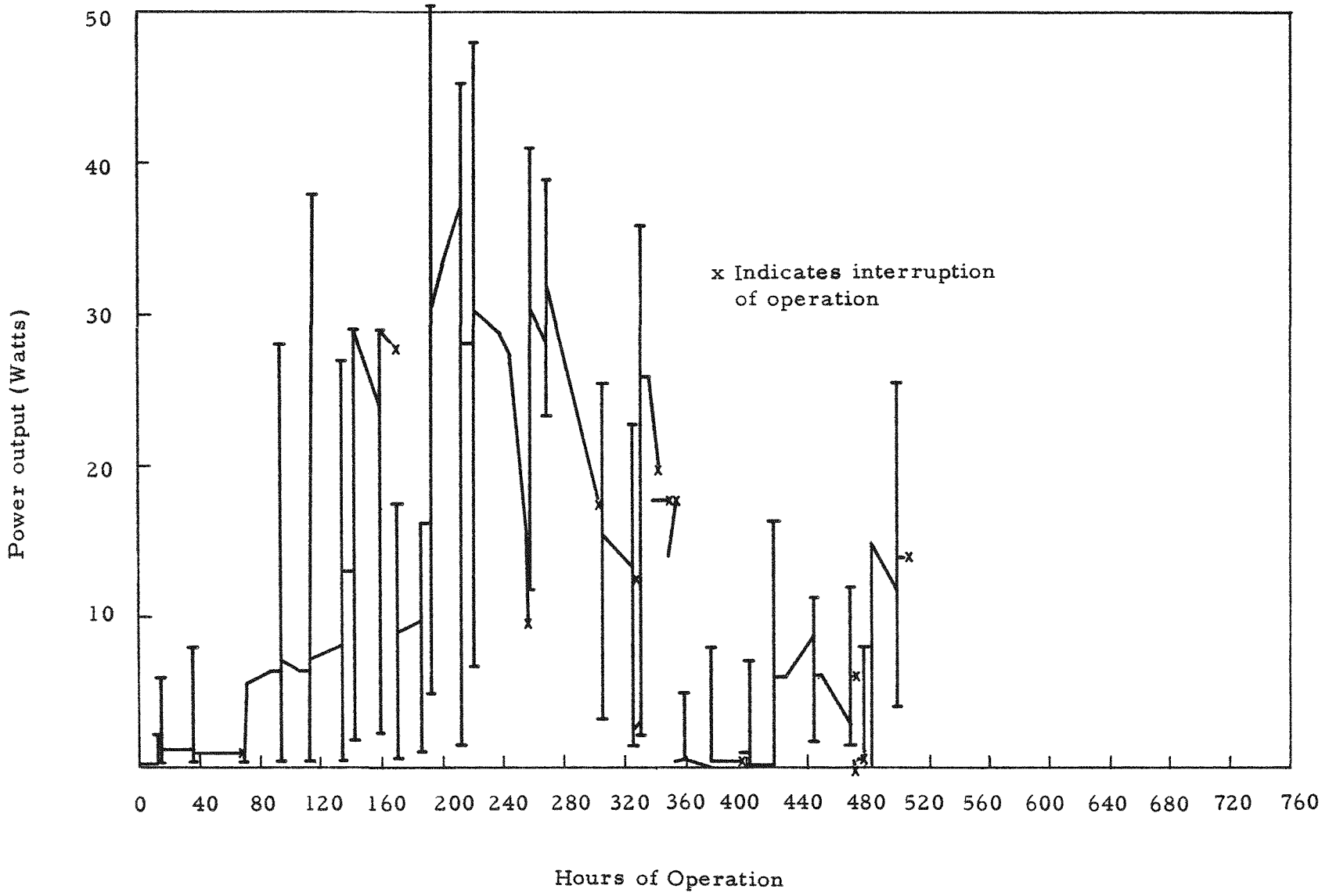

Fig. 4--Power output of Cell F as a function of hours of operation

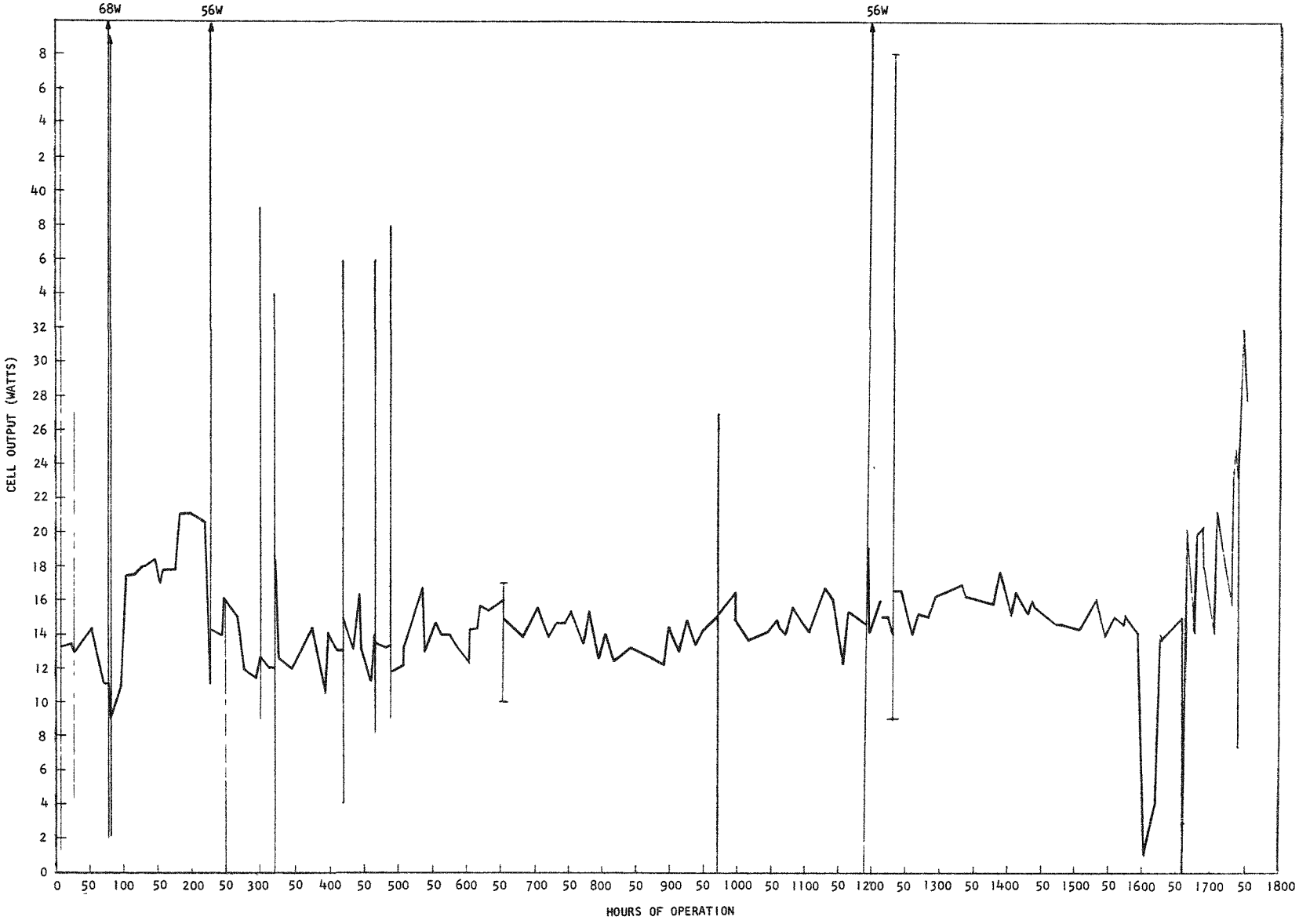

Fig. 5--Power output of Cell G as a function of hours of operation

input data for the remainder of the run. After the third electron-gun filament failure, a sharp degradation of power output with all indications of loss of cesium made termination of operation of this cell advisable. Cell G was operated for 1753 hr--longer than any other cell in this program. The only operational difficulties experienced through this long run aside from the filament burnout mentioned above were occasional collector cooling-flow interruptions, which caused the collector to operate at higher temperatures but did not result in cell shutdown.

CELL H

Cell degradation of all previous cells was attributed to loss of cesium. To varify this conclusion, two cesium vials were installed in Cell H. Operation of this cell was delayed until May, 1963, because of setbacks experienced during assembly, which followed the procedure established for Cells F and G. To initiate operation, one of the two cesium vials was broken and the effect of cesium temperature on cell output was investigated at 2000° and 2200°K. In spite of an improved collector cooling coil, the effect of collector temperature could only be investigated over a range of 120°K.

The output of Cell H was lower by a factor of 3 than the output of Cell G under the same conditions. It is noteworthy that the vacuum-emission current of Cell H was also lower than that of Cell G by the same factor. The maximum output recorded for Cell H was 56 watts at an emitter temperature of 2380°K, a collector temperature of 1023°K, and a cesium-well temperature of 638°K.

After the characteristics of the cell had been established, operation at a continuous average cell output of 15 watts was begun. The cell output is shown in Fig. 6, along with the emitter temperature. The fluctuations in the cell output were in part due to a faulty cesium-well controller, which caused that temperature to go off optimum. Deviation from the optimum cell voltage caused further apparent output variation. The emitter

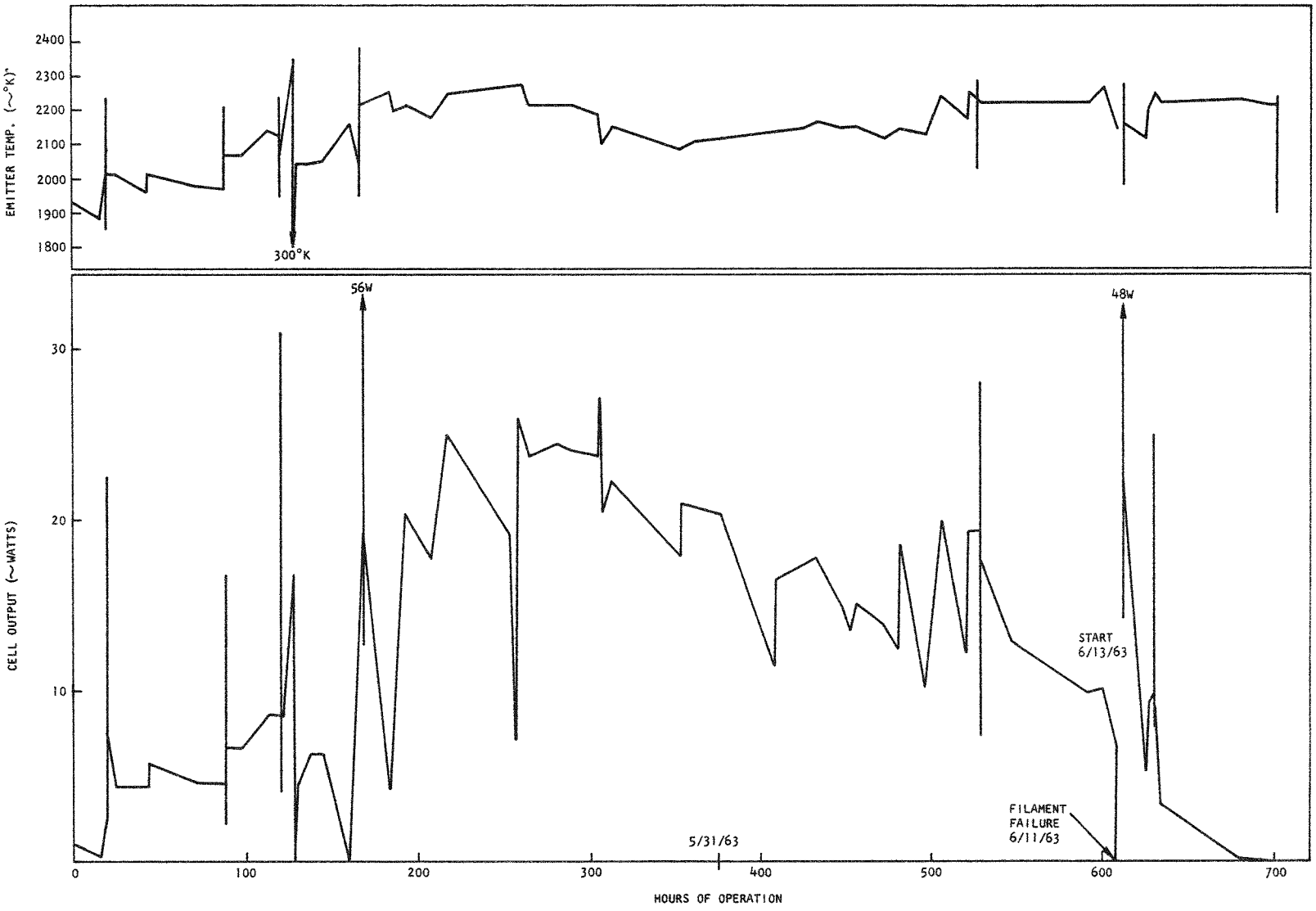

Fig. 6--Power output and emitter temperature of Cell H as a function of hours of operation

temperature varied between 1980° and 2270°K, and the cesium temperature varied between 628° and 638°K. During the first 530 hr of operation, only a slight power degradation was observed. In the following 78 hr, the power dropped to 12 watts at 2230°K (Fig. 7). Lack of response to increased cesium-well temperature, a condensation on the bell jar, and change of the current-voltage characteristics traced on the scope indicated that the cesium had leaked from the cell envelope. After a total of 608 hr, the filament burned out and was replaced. The second cesium vial was broken at this time.

A study of cell output versus emitter temperature showed that the performance of the cell was again restored to the values obtained from the first cesium charge (Fig. 7). A power output of 48 watts was observed at an emitter temperature of 2270°K, a collector temperature of 988°K, and a cesium-well temperature of 638°K. Thus, it was shown that the degradation observed before the filament failure was due to the depletion of cesium and not a deterioration of the carbide emitter. Within 24 hr after introduction of the second charge of cesium, another sharp degradation was observed. The cell voltage was abnormally low (Fig. 8). Apparently, an internal short between the emitter and collector existed. Because this short did not open up after several days, cell operation was discontinued with a total of 700 hr accumulated for Cell H.

CELL J

Cell J was identical to Cell G in every respect inclusive of the assembly procedures. Operation of this cell began in mid-January. Very little time was taken to evaluate cell characteristics. The optimum cesium temperature for maximum power was established at 610°K. In the emitter-temperature range from 1800° to 2200°K, the parameters of power output, short-circuit current, collector-temperature effect, and open-circuit voltage were studied.

For long-term operation, the output of Cell J was, as in previous cells, connected to an adjustable load. The output varied between 12 and 17

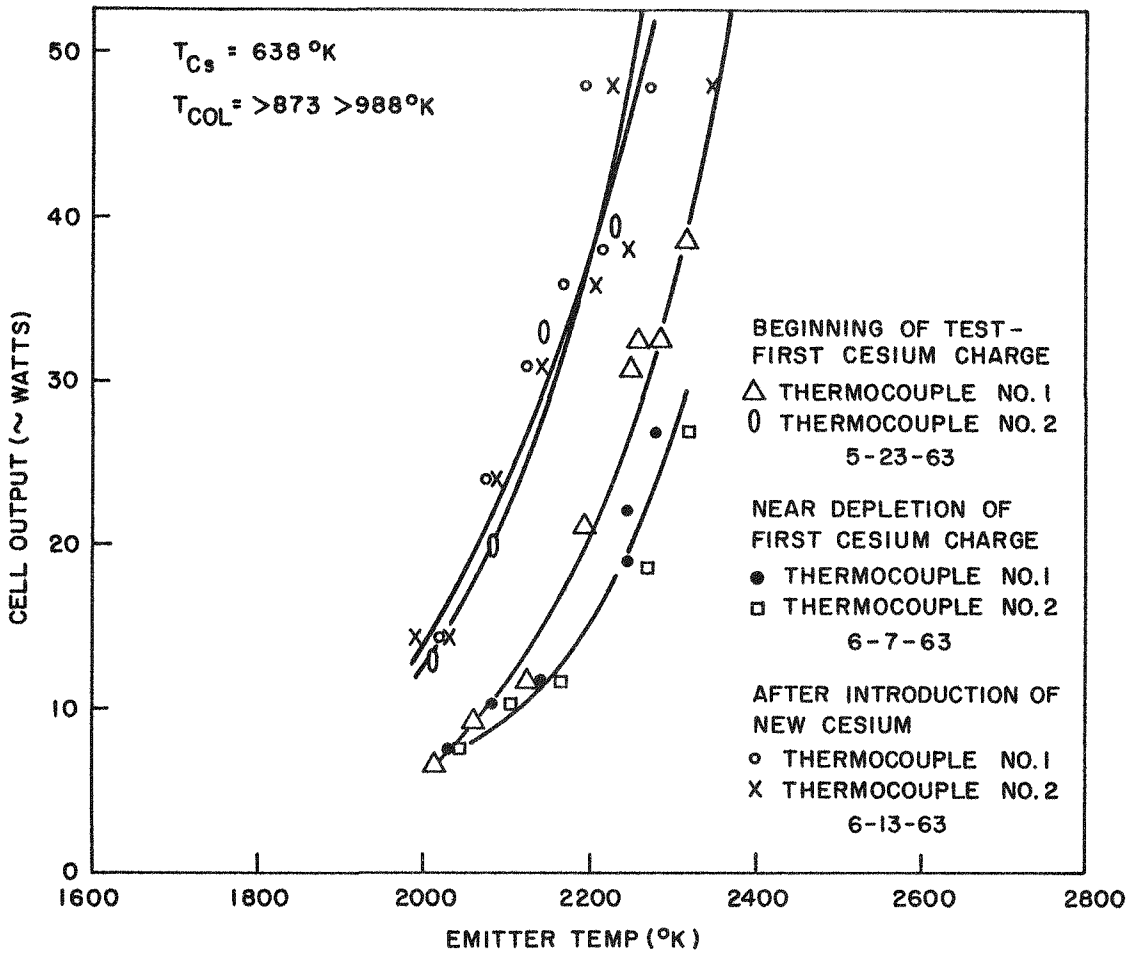

Fig. 7--Output of Cell H versus emitter temperature for operation with first and second charge of cesium

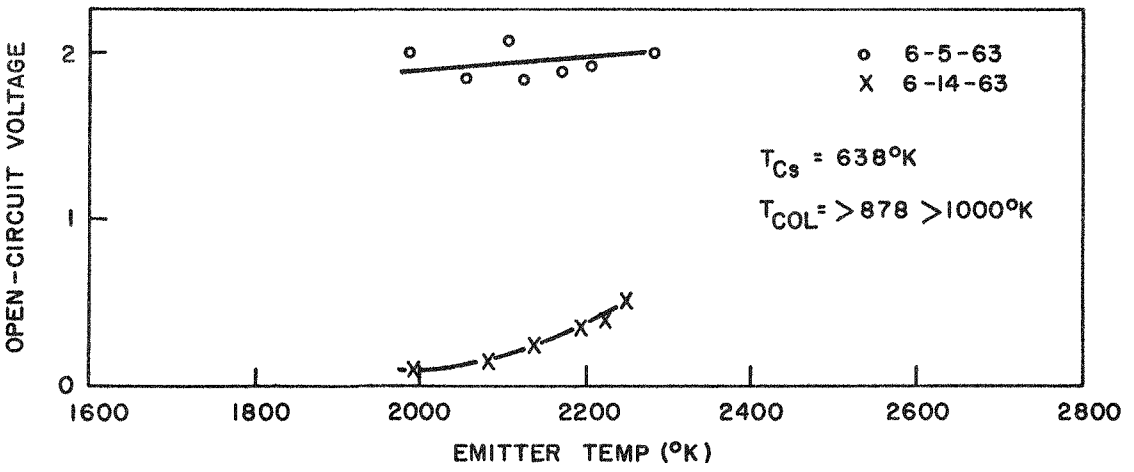

Fig. 8--Open-circuit voltage of Cell H versus emitter temperature for normal and degraded operating conditions

watts at an emitter temperature of 1900° to 2000°K for 1249 hr without any indication of power degradation (Fig. 9). The variations were due to input-power fluctuations. The electron-gun filament was replaced after 840 hr and again after 1320 hr of operation. After a period of 24 hr with a power output above 30 watts, the emitter temperature was further increased to obtain an average output of 40 watts with a maximum of 47 watts. A total of 151 hr were logged at this level before the third filament failure occurred. During the final days of operation, the collector coolant system became plugged and the collector temperature rose to 1160°K. After filament replacement, the power output decreased by a factor of 10, and cell operation was discontinued with a total of 1424 hr recorded for this cell. Again, the evidence conclusively pointed to a loss of cesium.

CELL K

The cell base of the diode for Cell K had been assembled in a hydrogen furnace, which assured a cleaner assembly and reduced bakeout time. Repeated sheath failure during installation of the two emitter thermocouples resulted in elimination of one thermocouple and sealing of the cell with a single emitter thermocouple.

An improved collector radiator and Dowtherm cooling coil were attached to the collector. The cell was instrumented with nine Chromel-Alumel thermocouples. Then the cesium vial was opened, and the cell was placed in operation in mid-August. The optimum cesium temperature for maximum output power of the cell was established at 608°K. Open-circuit voltage, emissivity, and power-output studies were conducted in the emitter-temperature range 1900° to 2250°K. The maximum power output from this cell was 54 watts, obtained at 2298°K with a collector temperature of 873°K and a cesium-well temperature of 609°K.

For the lifetime study, the diode was connected to the adjustable load. During the first 100 hr, the average cell output was 35 watts at an average emitter temperature of 2200°K (Fig. 10). Then the emitter temperature

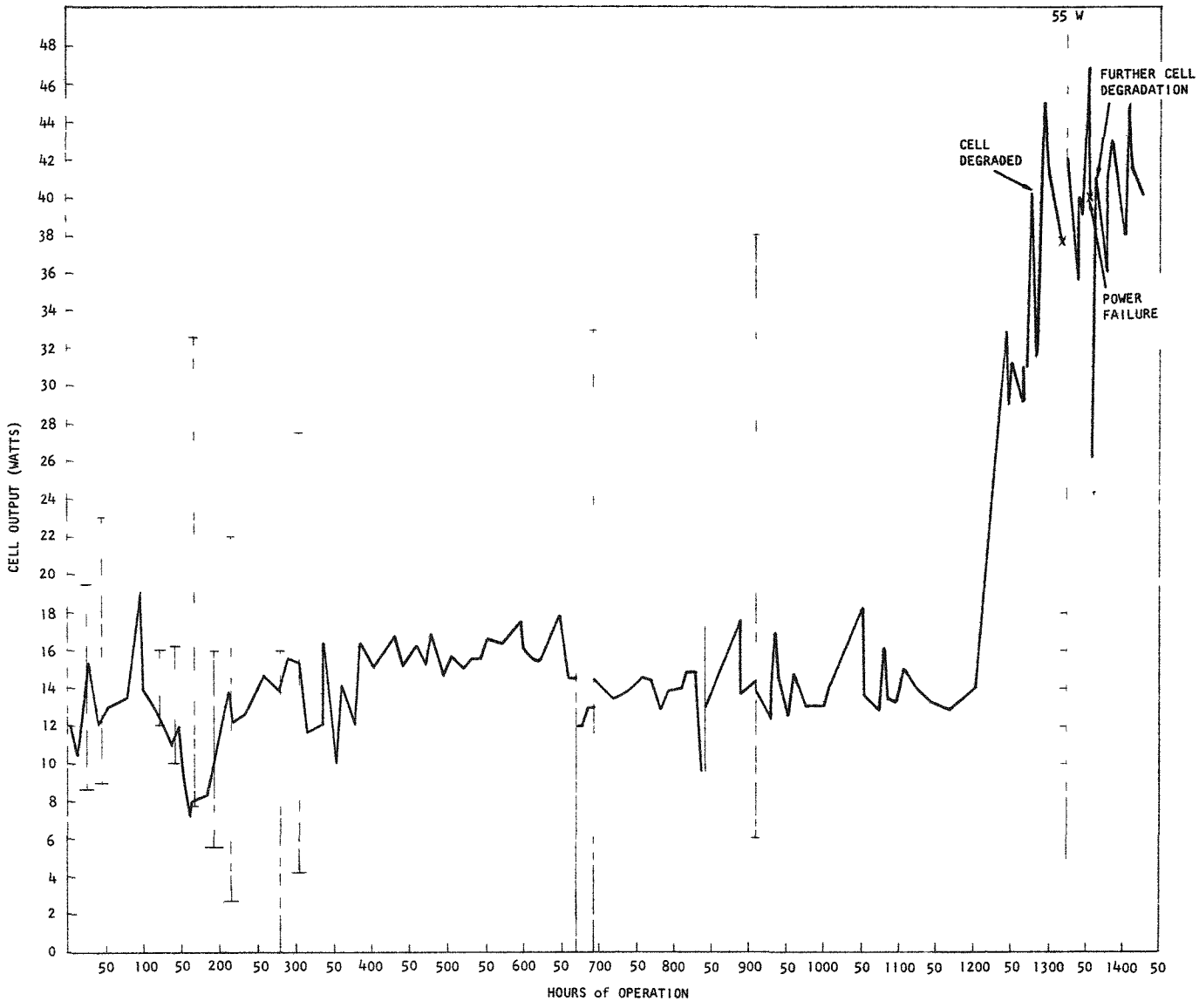

Fig. 9--Power output of Cell J as a function of hours of operation

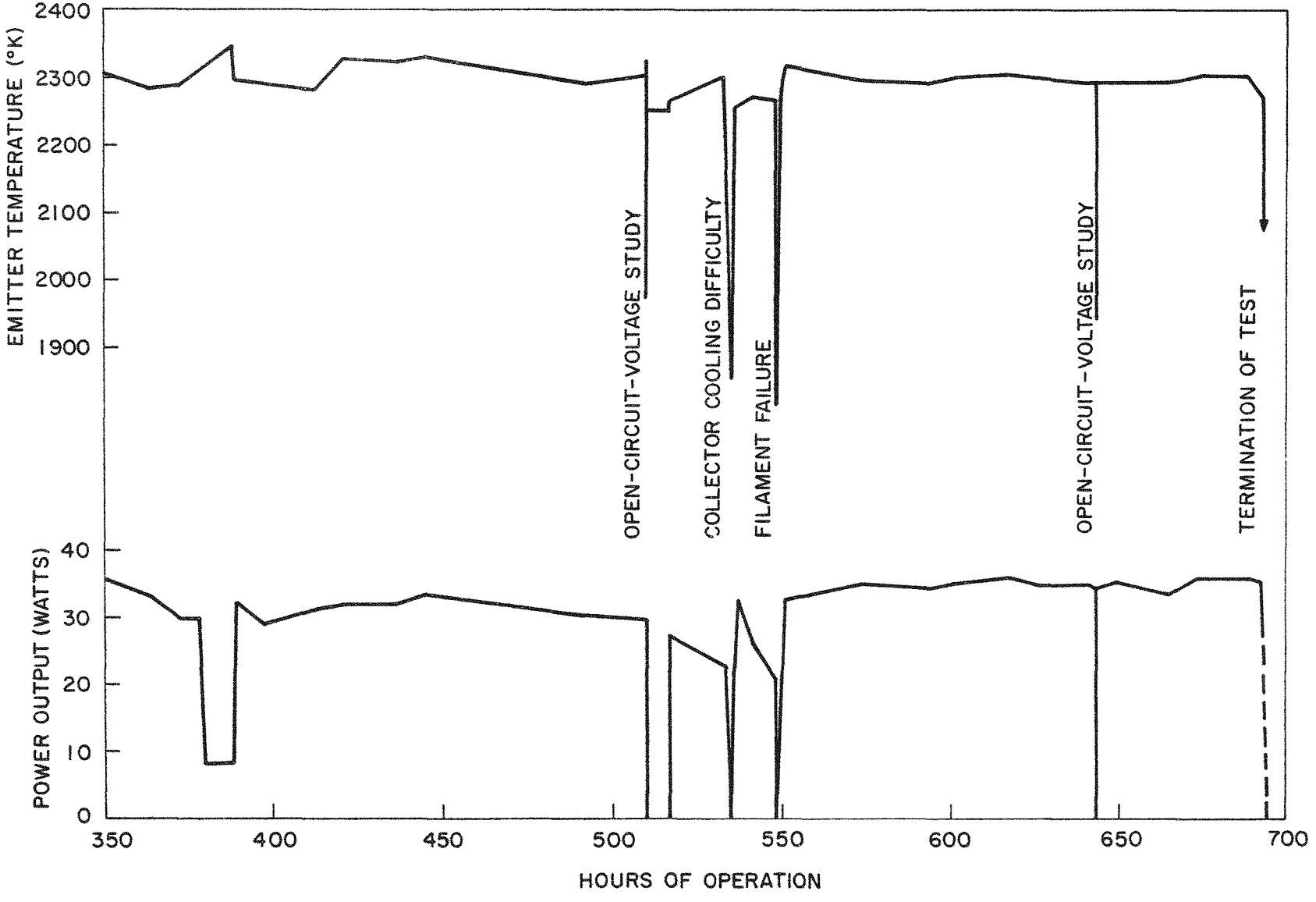

Fig. 10--Power output and emitter temperature of Cell K as a function of hours of operation

was increased 50°, resulting in an average output of 42 watts. Following an electron-gun filament replacement at 178 hr, the output decreased to an average of 33 watts for an average emitter temperature of 2300°K. However, at the same power input previously required for 2250°K operation, an emitter temperature of 2300°K was observed. This indicated that the emitter thermocouple calibration had changed. A post-test recalibration revealed that the temperature indication was indeed about 50° higher. Thus, a true emitter temperature of 2250°K existed when 2300° was indicated during the last 500 hr of operation. The second filament was replaced after 548 hr of operation. Owing to the termination of the contract, operation of Cell K was halted on September 20, 1963, with a total of 693 hr recorded. The cell was then cut apart for post-test analysis.

A summary of cell-performance data for all the cells is given in Table 1.

Table 1

SUMMARY OF CELL-PERFORMANCE DATA

Cell	Hours of Operation	Maximum Continuous Power Output (watts)	Maximum Output (watts)	Operating Conditions at Maximum Power			Efficiency (%)		Diode Spacing (mils)
				Emitter Temp. (°K)	Cesium Temp. (°K)	Collector Temp. (°K)	Max.	Continuous	
E	1034	2-8	14	2413	608	998	2.2	1	40
F	484	10-30	50	2365	606	1153	6.2	1-4.5	20
G	1753	12-20	68	2250	628	953	6	1.7-2.4	12-15
H	700	15-22	56	2380	638	1023	4.3	1.9-2.4	12-15
J	1427	15-40	56	2470	603	1150	5	2-4	12-15
K	693	30-40	54	2300	608	873	4.2	3	12-15

V. PERFORMANCE EVALUATION OF CELLS

EMITTER-TEMPERATURE MEASUREMENT

The emitter thermocouples penetrated into the tantalum substrate of the emitter approximately 3/16 in. They were calibrated by measuring the emitter surface temperature with an optical pyrometer sighted through two holes in the nickel test collector. The sight holes were vertically aligned about 5/16 in. apart, the bottom hole being located at the axial centerline of the emitter. A difference of ~60° was observed with the two holes. For the purpose of thermocouple calibration, the highest temperature observation was always used. The reading was corrected for emissivity and losses through the bell jar. The millivolt output from the two thermocouples was recorded and plotted versus the corrected pyrometer reading. After the removal of the test collector, the two thermocouples were the only direct means of determining emitter temperature. While thermocouples are less reliable than an optical pyrometer, it was felt that the cell design would suffer from the standpoint of reliability if pyrometer windows were required. In actual operation, at least one of the thermocouples gave consistent results for hundreds of hours. Frequently, one of the thermocouples abruptly gave much lower readings (~150°) and had to be disregarded. Large temperature changes such as those during filament failure often caused step changes in thermocouple output. During post-test analysis following termination of the life test, it was usually found that the thermocouple which had shown much lower readings had pulled out of its cavity.

The temperature gradient observed over the surface of the emitter was due to uneven density and uneven bonding of the carbide to the tantalum substrate, and to a large extent the method of heating. The center portion of the cavity was heated by electron bombardment from the largest number

of turns of the electron-gun filament wire. The entire top of the emitter was heated by a single turn, while a relatively large test sink was present in the form of the emitter stem; thus, heat was conducted away from the bottom portion of the emitter, lowering the temperature in that region. The center of the emitter was always the hottest portion. A temperature-profile study of the emitter, conducted without a collector, is given in Table 2. A, B, and C represent three angular positions approximately 120° apart. In the same radial plane, the maximum deviation was 35°K, while in the axial plane a maximum difference of up to 130°K was observed.

Table 2

TEMPERATURE PROFILE OF EMITTER SURFACE

	Temperature (°K)					
	Angular Position, Run 1			Angular Position, Run 2		
Axial Position	A	B	C	A	B	C
Top	1770	1735	1745	1875	1891	1882
Upper	1800	1800	1785	1915	1950	1930
Middle	1811	1811	1805	1949	1970	1972
Lower	1735	1778	1751	1909	1908	1899
Bottom	1708	1708	1710	1852	1868	1842

The emitter-temperature indication was most questionable in Cell E, where power input was used for the majority of the test owing to failure of the thermocouple. In Cell F, one thermocouple was reliable but the other thermocouple started giving low readings and was disregarded. In Cell G, the spread between the two emitter thermocouples increased from 20° to 70°, and at times to 100°. The higher temperature was considered more reliable and was used throughout the life test. In Cell J, the emitter-thermocouple indications were only about 50° apart for the entire run of over 1400 hr. The indicated temperature differential between the two thermocouples of Cell H varied between 25° and 80°. In Cell K, only one

thermocouple was used, which showed a step change of 50° after the replacement of the first filament.

Emitter-temperature control was achieved by adjusting the bombardment voltage. Since there was no fine control for this adjustment in the early part of the program, step changes in the input were made and the temperature was recorded after thermal equilibrium was observed. No attempt was made to adjust to a specific emitter temperature. For the latter part of the program, a fine control permitted setting of the emitter at a fixed, predetermined temperature.

VACUUM-EMISSION STUDIES

Cell performance is highly dependent upon the work function of the emitter. This parameter can best be studied under vacuum conditions by relating the saturation current to the temperature according to Richardson's equation. The large size of the emitter (12 cm^2) plus the large spacing (0.010 to 0.040 in.) required special equipment capable of high currents (50 amp) at high voltages (5 kv). To reduce the input requirement and prevent overheating of the collector, a 10-μsec square-wave pulse generator was designed and built. The repetition rate was 10 pulses per second. The voltage applied to the emitter was varied by means of a variable transformer from 0 to 4000 volts. Using a special oscilloscope with independent external horizontal and vertical input, a current-voltage plot could be presented on the scope. Each dot represented a current pulse and the trace is similar to a Schottky plot. For convenience it was recorded with a camera (Fig. 11). The current was presented on the ordinate and the applied voltage on the abscissa. To be certain that saturation had occurred, the current was read at a voltage of 3.5 kv. This was divided by the emitter area to obtain current density and was plotted against the emitter temperature on semi-log paper. The emission was investigated in about 10 increments over the emitter-temperature range 1600° to 2200°K.

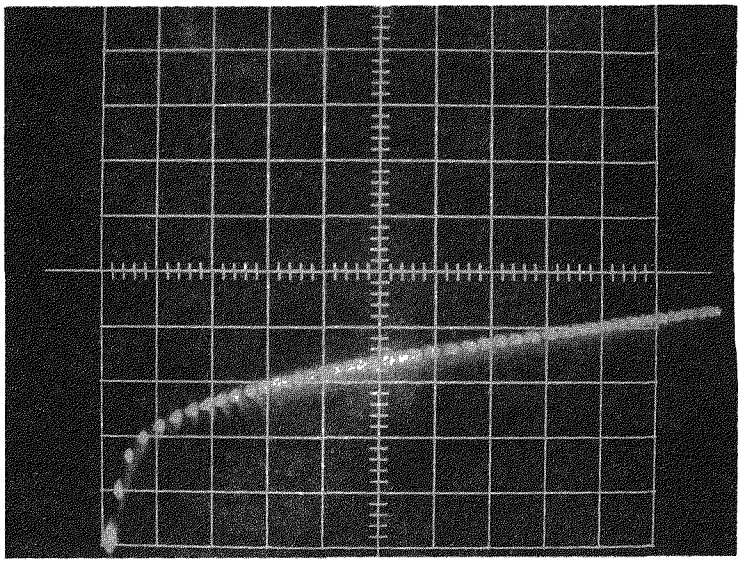

DATE: 10-23-62

Abscissa: 0.5 kv/div

Ordinate: 2 v/div (obtains 2 amp/div across 1-ohm resistor)

Current: 7.8 amp at 4 kv applied voltage

Emitter temperature: 1883°K

Emitter: No. 28

Fig. 11--Representative waveform of emission current as a function of applied cell voltage

Vacuum-emission measurements were made on each emitter following final machining and abrasive cleaning. It was learned from other studies[3] that heating the emitters for 40 hr at temperatures in excess of 2000°K would enhance the emission of bare carbides. This procedure was also applied to the emitters used in Mark V diodes. After the 40-hr bakeout, another vacuum-emission study was conducted. The increase in saturation current observed on emitter No. 39 is shown in Fig. 12. It is believed that an activation of the surface was accomplished by evaporating the uranium oxide and allowing new uranium to diffuse to the surface. A number of similar emission studies were conducted during assembly. During the first emission measurements, the temperature was observed with an optical pyrometer sighted through holes in the test collector. After installation of the regular collector, the temperature was read by means of the thermocouples. The final vacuum-emission curves for Cells F, G, H, J, and K are shown in Fig. 13. It can be noted that a considerable difference existed between these five emitters. In part, this is a result of the nonisothermal temperature existing over the emitter surface. Although all data are reported on the basis of the maximum emitter surface temperature, in actuality the emission current is a function of the weighted surface temperature. No correction or normalization between emitters due to temperature distribution was made, so direct comparison is not completely valid. Slight variations in fabrication and subsequent handling of the emitter also affected the saturation current. The slope of the curve is the same in all cases; however, there is a shift of nearly 200° from the best emitters (Cells F and G) to the poorest emitter (Cell H). For a given emitter temperature, the emission of Cell F was five times as high as that of Cell H.

THERMIONIC CELL PERFORMANCE

The thermionic performance data were obtained by two means. For fast evaluation of cell performance over the complete current range of the cell, a 60-cycle sweep was applied to the cell terminals. The circuit diagram

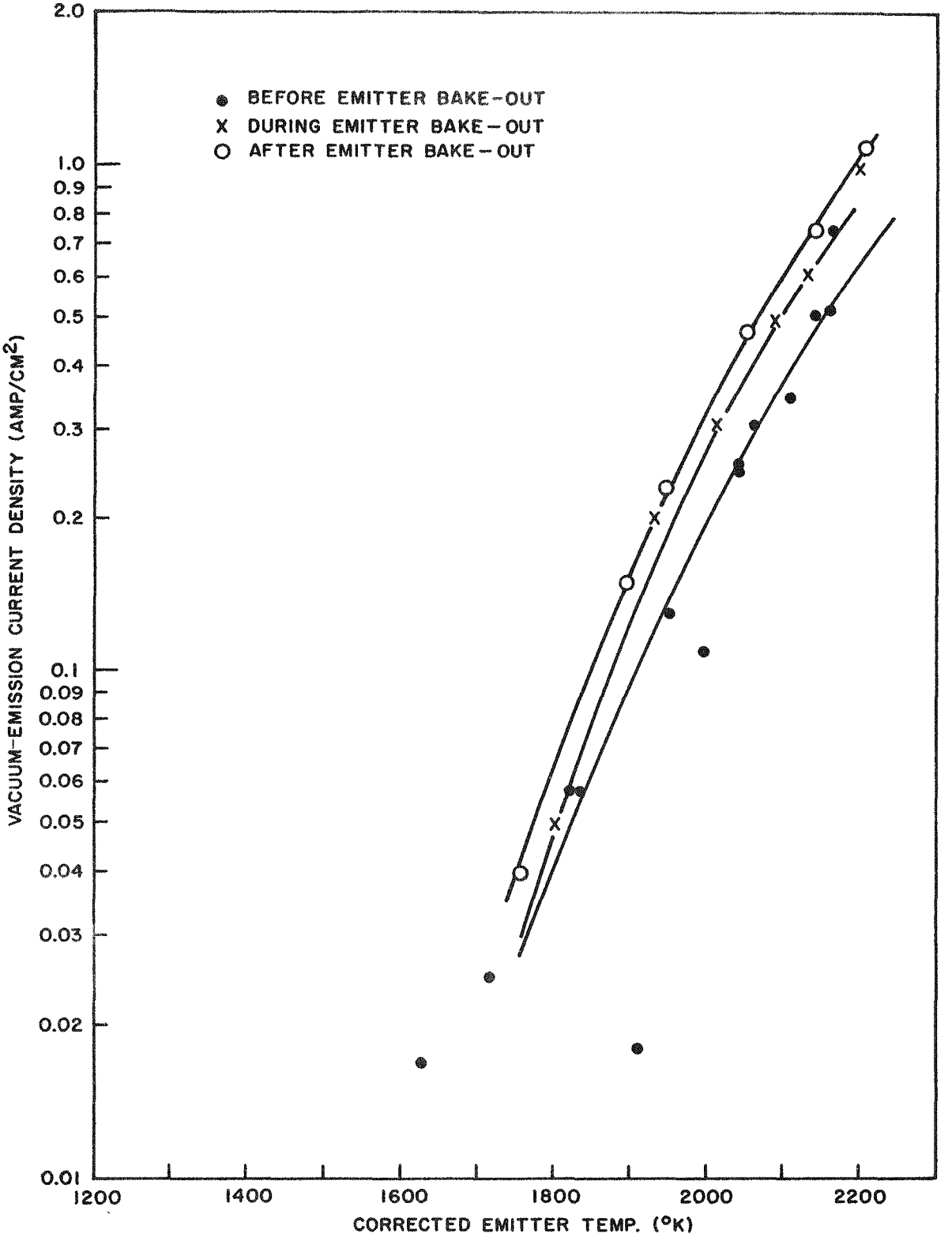

Fig. 12--Current density versus emitter temperature for emitter No. 39 (10UC-90ZrC)

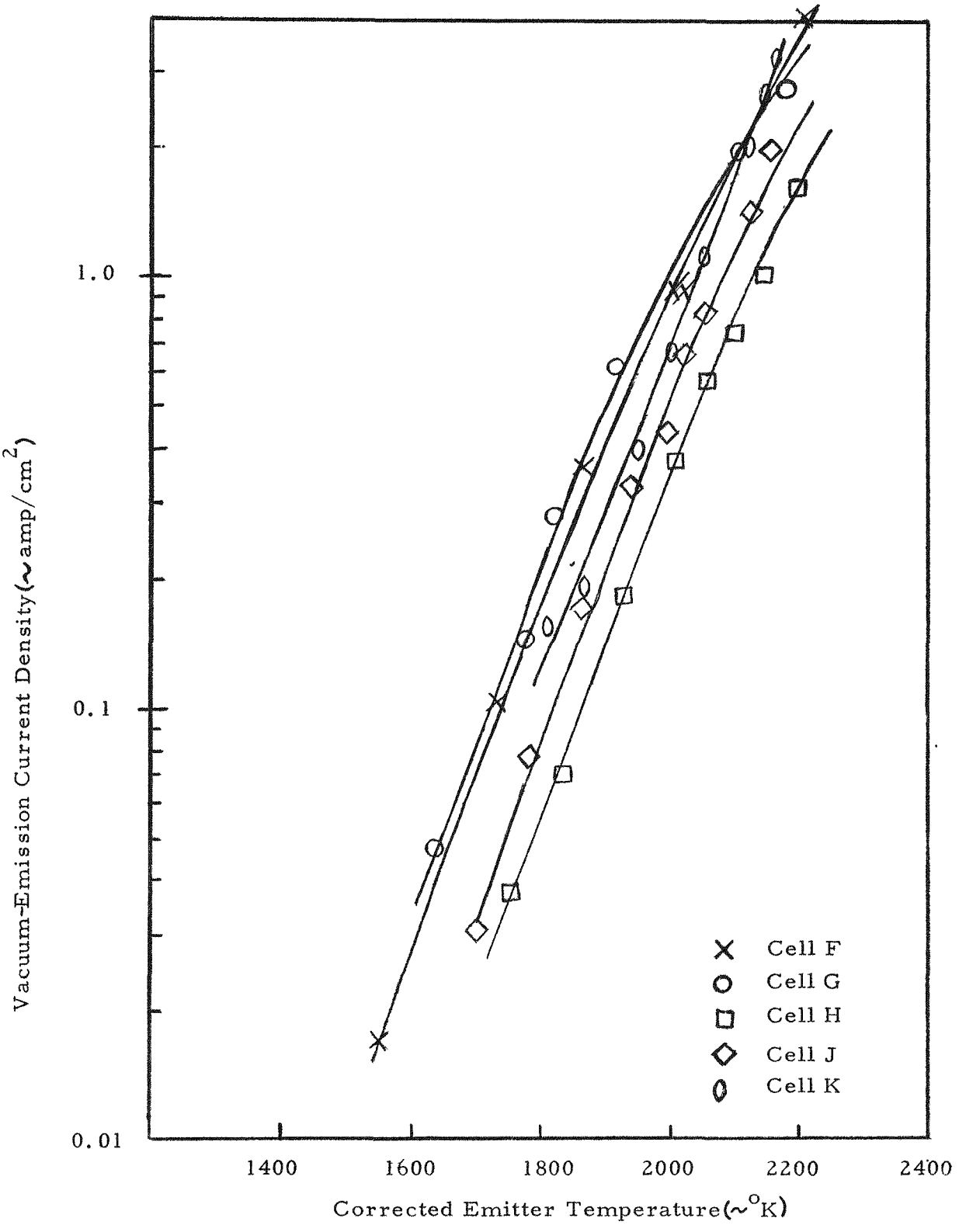

Fig. 13--Current density versus emitter temperature for Cells F through K

is shown in Fig. 14. The resulting current-voltage plot was displayed on an oscilloscope and recorded with a Polaroid camera (Fig. 15). The hysteresis in the curve has not been explained. The lower curve usually corresponded to steady-state data. The dot is the origin of the axes. Because the entire current trace was instantaneously presented as a function of cell voltage, it afforded a revealing insight to cell operation. A flat current-voltage curve with the classical knee at a potential of about 1.2 volts indicated low cesium pressure, while very low current indicated a lack of cesium plasma (Fig. 15). Maximum power output for given emitter and cesium-well temperatures was easily computed by calculating the power at various cell voltages. To obtain these traces, only the cell voltage was varied by means of the external sweep. The assumption was made that during the short period of sweeping the cells, all parameters including the emitter temperature remained constant. This assumption, however, was not entirely correct. This method, though expedient, lacked the accuracy achievable with steady-state measurements. It must be kept in mind that these cells were designed for life-testing, so little emphasis was placed on obtaining precise physics data.

After obtaining a trace, one parameter--usually the emitter temperature--was changed and another data point was recorded.

During long-term, steady-state operation, the cell output was switched over to a resistor (Fig. 16) which was adjusted to obtain the maximum power output for the given operating conditions. Occasionally, the second method was used to study the effect of cesium pressure or collector temperature. With the steady-state method, the voltage was read on a voltmeter with 0.02-volt divisions and the current was read as a millivolt output across a 50-amp (50 mv) precision shunt.

EMITTER-TEMPERATURE EFFECT

The emitter-temperature data were predominantly taken in the following manner. The cesium-well temperature and the emitter temperature

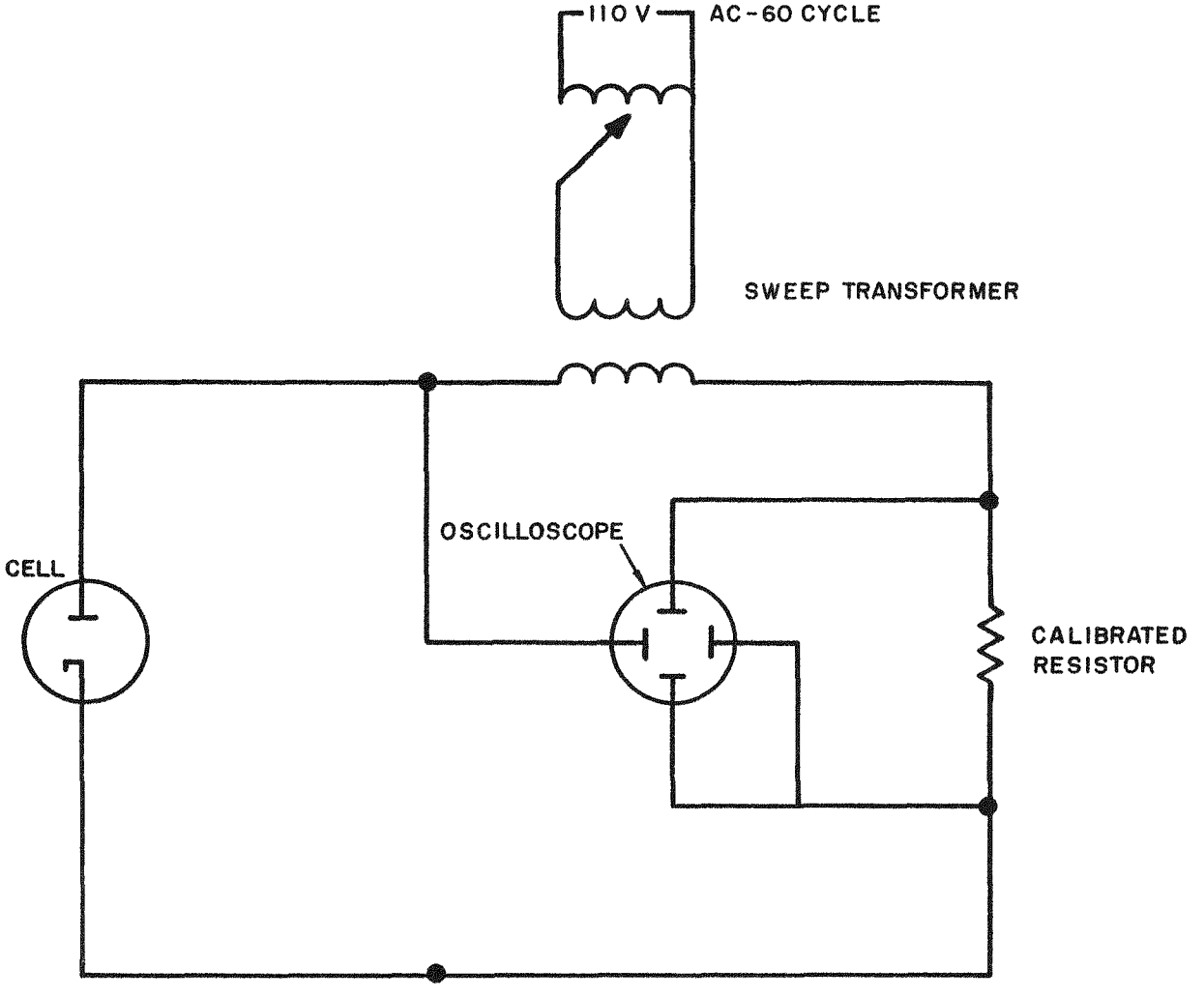

Fig. 14--Circuitry for dynamic data-taking

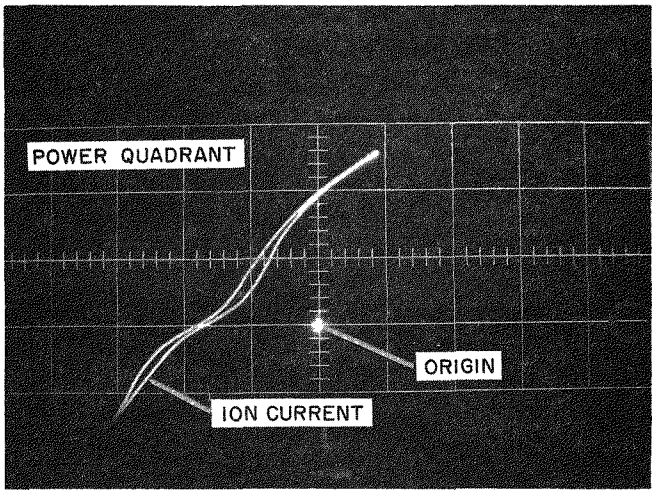

(a) CURRENT - VOLTAGE TRACE AT NORMAL OPERATION
ABSCISSA: 1 VOLT/DIV; ORDINATE: 40 AMP/DIV.
EMITTER TEMPERATURE: 2195°K; COLLECTOR TEMPERATURE: 888°K
CESIUM - WELL TEMPERATURE: 617°K
NOTE LARGE ION CURRENT.

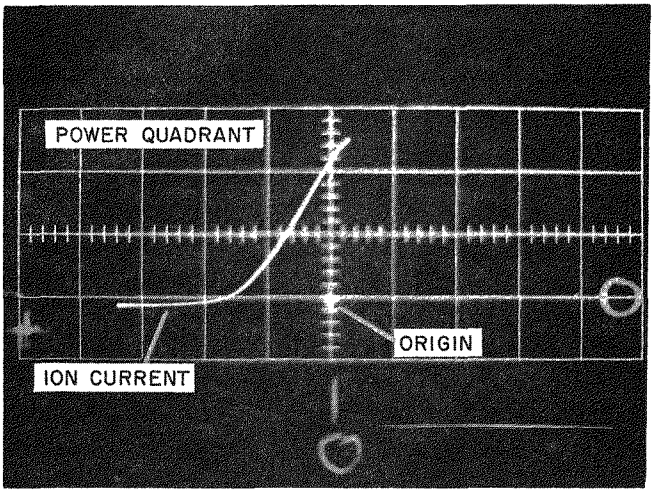

(b) CURRENT-VOLTAGE TRACE WITH LACK OF CESIUM PLASMA
ABSCISSA: 1 VOLT/DIV; ORDINATE: 20 AMP/DIV
MAXIMUM POWER OUTPUT: 9.8 WATTS.
EMITTER TEMPERATURE: 2265°K; COLLECTOR TEMPERATURE: 1183°K
CESIUM - WELL TEMPERATURE: 623°K
NOTE LACK OF ION CURRENT AND LOW POWER OUTPUT.

Fig. 15--Current-voltage trace (a) at normal operation and (b) with lack of cesium plasma

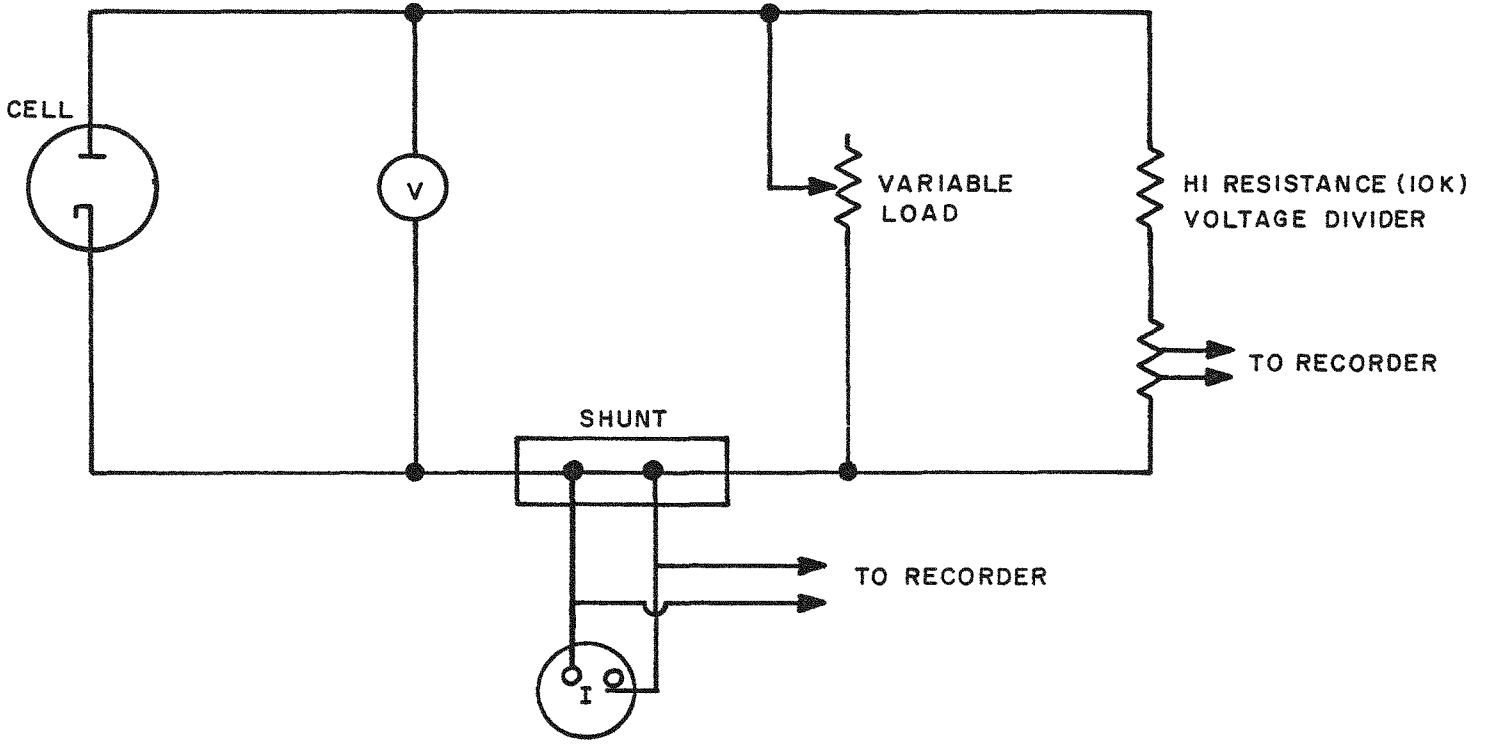

Fig. 16--Circuitry for steady-state data

were adjusted to a desired value. After equilibrium had been reached, a current-voltage trace was recorded. Then the emitter temperature was changed and another current-voltage trace was recorded. The emitter-temperature range from 1900° to 2200°K was investigated in 5 to 7 steps, with 3 to 8 min being allowed at each step for equilibration of all parameters. From each current-voltage curve the maximum power was computed. The power output was plotted as a function of emitter temperature for all cells tested (Fig. 17). It is noted that the power was an exponential function of the emitter temperature, which emphasizes the significance of an accurate emitter-temperature measurement. Some of the differences between cells were attributed to different average surface temperatures. The reason for the low output of Cell E is not fully known. It is believed, however, that the emitter surface was contaminated and that the bakeout and outgassing procedures for the emitter and the cell were inadequate.

CESIUM-TEMPERATURE EFFECT

In Cell E, the tubing connecting the cesium well to the cell was long and had a small cross-sectional area. In addition, the long tubing to the high-temperature valve produced thermal lags so that cesium-pressure equilibrium was not reached for hours. Therefore, data were taken at fixed cesium pressures over the whole emitter-temperature range. After a cesium-pressure change, several hours (preferably 16 to 20) were allowed for equilibration. With the improved cell design, equilibrium was achieved within minutes and cesium-pressure effects could be studied more expeditiously and effectively. With the exception of the last two cells, data were taken at a fixed cesium pressure over a wide emitter-temperature range before changing to another cesium-well temperature. The maximum power output was plotted as a function of emitter temperature with cesium pressure as a parameter (Fig. 18). From this family of curves, the effect of cesium pressure was evaluated by cross-plotting the data at a fixed emitter temperature (Fig. 19).

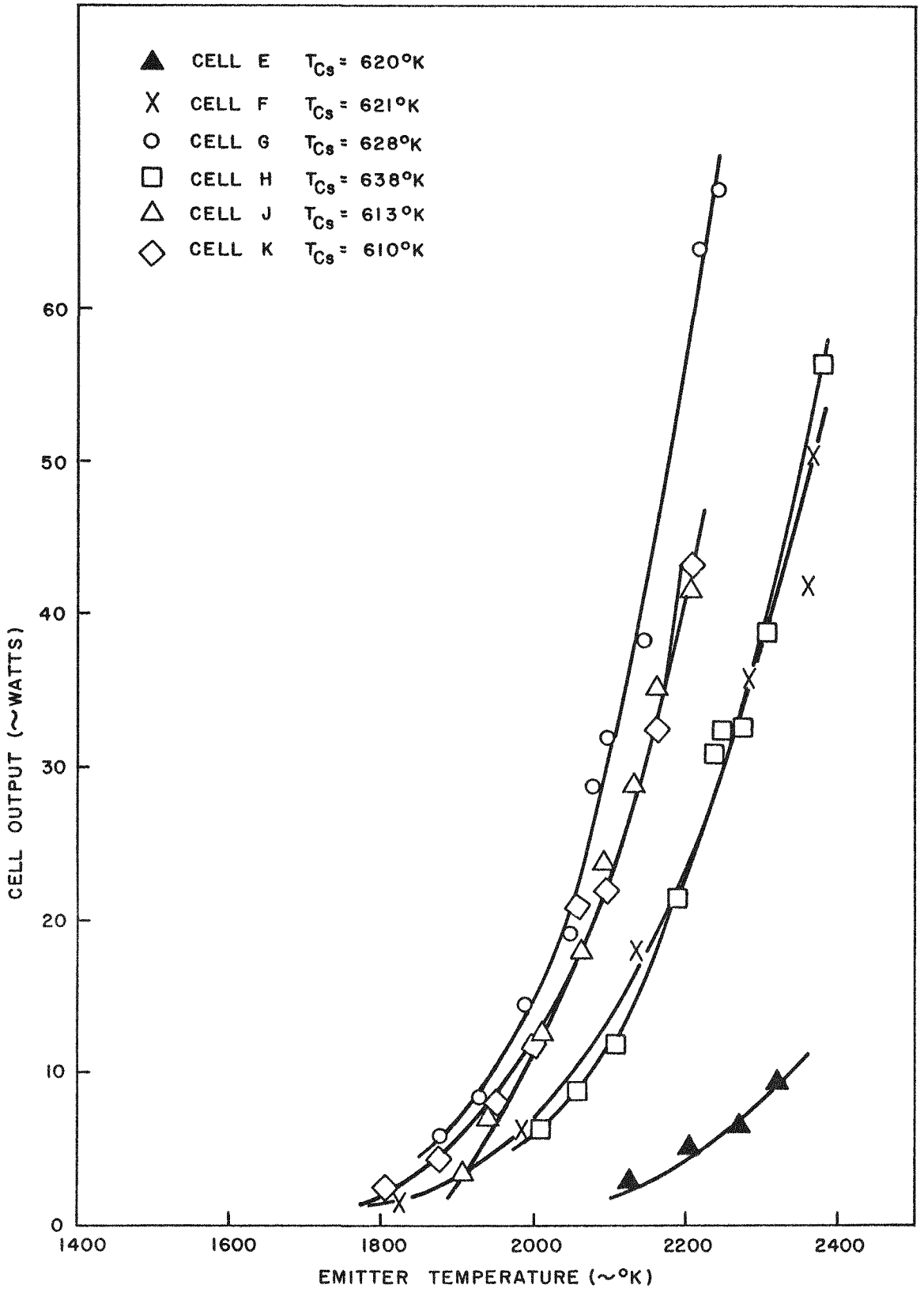

Fig. 17--Power output of Cells E through K as a function of emitter temperature

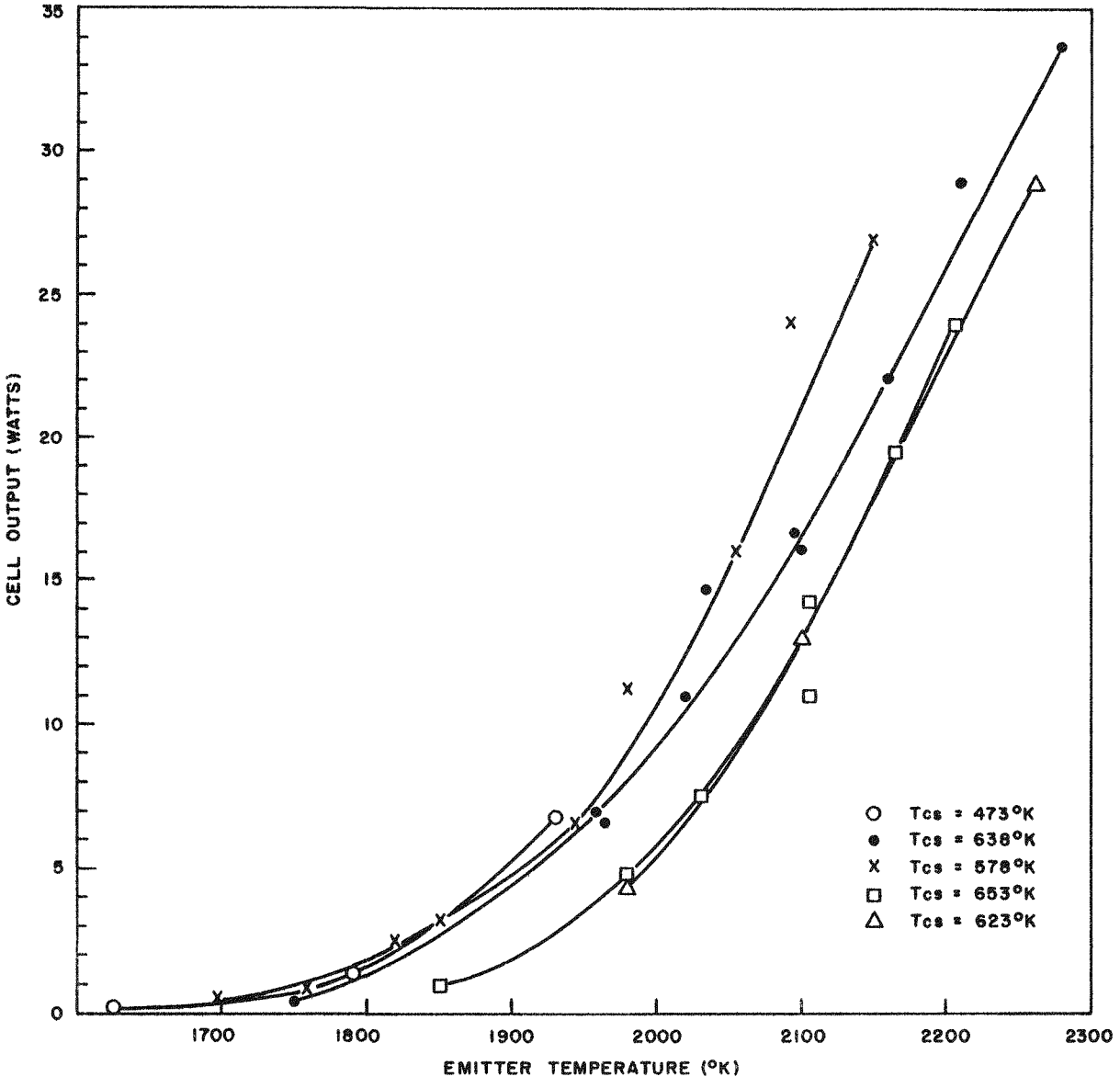

Fig. 18--Cell performance as a function of emitter temperature at several cesium temperatures

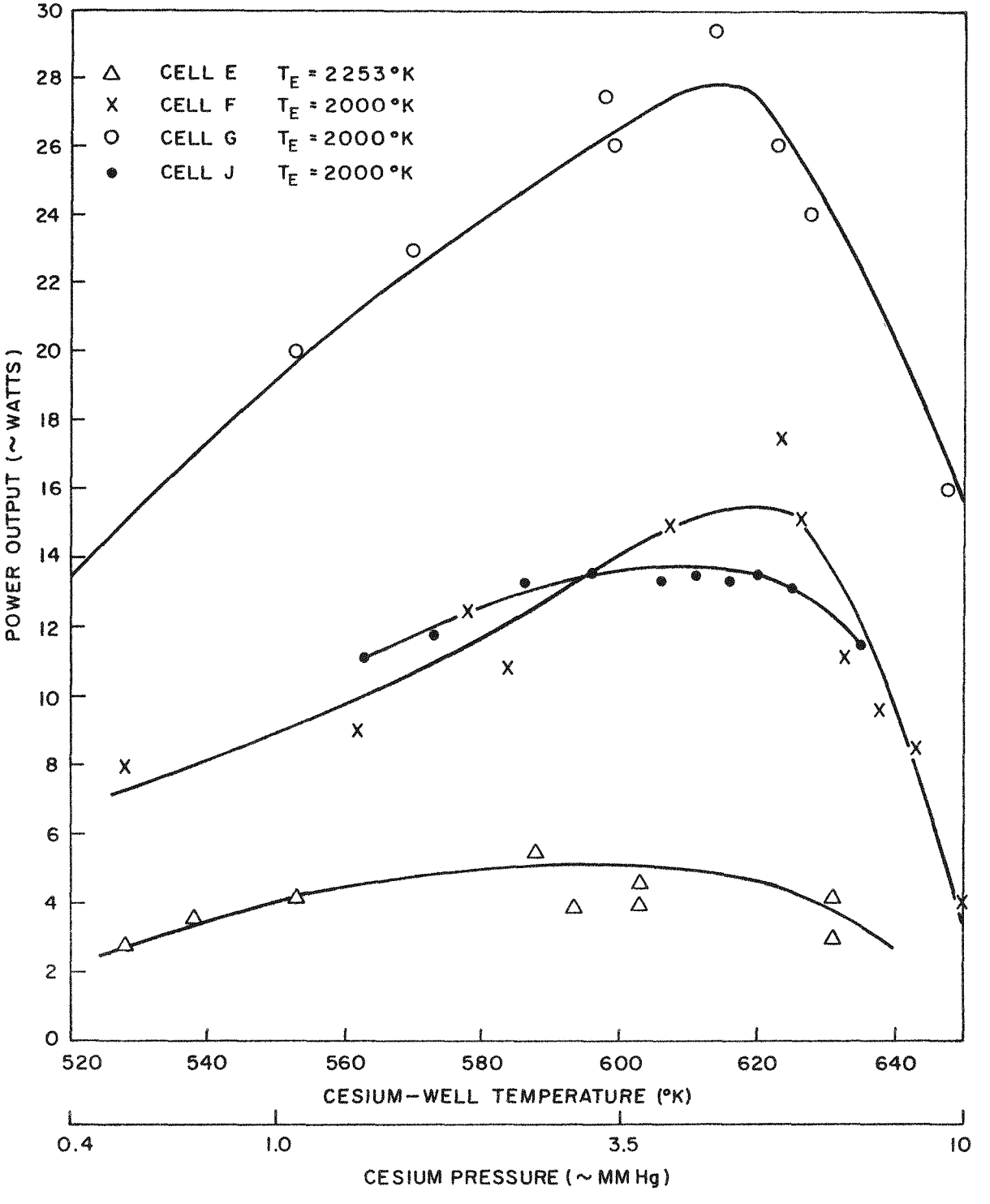

Fig. 19--Power output versus cesium-well temperature and pressure for Cells E, F, G, and J

The cesium-pressure effect was investigated in Cells E, F, G, and J from 0.04 to 9 mm Hg (from 460° to 640°K). There was a gradual increase in cell output with increasing well temperature up to 600°K, with a steep decrease in output at temperatures above 620°K. The data of Cell E were less conclusive. While there seems to be a peak at 590°K, the maximum power obtained from this cell was at a cesium-well temperature of 608°K. In subsequent cells, the pressure range investigated was narrowed to 1 mm to 10 mm Hg. Figure 20 shows the power output for Cell H at two emitter temperatures, 2012° and 2200°K, as a function of cesium-well temperature. The peak in cell output is very apparent at 637° ±4° and seems to occur at essentially the same cesium-well temperature for both emitter temperatures.

In Cells H and K, it was possible to maintain a fixed emitter temperature by means of a fine adjustment on the input voltage. The effect of cesium pressure was investigated by maintaining the cell voltage constant and recording the cell current at cesium pressures from 2.5 to 7 mm Hg (583° to 635°K). The optimum in this case appears at 608° ±2°K (Fig. 21). At lower cesium pressures insufficient ions were present for complete space-charge neutralization, while at pressures above 7 mm Hg (630°K) collisions with cesium atoms reduced the current flow.

SHORT-CIRCUIT CURRENT

To investigate the maximum current output from the cell, measurements were made with the external resistance reduced to a minimum. It was observed, however, that this operating condition was not stable enough to permit the taking of reliable data, primarily because of Peltier cooling of the emitter. More consistent results were obtained by reading the current from the trace on the scope at the intercept with the ordinate. Since the trace swept the whole voltage range in 1/120 sec, the assumption was made that the mass of the emitter was sufficient to maintain the emitter temperature nearly constant. The short-circuit current density is shown as a

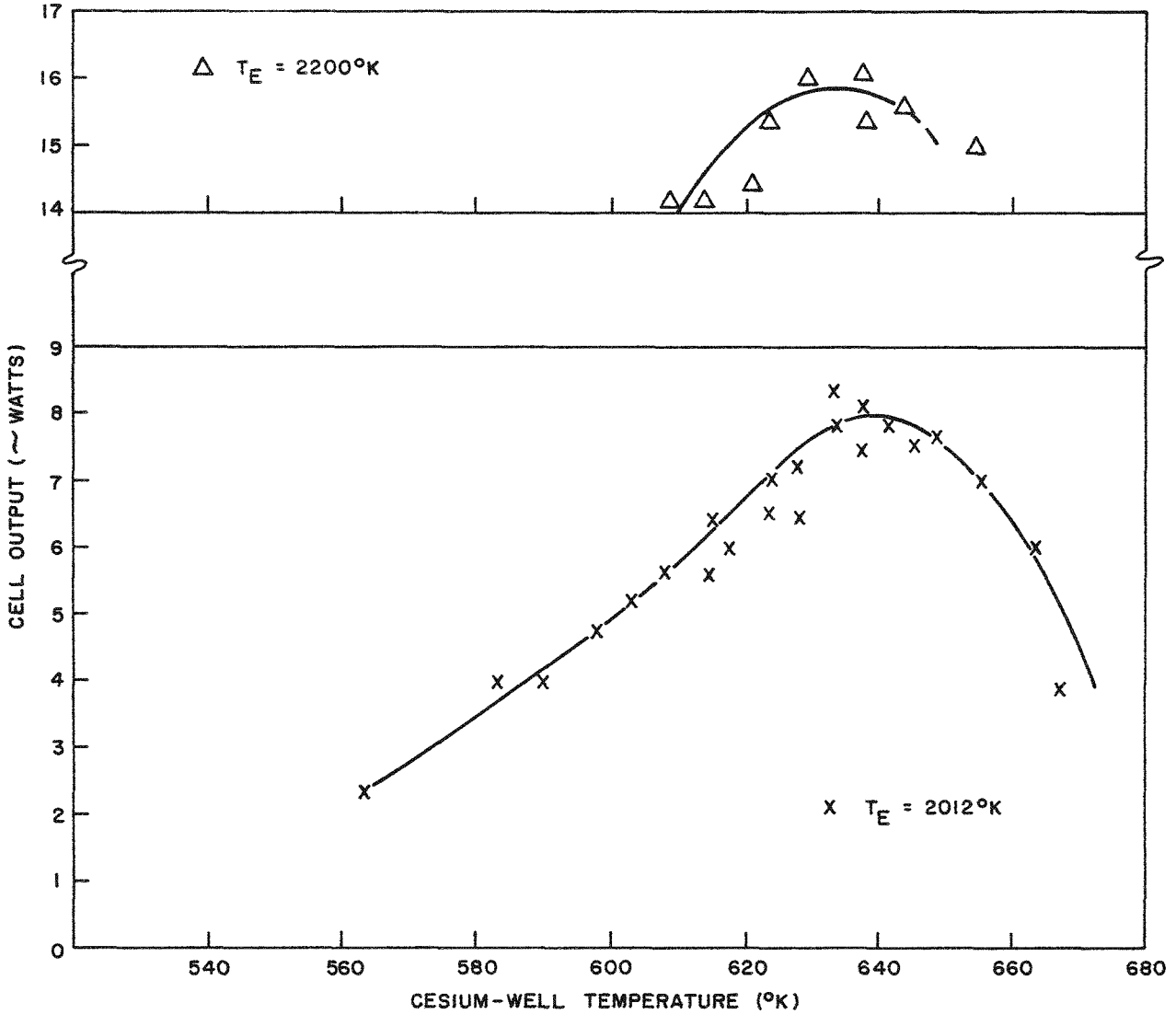

Fig. 20--Effect of cesium-well temperature on output of Cell H

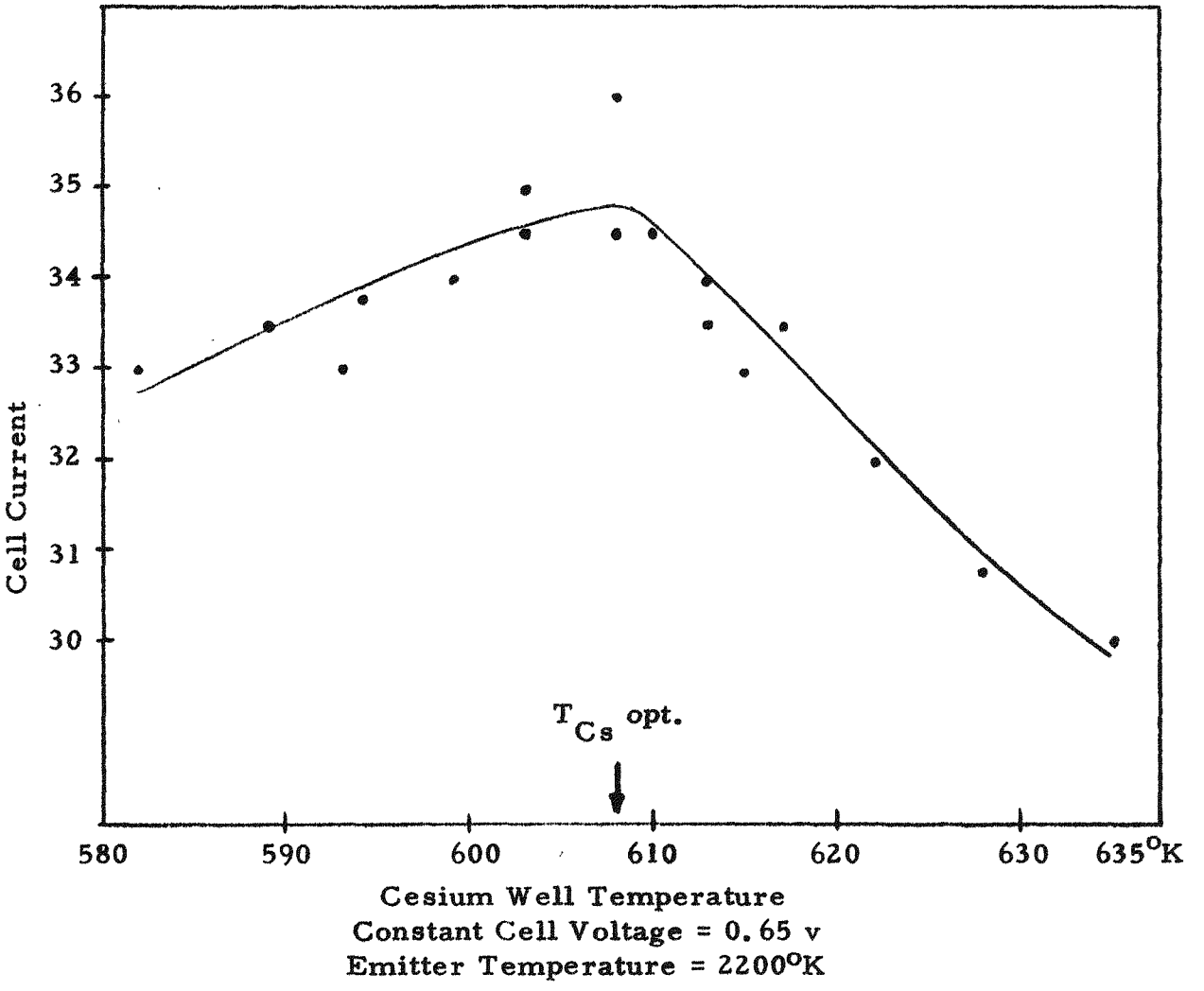

Fig. 21--Cell current versus cesium temperature of Cell K

function of emitter temperature in Figs. 22 and 23 for Cells G and J, respectively. The maximum current obtained from a cell in the presence of cesium exceeded the vacuum-emission current by a factor of 5 to 6. In Figs. 22 and 23 the vacuum-emission currents for the corresponding emitters are shown as a dashed line for comparison.

The scatter of the points in Figs. 22 and 23 somewhat obscured the fact that the short-circuit current for a given emitter temperature was a function of the cesium pressure. In Fig. 24, the relation of cesium pressure to short-circuit current is plotted for Cells G and J. It is apparent that the short-circuit current increased with increasing cesium-well temperature, and that the curve also has a maximum similar to that observed for power output (Fig. 19). A comparison of these three figures reveals, however, that the maximum of the current curve lies about 10° higher than that of the power curve, and that the decrease is much more gradual. This points to the fact that decrease in cell power at higher cesium pressure is due to factors other than the transport defects mentioned above.

Open-circuit Voltage

Since power is the product of current and voltage, cell voltage was investigated. The cell voltage measured with an infinite external resistance is referred to as the open-circuit voltage. The experimental values obtained from Cell G are shown as a function of cesium-well temperature in Fig. 25. Theoretically, this voltage is the difference between the effective emitter work function and the collector work function. A change of the wetting of either of the surfaces will affect their work functions. It is not readily seen why the cesium-pressure effect on cell voltage should be linear, as it appears to be in Fig. 25. An open-circuit voltage of 2 volts was recorded at 470°K, while at a cesium-well temperature of 650°K the voltage had dropped to 1.6 volts.

The cell voltage at maximum power output is also plotted in Fig. 25. At a cesium-well temperature of 470°K, the voltage is 1.3 volts and it decreases to 0.6 volt at 650°K. The two curves are nearly parallel. The

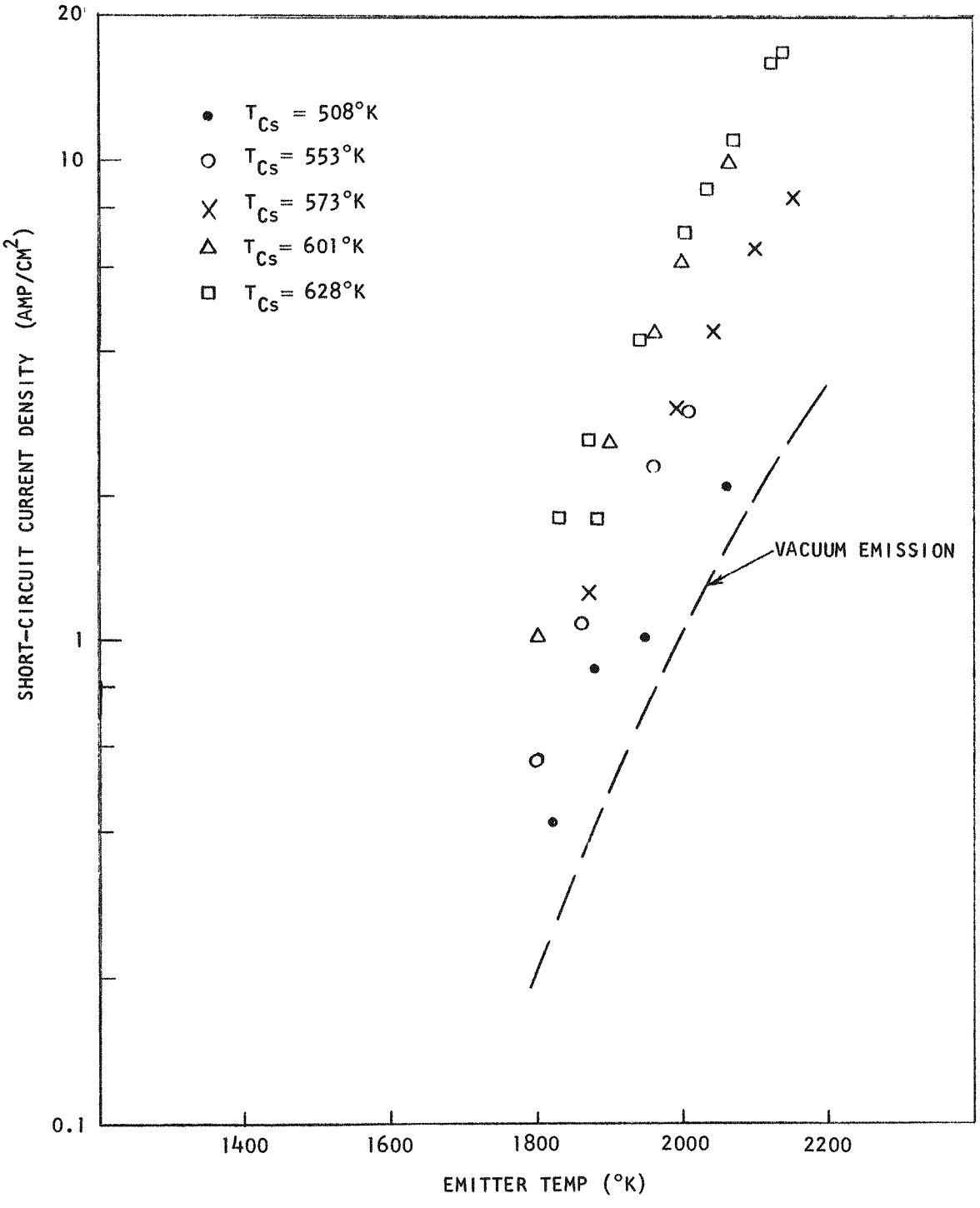

Fig. 22--Short-circuit current density of Cell G as a function of emitter temperature at various cesium temperatures

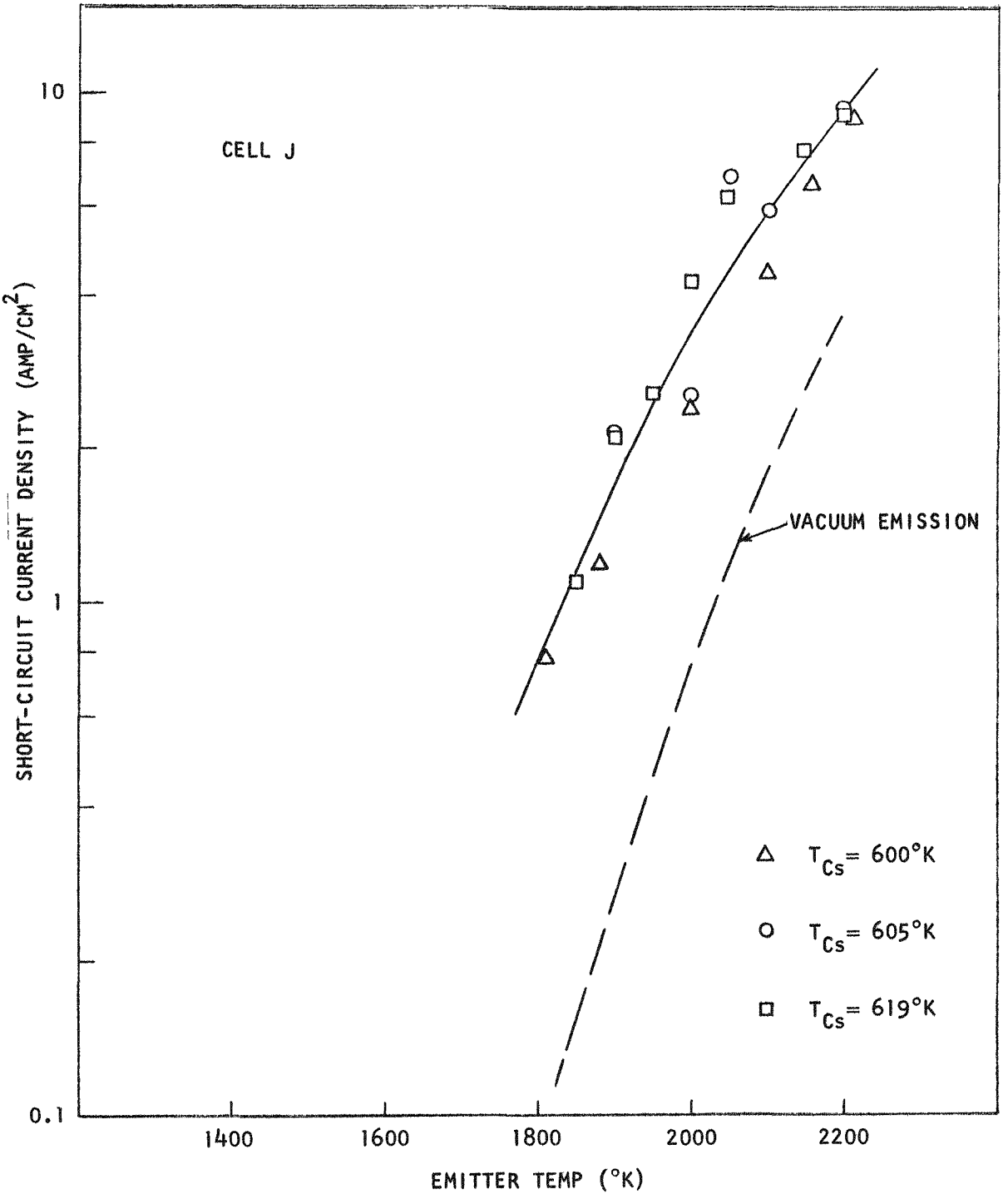

Fig. 23--Short-circuit current density of Cell J as a function of emitter temperature at various cesium temperatures

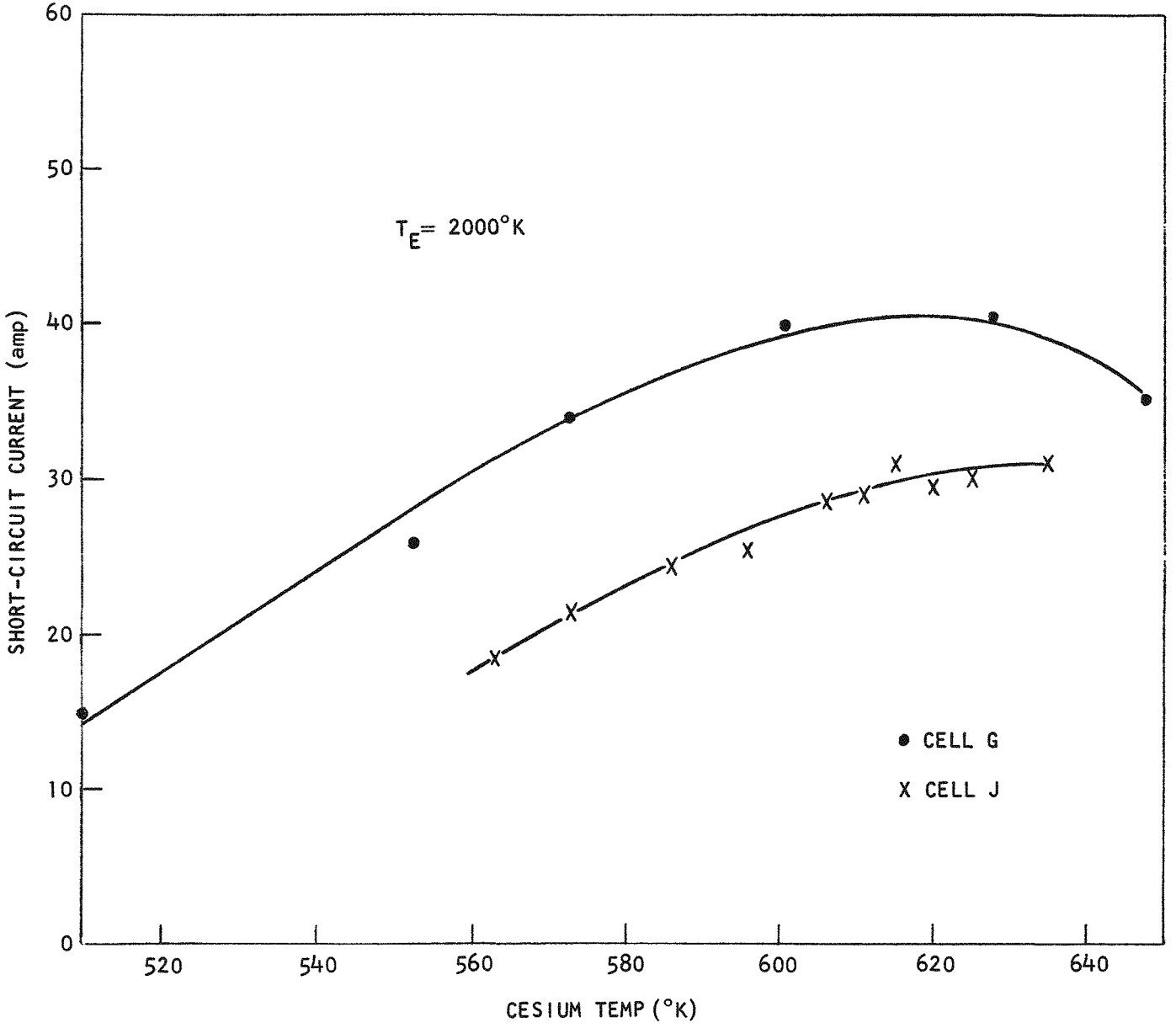

Fig. 24--Short-circuit currents of Cells G and J as a function of cesium-well temperature

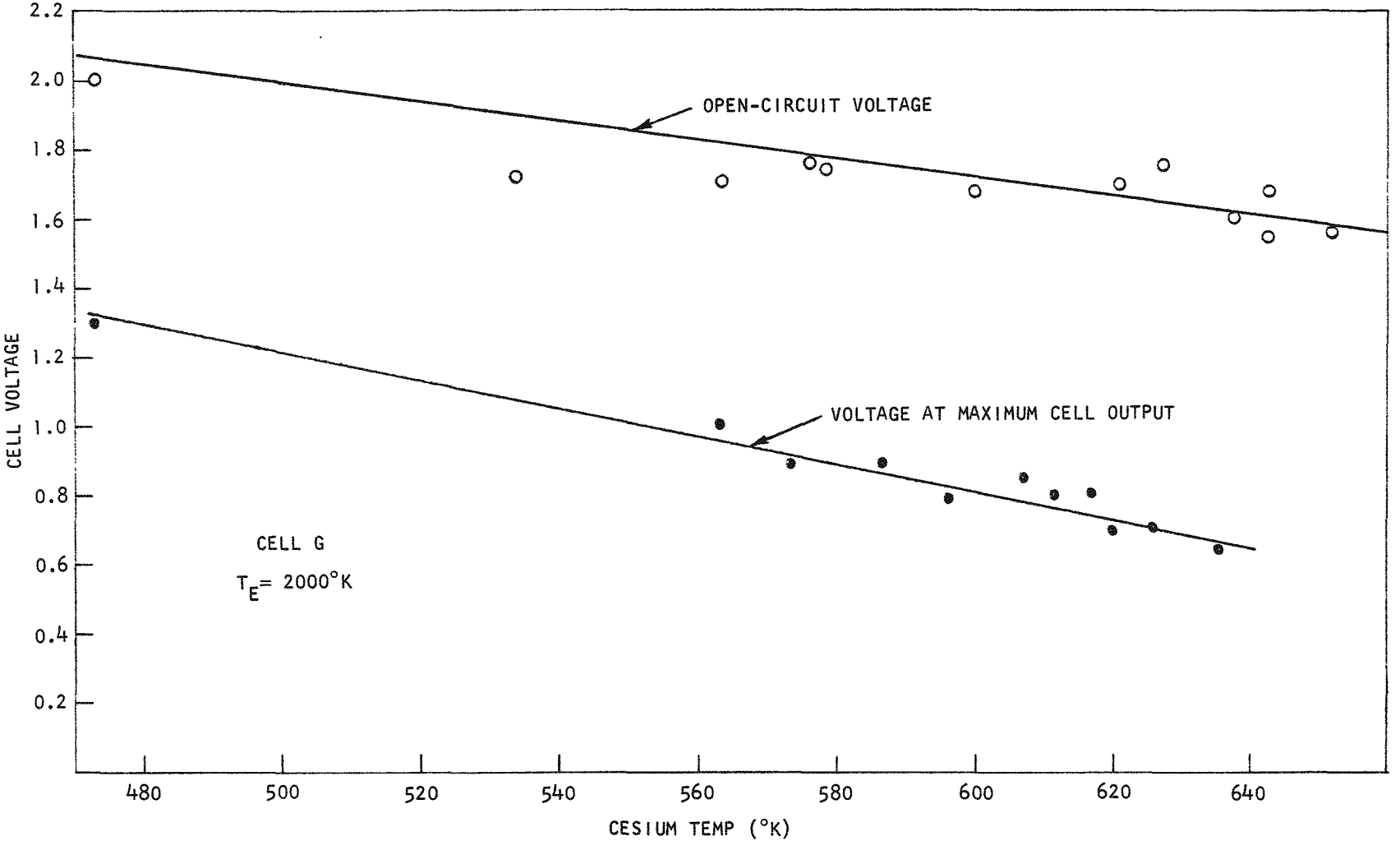

Fig. 25--Variation of cell voltage with cesium temperature

cell voltage for maximum cell power output at the optimum cesium pressure is between 0.7 and 0.8 volt, which is considerably less than the contact potential of the theoretical model. The open-circuit voltage is also dependent upon the emitter temperature, since it depends on emitter work function (Fig. 26). An increase from 1.75 at 1800°K to 2.05 at 2200°K was observed. The voltage at maximum power followed the same trend. A similar study was conducted on Cell K. When the collector temperature was held constant, a linear relation between voltage and emitter temperature was recorded (Fig. 27). Much lower open-circuit voltages were measured when the collector temperature was allowed to increase with increasing emitter temperature.

COLLECTOR-TEMPERATURE EFFECT

Since one objective of this program was cell operation at high collector temperature (~1000°K), little provision was made to achieve optimized collector temperatures, since this temperature might be well below 1000°K. Thus, the cooling provisions were inadequate and the collector temperature was primarily a function of the emitter temperature. Stopping collector coolant flow or supplying additional heat with the collector heater (Fig. 1) resulted in higher collector temperatures. The range over which collector temperature could be investigated was about 150°K. The results were not very conclusive. At an emitter temperature of 2000°K, the cell output was independent of collector temperature between 850° and 1040°K (Fig. 28). In Cell E, it appeared that an increased power output occurred at higher collector temperatures. In a study on Cell H, two operations, with and without collector coolant flow, were compared. The curve in Fig. 29 corresponding to the lower collector temperature (730° to 900°K) is about 20% higher than the curve for the higher collector temperature (900° to 980°K). In Cell K, the study of collector temperature again proved that a substantial increase in output was obtained at lower collector temperatures (Fig. 30). At 2200°K, the cell output increased from 21 to 41 watts when the collector

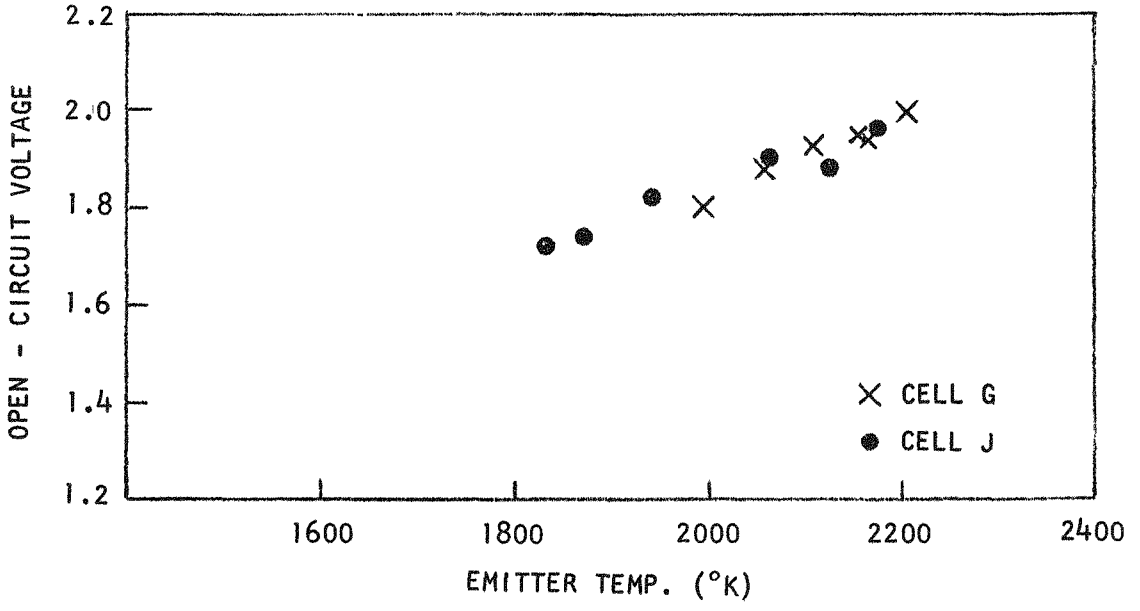

Fig. 26--Variation of open-circuit voltage of Cells G and J with emitter temperature

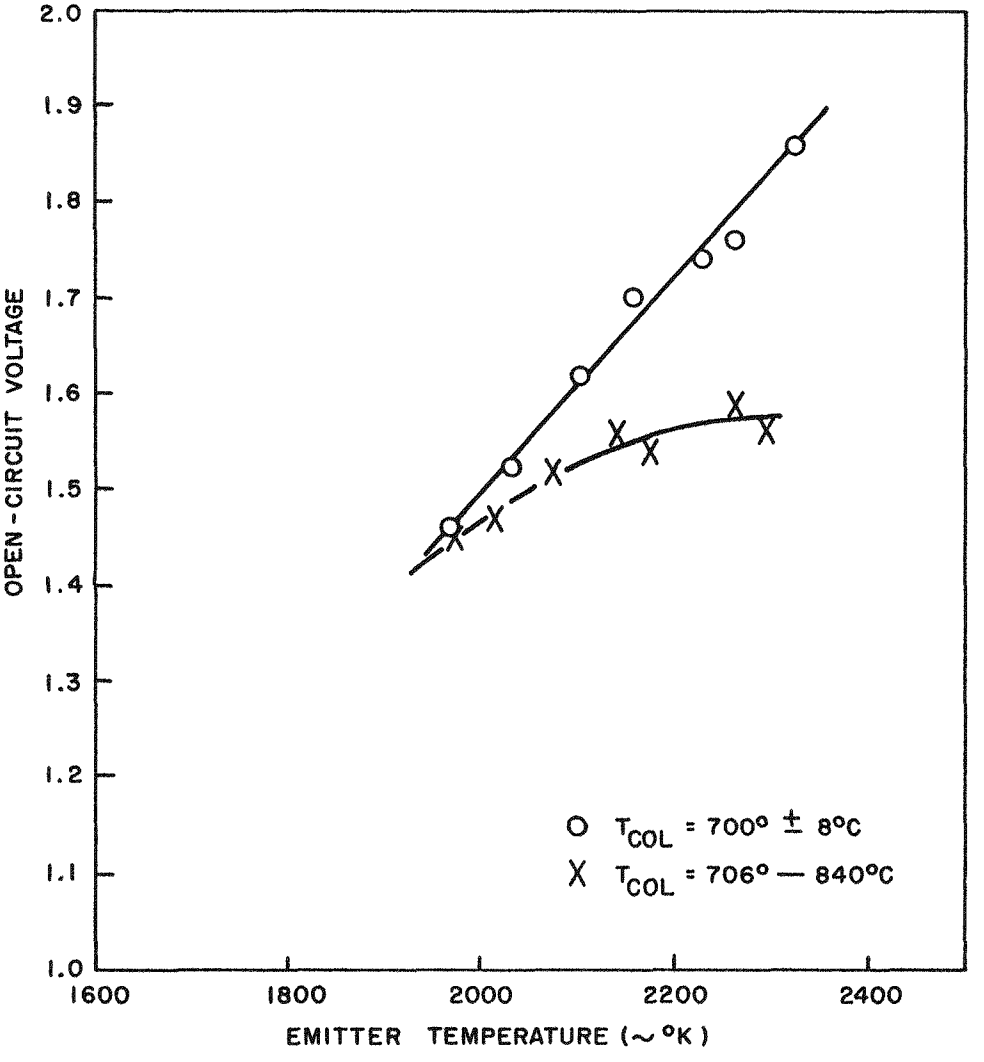

Fig. 27--Open-circuit voltage as a function of emitter temperature of Cell K

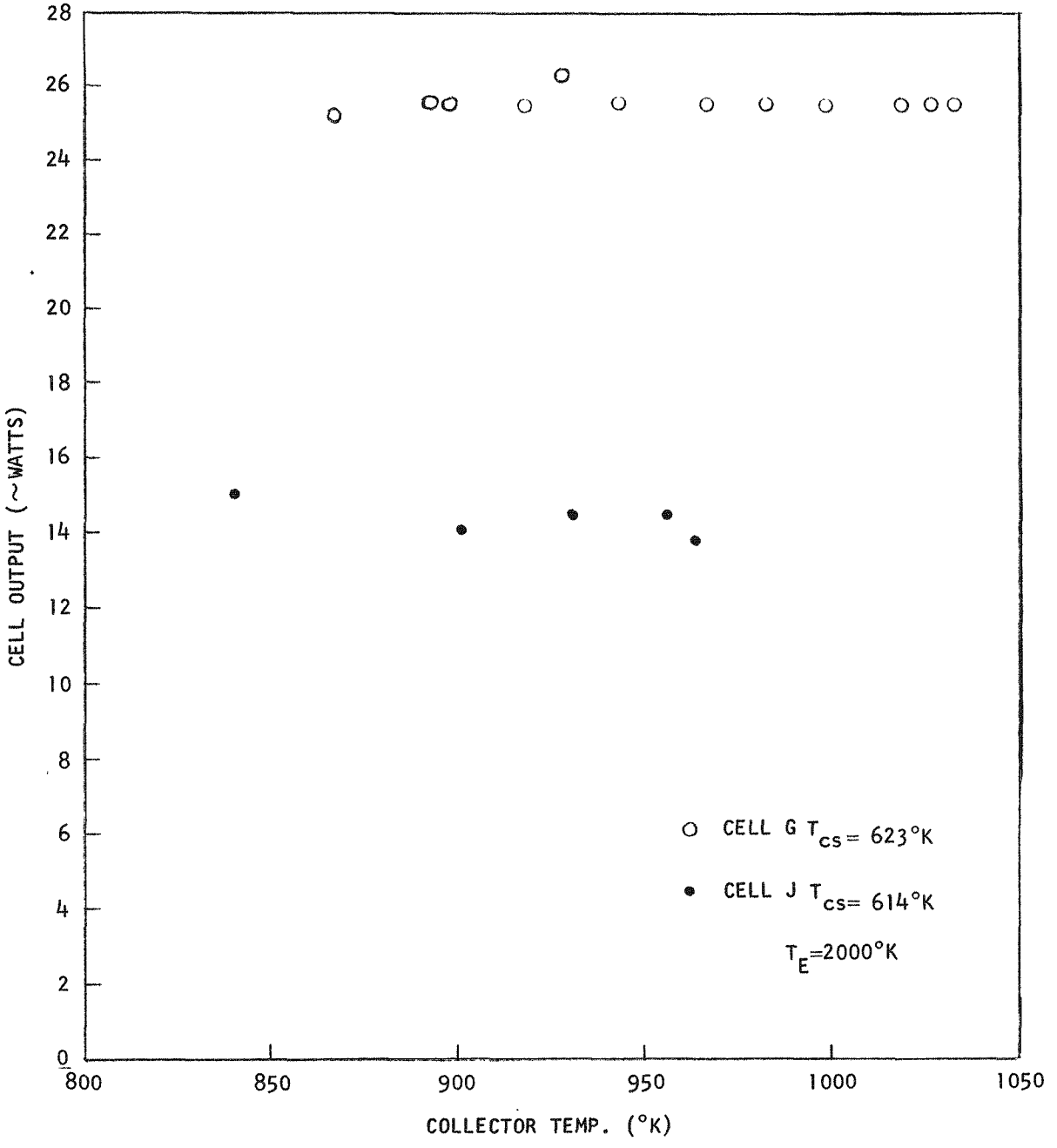

Fig. 28--Effect of collector temperature on power output of Cells G and J

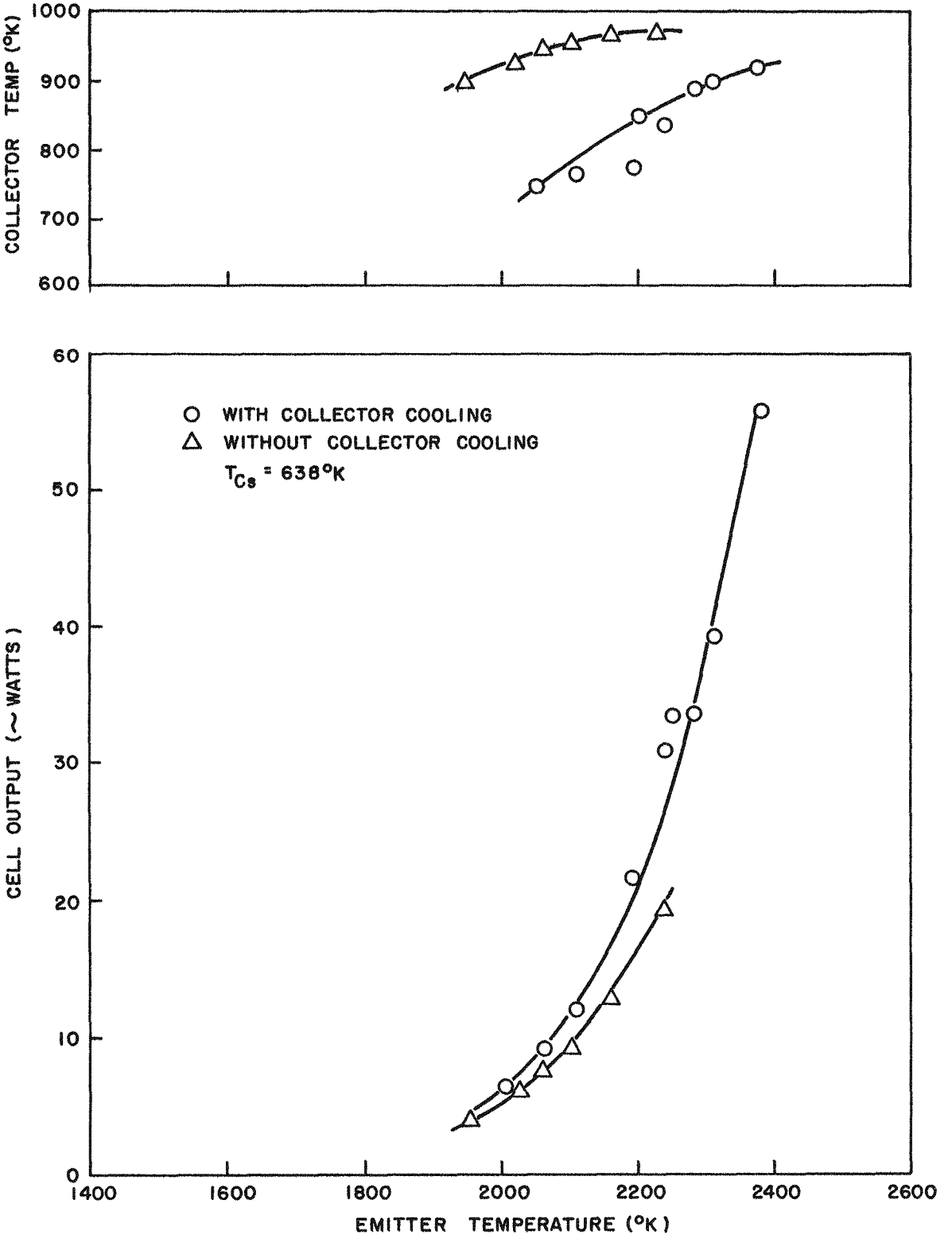

Fig. 29--Effect of collector cooling on power output and collector temperature of Cell H at various emitter temperatures

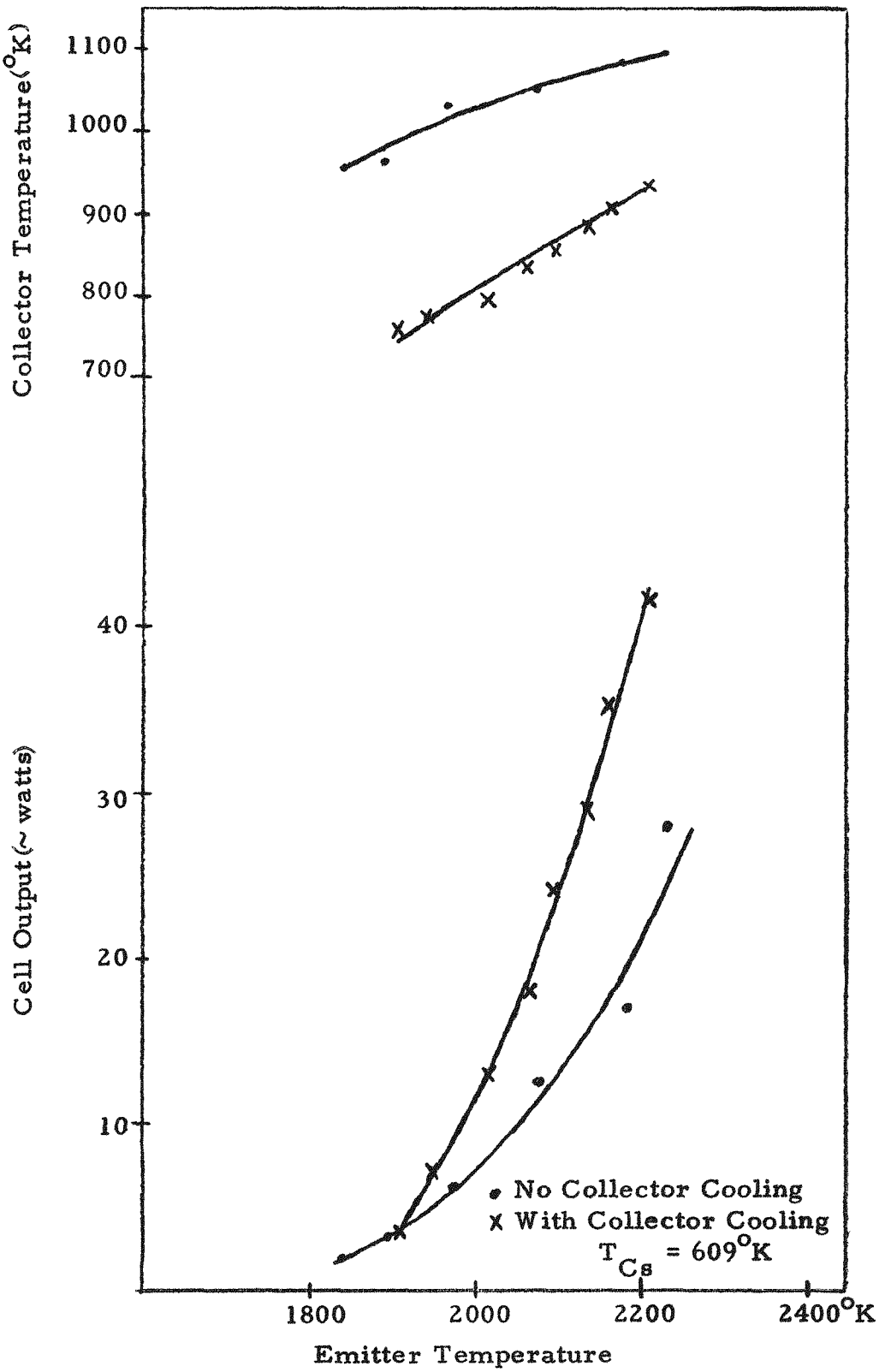

Fig. 30--Cell output and collector temperature versus emitter temperature

temperature decreased from 1090° to 923°K. At 1900°K, however, there was no increase in power for a 230°K drop in collector temperature.

The data obtained in this program have been inadequate to establish if an optimum collector temperature does exist for carbide emitters with nickel collectors. At low emitter temperatures, 1900° to 2000°K, there does not appear to be a noticeable effect of collector temperature on power output, but at an emitter temperature of 2200°K a substantial increase has been noted. This increase in power was due not only to a higher cell voltage but also to a higher cell current. While an increase in cell voltage may be attributed to a lower work function of the collector at lower collector temperature, the increased cell current is not so readily explained.

A subsequent collector-temperature study on Cell K at a fixed emitter temperature of 2300°K showed a time-dependent decrease in cell output as well as a collector-temperature effect. Preliminary to this study, the emitter temperature was decreased from 2300° to 1940°K, allowing the collector to cool to 826°K. Then the emitter was quickly increased to 2300°K, and a power output of 54 watts was recorded at a collector temperature of 873°K. With the emitter temperature held constant, the cell output was monitored as the collector temperature was increased to 992°K within 30 min (Fig. 31). At this point the output had dropped to 47.5 watts--a 12% decrease. A gradual but continuous decrease occurred over the next 6-1/2 hr until the power had degraded to 34.5 watts. The only change of any parameter was a 16°K increase in collector temperature. The output of 34.5 watts was the same as that observed before this study under the same conditions, while 54 watts was the highest output observed on Cell K. The first rapid degradation was primarily attributed to a change in work function of the collector. The slower change, which occurred at essentially constant collector temperature, was more complex. Similar time-dependent changes in output have been observed during this program, although they are not as well-documented as in the above case. A time-dependent change in vacuum-emission current was

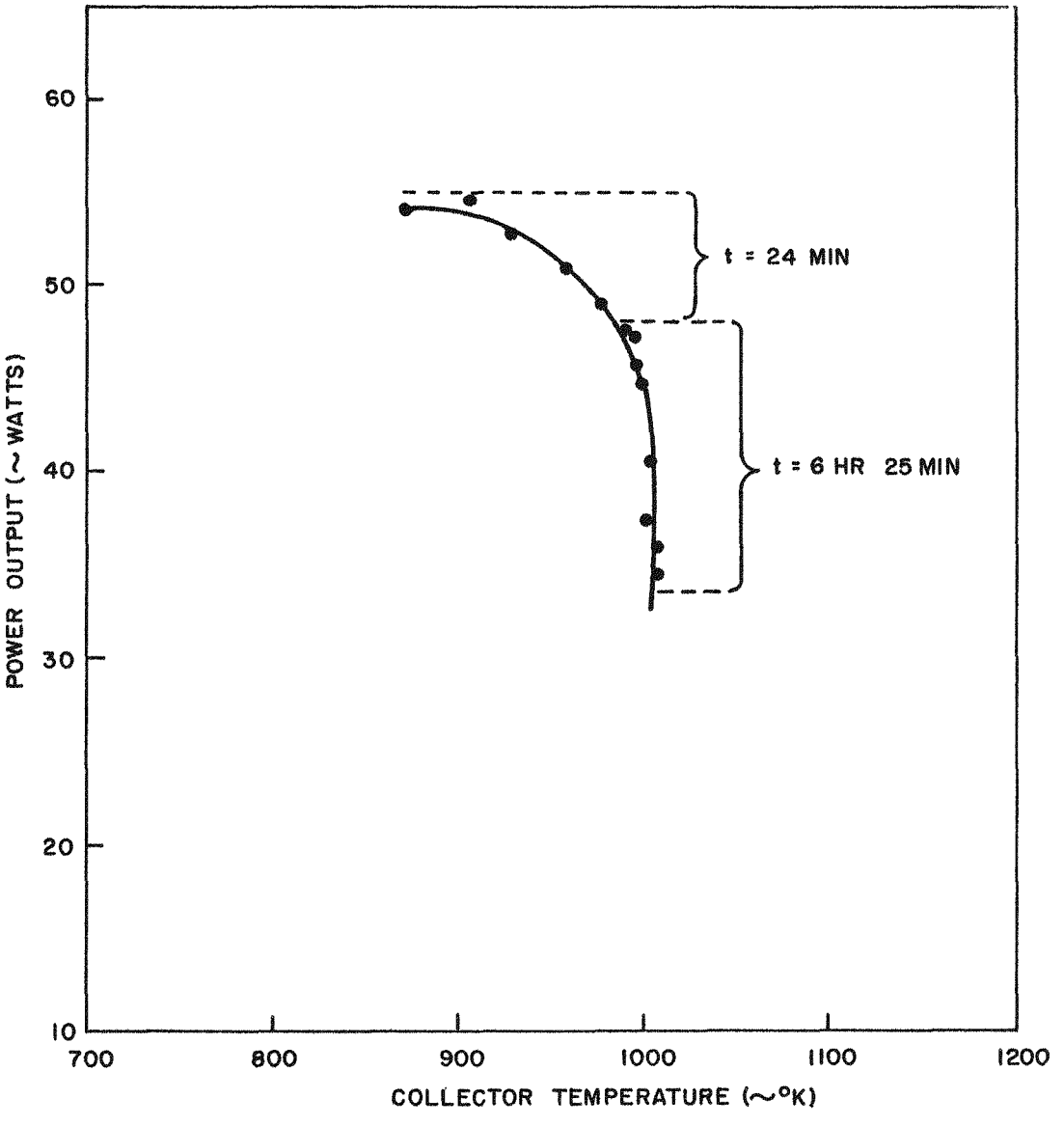

Fig. 31--Effect of time and collector temperature on power output of Cell K

also observed in related research.[3] It is postulated that surface depletion of uranium occurred owing to the evaporation that occurs when carbide emitters are operated above 2100°K; at temperatures below 1950°K, the rate of diffusion of the carbide to the surface exceeded the evaporation rate and additional uranium was available on the surface, which resulted in increased emission. The data available at this time are inadequate to prove or disprove this hypothesis. It may well be that changes in surface conditions such as those described above have contributed substantially to the scatter of the points observed during this program.

EFFECTIVE EMISSIVITY

A knowledge of the effective emissivity of a thermionic converter is important because heat losses by radiation may be computed if the emissivity is known and changes in surface conditions can be related to changes in emissivity. At a steady-state condition, and without current flow, it was assumed that the power input (p_{in}) was equal to the power loss due to radiation, $p_{in} = \sigma EAT^4$. Conduction losses down the emitter stem and convection through the plasma were considered negligible for the purpose of this analysis. Furthermore, it was assumed that the total electrical power input was dissipated in the emitter cavity, which meant that there were no lead losses. For blackbody radiation, E = 1 and $P_{BB} = \sigma AT^4$. For a given temperature, T, and an emitter area A = 12 cm^2, P_{BB} was computed. Equating the two terms for power and solving for the effective emissivity, E, gives $E = P_{in}/P_{BB}$. This emissivity is plotted in Fig. 32. While there was a considerable scatter of the points, there existed a definite decrease in emissivity with increasing emitter temperature. One explanation is that the conduction losses of the stem are a smaller portion of the total power input at higher emitter temperature than at lower temperature. The average emissivity of the diodes was found to be 0.55. This is lower than might be expected considering that the collector was coated with a heavy layer of carbide even after short periods of operation.

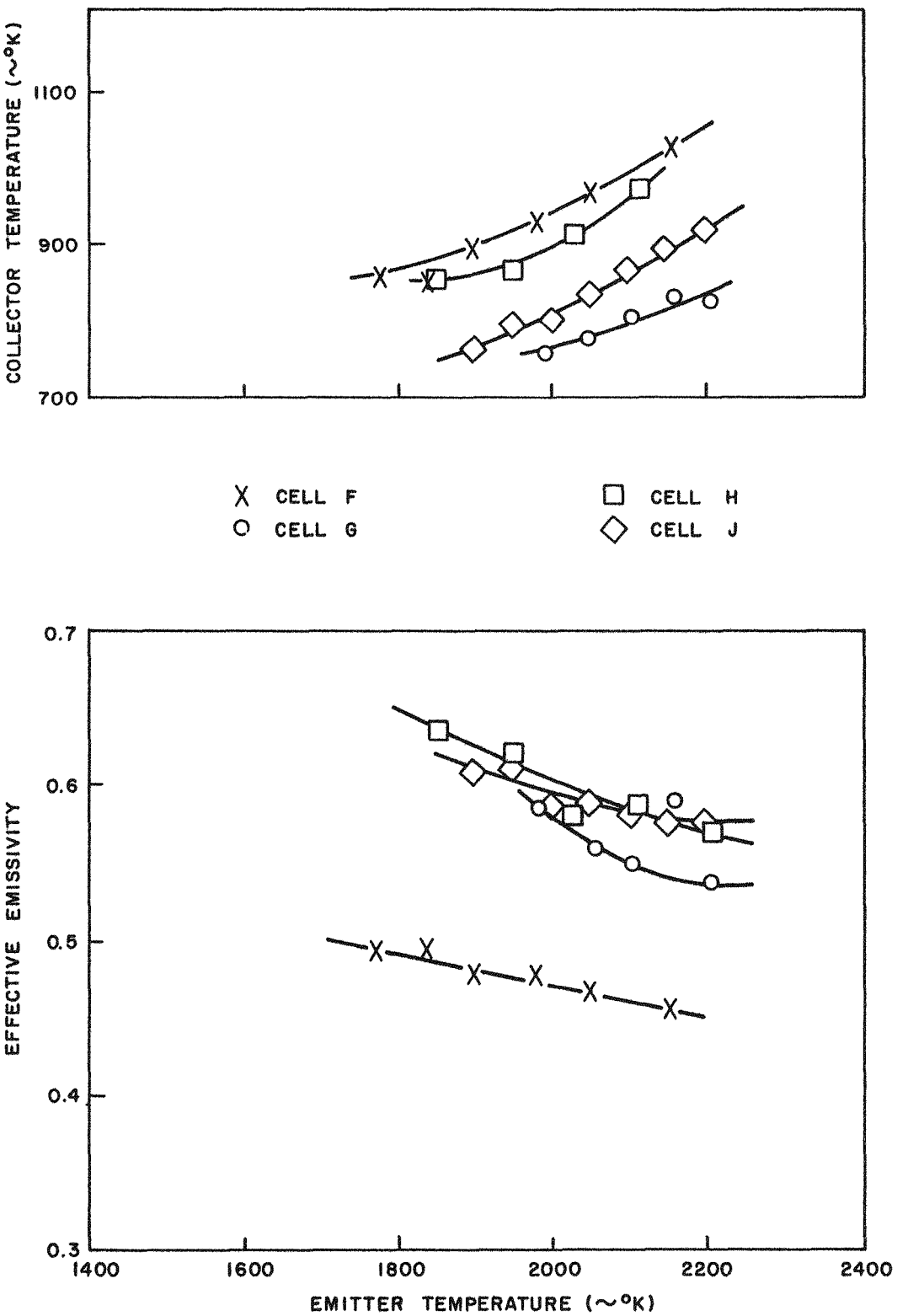

Fig. 32--Effective emissivity and collector temperature of Cells F, G, H, and J as a function of emitter temperature

The collector temperature obtained at the same time is also plotted in Fig. 32, but there does not seem to be a relation between the collector temperature and the emissivity, although the highest collector temperature resulted in the lowest emissivity curve. In Cell K, the emissivity was determined over the entire life test (Fig. 33). The highest emissivity (0.8) was observed at the start of operation. The emissivity decreased during the test to 0.55 and then increased again to 0.65 at 1900°K. One study was made at a constant collector temperature, but the trend of the curve did not differ from data taken when the collector was allowed to vary with emitter temperature.

CELL OPERATING EFFICIENCY

Throughout this research, the efficiency of the converter was determined by dividing the cell output by the electrical power input. Because the emitter temperature was a linear function of power input, while the cell output increased exponentially with emitter temperature, the efficiency of this device was highest at the highest emitter temperature. It must be noted at this time that the power output referred to here and throughout the entire report was computed from load voltages and not voltages measured at the cell terminals or at the emitter and collector proper. While heavy leads were used between the cell and the lugs external to the bell jar, small contact and lead losses of 0.002 ohm resistance could result in a 10% loss of power (at 40 amp), or a 10% decrease in efficiency.

The maximum efficiency of 6.2% was computed from sweep data for Cell F. Also, in Cell G a 6% efficiency for short operation was observed. During continuous operation of the cells at a reduced power output, the efficiency was as low as 1% for Cell E and as high as 4% for Cells J and K. The efficiency of the cells is given in Table 3.

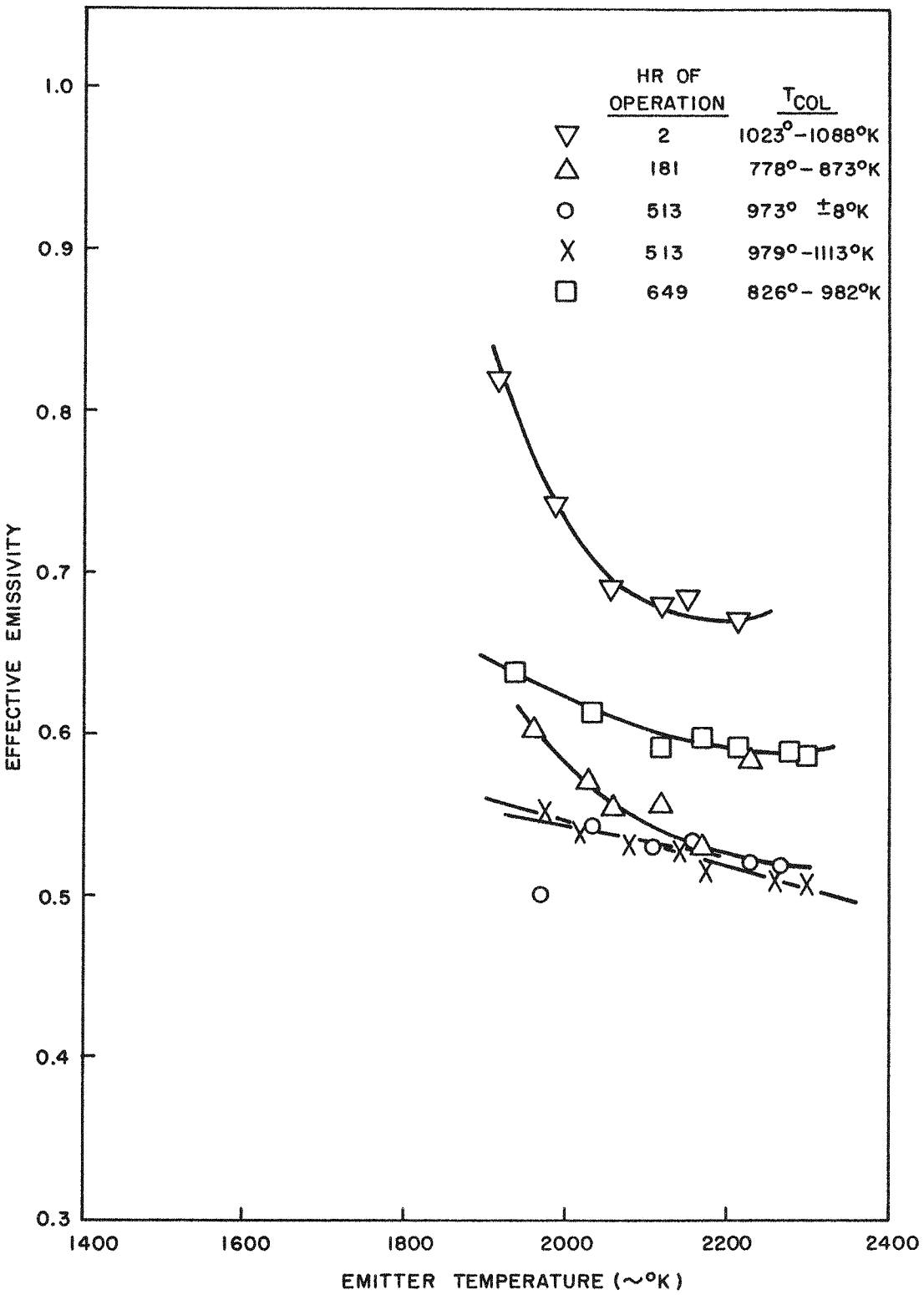

Fig. 33--Effective emissivity of Cell K as a function of emitter temperature with hours of operation and collector temperature as parameters

Table 3

OPERATING EFFICIENCY OF CELLS E THROUGH K
(In %)

	E	F	G	H	J	K
Maximum	2.2	6.2	6	4.3	5	4.2
Continuous operation	1	1-4.5	1.7-2.4	1.9-2.4	2-4	.3

VI. SERIES AND PARALLEL OPERATION OF CELLS

During the operation of Cells F, G, and J, the electrical output of two cells was connected either in series or in parallel. These studies were conducted under a variety of load conditions and with independently variable emitter temperatures in the two cells. The data obtained from Cells G and F are presented in Table 4. Because of the very low power output of Cell F, the information was not conclusive.

When Cells J and G were operating simultaneously, network studies were again conducted. The electrical circuitry used for these measurements is shown in Fig. 34. Since the two cells were completely independent of each other, except for the electrical connection, no interaction between the cells was observed. The data obtained are shown in Tables 5 and 6. The results agree with the principle of current conservation within experimental accuracy. Circuit-voltage conditions under parallel operation are consistent with lead resistances of 0.011 ±0.001 ohm in series with each cell. Current and voltage data for series operation are consistent with a circuit resistance of 0.006 ±0.002 ohm in addition to the variable-load resistance.

POST-TEST ANALYSIS

Upon completion of the life test, each converter was subjected to an extensive post-test analysis to determine the cause of failure and establish the condition of the individual components. The analysis covered the following major areas of investigation:

1. Leak-check of cell envelope.
2. Thermocouple recalibration and evaluation.
3. Vacuum-emission study of the emitter.
4. Chemical analysis of the emitter and collector.
5. Metallurgical analysis of the emitter, collector, and insulator.

Table 4

SERIES AND PARALLEL OPERATION OF CELL F AND CELL G

Cell F and Cell G in Parallel
(for various load resistances)

Cell F		Cell G		Total		Remarks
V (volts)	I (amp)	V (volts)	I (amp)	V (volts)	I (amp)	
0.85	3.2	0.95	7	0.84	9.5	
0.75	3.9	0.89	8	0.73	12.5	
0.62	6	0.75	10	0.58	16.5	
0.9	2.7	1.25	20	0.84	24	Increased emitter temp. of Cell G
0.47	9.9	0.87	22	0.40	34	

Cells F and G in Series

Cell F		Cell G		Total		Remarks
V (volts)	I (amp)	V (volts)	I (amp)	V (volts)	I (amp)	
0.6	8	0.3	8	0.74	8.2	
0.24	15	1.42	14.6	1.34	15	Increased emitter temp. of Cell G

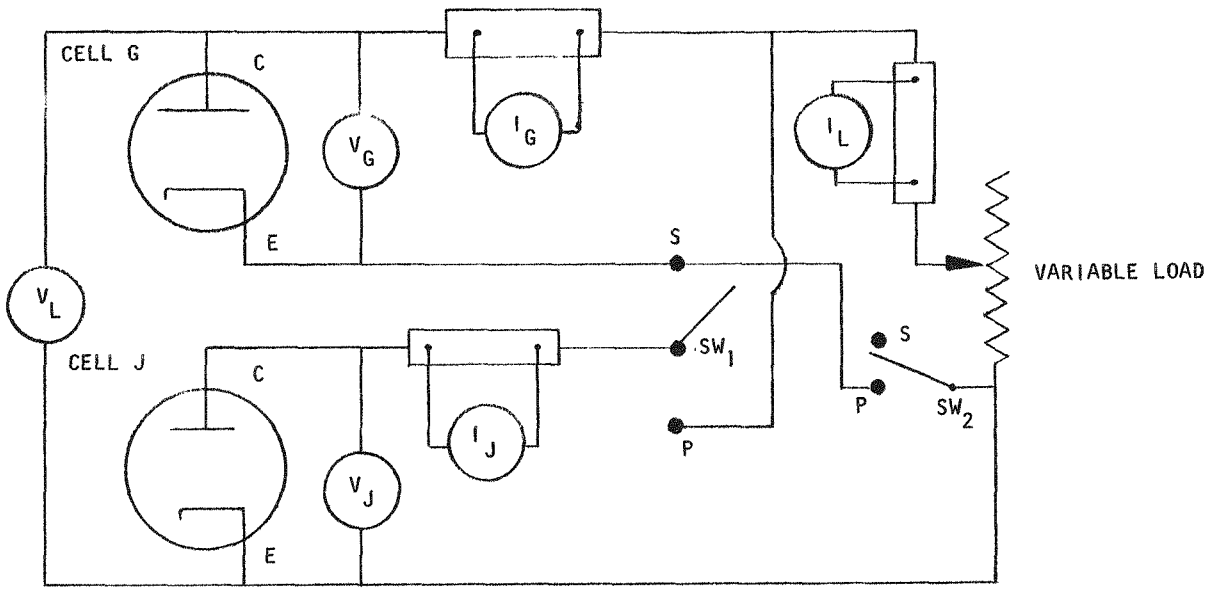

V = VOLTAGE

I = CURRENT

E = EMITTER

C = COLLECTOR

S = SERIES CONNECTION

P = PARALLEL CONNECTION

SW = SWITCH

SUBSCRIPT

G = CELL G

J = CELL J

L = LOAD

Fig. 34--Circuit to measure operation of Cells G and J in series and parallel

Table 5

PARALLEL OPERATION OF CELLS G AND J

(Cesium Temperature - 618°K)

CELL G			CELL J			LOAD		
Emitter Temp. (°K)	Cell Voltage (V_G)	Cell Current (I_G)	Emitter Temp. (°K)	Cell Voltage (V_J)	Cell Current (I_G)	Voltage (V_L)	Current (I_L)	Power (watts)
2051	0.98	15	2010	0.95	12.5	0.81	27	21.9
2102	1.19	10.5	2022	1.17	9.2	1.08	19	20.5
2080	0.94	16	2005	0.91	13.5	0.76	29	22.1
Increased Cell G Emitter Temperature								
2146	1.05	19	2005	0.99	12	0.84	31	26
2120	0.8	25.5	2000	0.73	15.8	0.52	41	21.3
2195	1.33	13	2040	1.28	7.8	1.19	20	23.9
Increased Cell J Emitter Temperature								
2182	1.15	17.5	2115	1.14	18.5	0.94	36.5	34.4
2085	0.82	24.5	2082	0.82	24.5	0.54	48.5	26.2

Table 6

SERIES OPERATION OF CELLS G AND J

CELL G			CELL J			LOAD		
Emitter Temp. (^{o}K)	Cell Voltage (V_G)	Cell Current (A_G)	Emitter Temp. (^{o}K)	Cell Voltage (V_J)	Cell Current (A_J)	Voltage (V_L)	Current (A_L)	Power (watts)
2109	0.46	33	2088	0.58	31	0.88	31	27.2
2108	0.55	29	2088	0.67	28.5	1.08	28.5	30.8
2120	0.70	27	2098	0.80	27	1.38	27	37.4
2122	0.73	24	2110	0.97	23	1.57	23.5	37
2150	0.99	21.5	2120	1.10	21	1.95	21.0	41
2155	0.96	18.75	2130	1.18	18.5	2	18	36
Decreased Cell J Emitter Temperature								
2185	1.14	18	2045	0.94	17.5	1.95	17.5	34
2156	1.0	21	2028	0.71	20.5	1.57	20.5	32.2
Decreased Cell G Emitter Temperature								
2022	1.6	18.5	2040	0.9	18	1.35	18	26
2025	0.75	16.5	2045	0.99	16	1.63	16	26
2020	0.82	15.8	2050	1.05	15	1.75	15	26.4
2026	0.91	14	2060	1.14	13	1.95	13.5	26.4

LEAK-CHECK OF CELL ENVELOPE

Since closure of Cell E had been accomplished by means of a high-temperature valve, an investigation of the pressure in the cell and the identity of the gases that might have accumulated was considered worthwhile. It was found, however, that a leak across the valve seat had existed during the life test and that the cell body had numerous leaks, which precluded any pressure or residual-gas study. In all other cells, the cesium vial was cut off and a leak-check of the cell body was conducted. All of these cells except K, which had five small leaks, had so many large leaks that they were difficult to locate accurately. The electron-beam weld between the copper of the emitter base and the Kovar ring of the insulator was leaking in each case. In Cell K, this weld was eliminated and a relatively better cell envelope resulted. In Cell F, a large leak was also found in the tantalum substrate of the emitter. Since the cells were operated in a vacuum environment, cesium leaked out through the cell envelope and was deposited in the bell jar. There has never been any evidence that the ceramic-to-metal bond of the insulator or the aluminum oxide itself had developed a leak. All of the brazes which were made with a copper-silver alloy remained leaktight throughout the entire life test of the cells. The nickel-to-copper weld joining the collector and the collector base, which was made in an electron-beam welder, also maintained its integrity.

THERMOCOUPLE RECALIBRATION

Following the leak-check, the collector was removed from each cell by filing off the collector-to-base weld so that the emitter thermocouples could be recalibrated with the use of the test collector.

For Cell E, a plot of the input power versus the emitter temperature read from a pyrometer after the test was found to fit the power-input versus emitter-temperature curve previously established and used throughout the life test.

In Cell F, it could be seen that thermocouple No. 1, which had given low readings during the test, had pulled out of its cavity. The recalibration of the other thermocouple agreed well with the original calibration.

In Cells G and J, no thermocouple recalibration was possible because the emitters were removed together with the collector. In Cells H and K, the thermocouples maintained their calibration throughout the test (Fig. 35). Thermocouple No. 1 read an average of 40° lower in Cell H, while thermocouple No. 2 was only about 20° off. The thermocouple in Cell K read 50° to 80° higher after the test. In this calibration, the two pyrometer readings made through the top and bottom sight holes agreed within 10°, indicating a good temperature distribution over the surface of the emitter.

VACUUM EMISSION AFTER LIFE TEST

To determine if the vacuum-emission characteristics of carbide emitters change after long operation at elevated temperatures, vacuum-emission studies were conducted on emitters from Cells E, F, H, and K after the life test. In Cell E, the top of the emitter was cut off and tested. An increase in current was observed at lower temperatures, but at higher temperatures the emission was the same as before the test. This information was substantiated by data obtained from Cell F (Fig. 36). In Cells H and K, it was found that the current density was higher over the entire temperature range (Fig. 37), an increase of a factor of 8 being observed in Cell H. After operation at 2100°K for 5 hr, another emission check resulted in slightly lower values. It is of considerable importance to note that the emission was higher after the test than before the test. Furthermore, the increased value is in good agreement with the maximum short-circuit current observed during the life test (Figs. 22 and 23). This strengthens the hypothesis that the carbide surface was cleaned up in the presence of cesium; but it apparently became contaminated again after operation in vacuum, as indicated by the lower values obtained on Cell H after 5 hr at

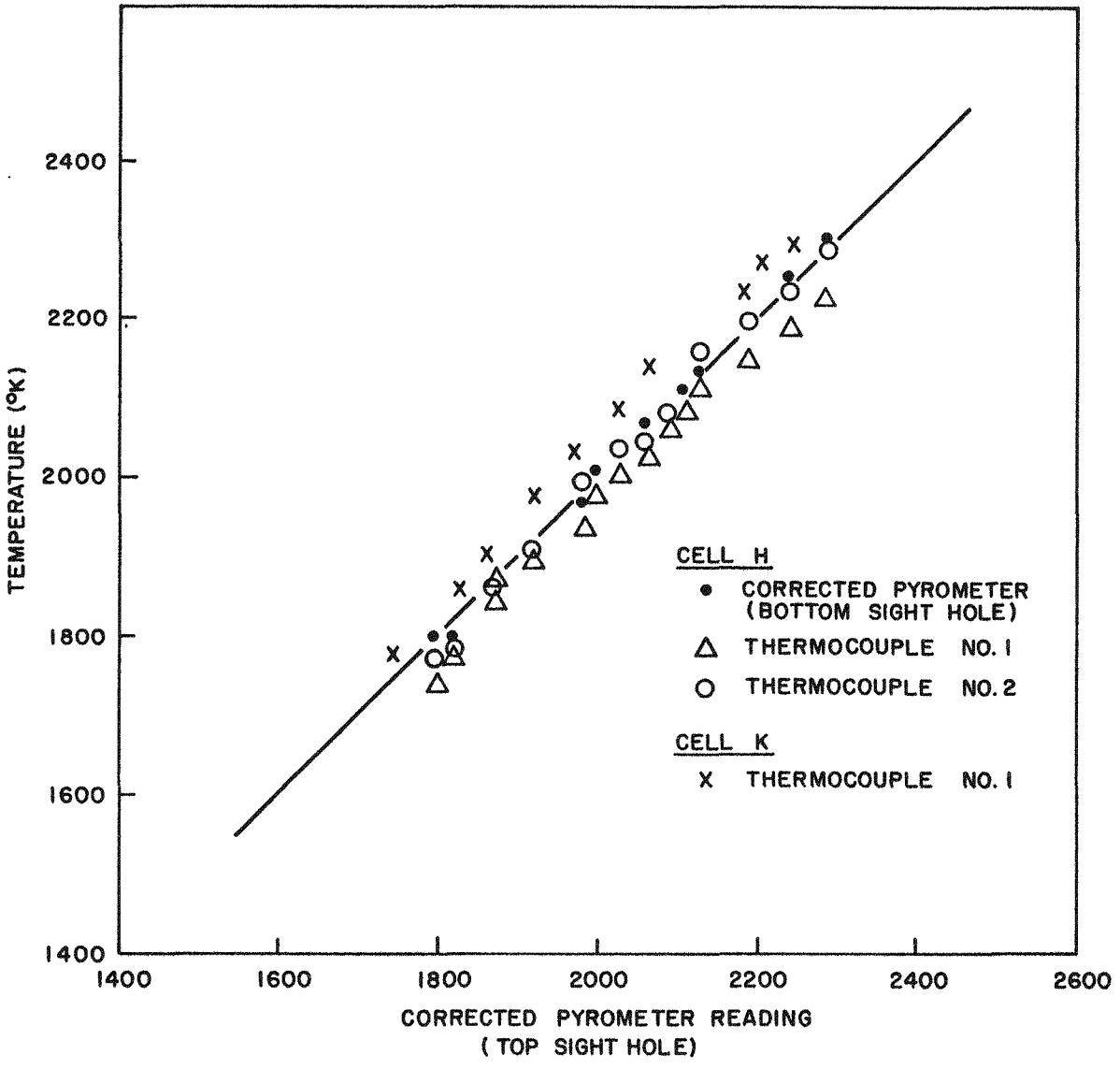

Fig. 35--Post-test thermocouple calibration for Cells H and K

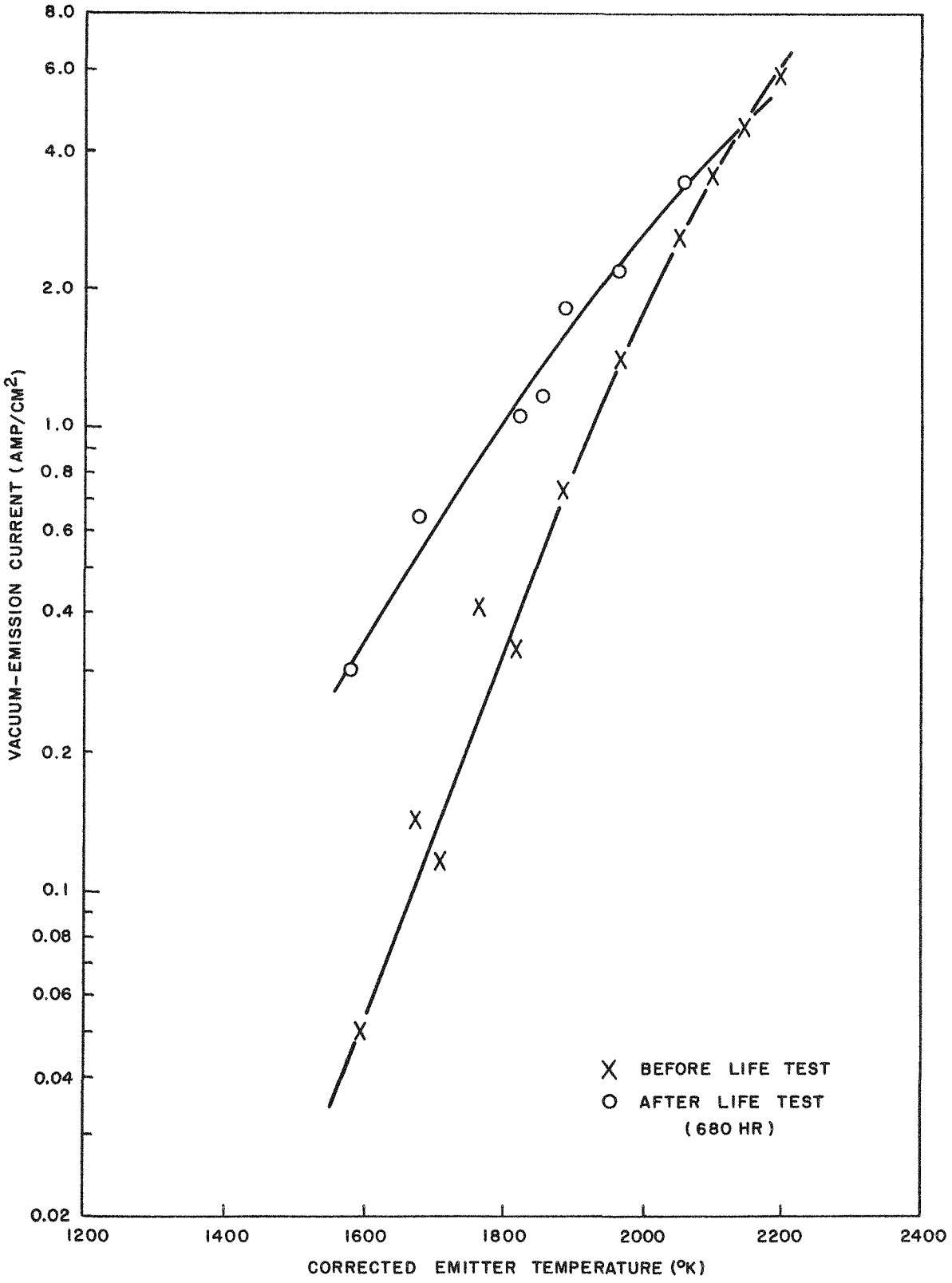

Fig. 36--Comparison of pre-test and post-test vacuum-emission current of Cell F as a function of emitter temperature

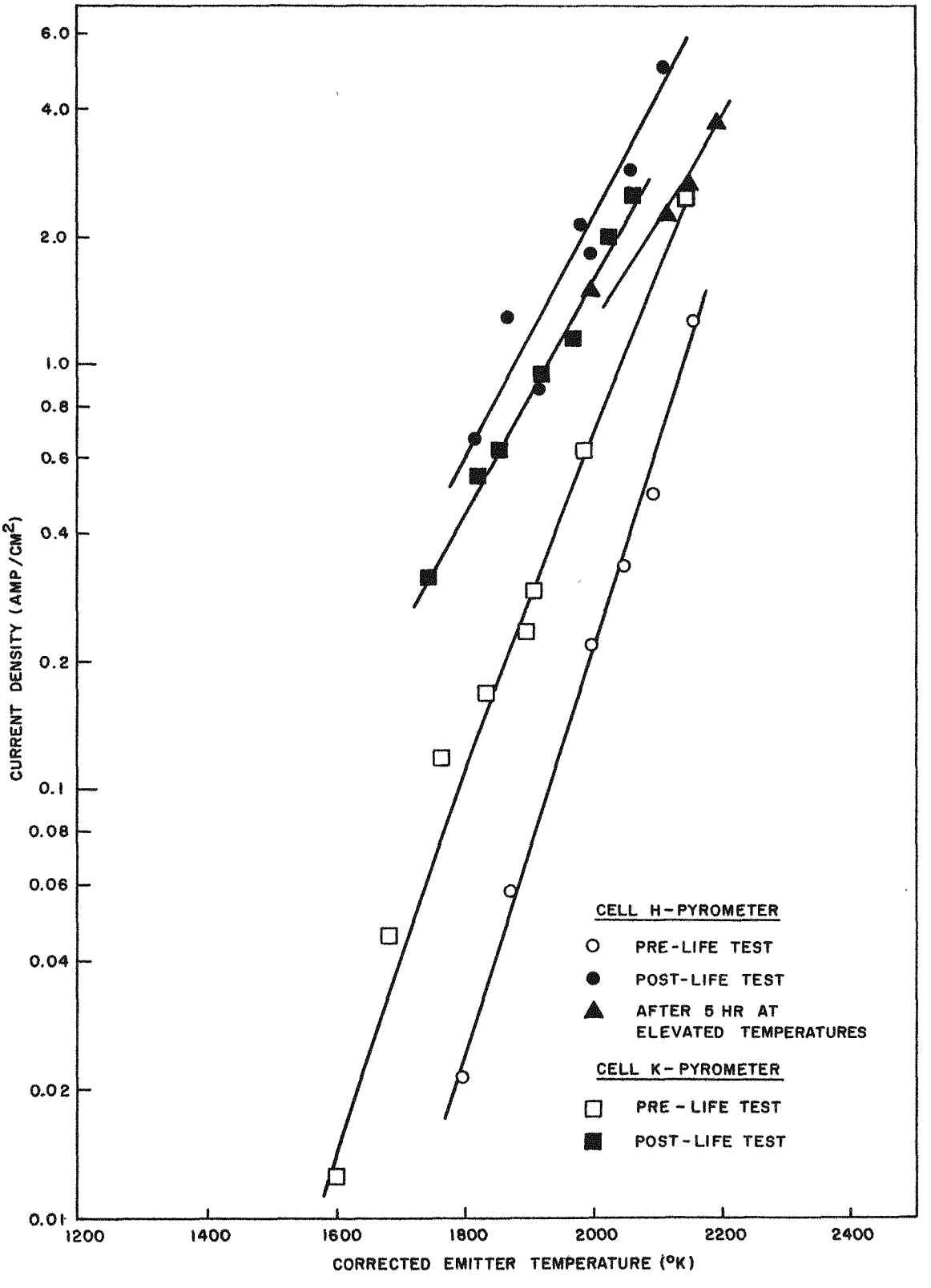

Fig. 37--Comparison of pre-test and post-test vacuum-emission current of Cells H and K as a function of emitter temperature

elevated temperature. In spite of the substantial evaporation of uranium from the emitter (to be discussed later in this section), the emission current had not decreased but instead increased after hundreds of hours of operation. The theory that carbide emitters act as dispenser-type cathodes requiring only a monolayer of uranium on the surface is supported by this data. Using the equation

$$\phi = \left[\frac{2.08\ T\ 2 \log T - \log I_s}{5042}\right] T \ ,$$

where ϕ is the effective work function, I is the vacuum-emission current, and T is the emitter temperature, the effective work function for Cell F increased from 3.1 volts at 1600°K to 3.6 volts at 2200°K before the life test, whereas it increased from 2.9 volts at 1580°K to 3.35 volts at 2075°K after the test. The highest effective work function (3.8 volts) was observed in Cell H at 2200°K.

ANALYSIS OF EMITTERS

Chemical Analysis

Portions of the carbide overlay of the emitters were broken off and subjected to a chemical analysis to determine the post-operation emitter composition. In Table 7, the post-test composition is compared with a pre-test analysis of the powder used to make the emitters.

A severe depletion of uranium was observed in all emitters, especially in Cells G and J, which had operated for 1700 and 1400 hr, respectively. Only Cell H had a comparatively large concentration of uranium left after the test, and it had decreased 25% from its original value. In all the cells, the carbon content changed relatively little, remaining close to its original value of 10%. With the exception of Cell J, the tantalum content increased from an undetectable level to about 2%. In Cell J, 39% tantalum was found. Since this emitter was very porous and had eroded more than any of the others, the sample may have included material much closer to the tantalum substrate than the other samples. It is apparent from the results for the two samples taken from Cell F that composition varies considerably with the origin of the sample. The top of the emitter was considerably cooler (~100°) than the sides; consequently, less uranium evaporated.

Table 7

CHEMICAL ANALYSIS OF EMITTERS
(In weight-percent)

Cell	U	Zr	C	Ta	W
ORIGINAL COMPOSITION					
E	19.67	67.02	10.2	----	4.16
H	20.37-20.40	68.50-68.81	10.32-10.50	----	1
POST-OPERATION COMPOSITION					
E	8.5	77.1	9.06	0.6	3.8
F					
Side	5.32	80.63	7.86	2.5	1.2
Top	13.6	72.5	8.16	3.8	1.7
G	0.1	76.7-77.8	10.3	10[a]	----
H	15	70	11.8	2	----
J	2.46	48-47.5	7.6	39	----

[a]Estimated value.

Diffraction-pattern Study

An electron diffraction analysis of Cell E indicated a strong ZrO_2 pattern and a weaker UO_2 pattern, without any indication of a carbide. The presence of the oxides is hard to explain, but the possibility that oxidation occurred following the life test is a strong one. X-ray diffraction, which penetrates the surface more deeply than electron diffraction, showed a strong pattern of 10 mol-% UC–90 mol-% ZrC (determined from lattice-parameter measurements), with only slight traces of UO_2 and ZrO_2.

X-ray diffraction studies were also made of the top of the emitter of Cell F. The strongest pattern was obtained for tungsten, that of ZrC being weaker. Although the original powder used to make the emitter contained some tungsten, it is believed that tungsten from the filament of the electron gun deposited on the tantalum and then diffused through it. The lack of a pattern corresponding to UC-ZrC indicated a severe depletion of UC at the emitter surface. No UO_2 or ZrO_2 pattern was observed.

Visual Inspection of Emitters

Visual inspection of the emitters was always very revealing. While the emitter from Cell H appeared in good condition with little sign of deterioration, the emitter from Cell J was heavily eroded along the cylindrical surface, with the top being in slightly better condition (Fig. 38). The emitters from Cells F and K had a number of large cracks but otherwise exhibited little signs of having operated for hundreds of hours at very high temperatures (Fig. 39). These cracks were vertical in Cell K, but were transverse in Cell F. The emitter from Cell G had a number of large areas which showed no apparent result of operating for 1700 hr in excess of 2000°K, and other areas which exhibited deep erosions, cavities, and low a carbide density (Fig. 40). These low-density areas protruded beyond the original dimensions of the emitter, causing it to be firmly lodged in the collector. The latter had to be cut apart to extract the emitter.

The diameter of the emitters was measured at various elevations, in even increments starting at the top and going toward the stem, to determine dimensional changes. The results are given in Table 8.

Metallurgical Analysis of Emitters

Longitudinal sections of the emitter were examined under large magnification to determine metallurgical reactions. In most cases, the top serrations of the tantalum slug had melted away. In some cases this had also occurred to some of the serrations on the sides (Fig. 41). Since the outside of the emitter and the filament cavity had sharp, straight edges, it is reasoned that the serrations had not melted during cell operation but during hot-pressing, which preceded the final machining on the inside and outside surfaces.

A series of photomicrographs was taken of several of the emitters. Figures 42 and 43 show representative samples of sections of the emitters. A reaction between the carbide and substrate had occurred. This same basic phenomenon was seen in all cases, only the extent of the reaction

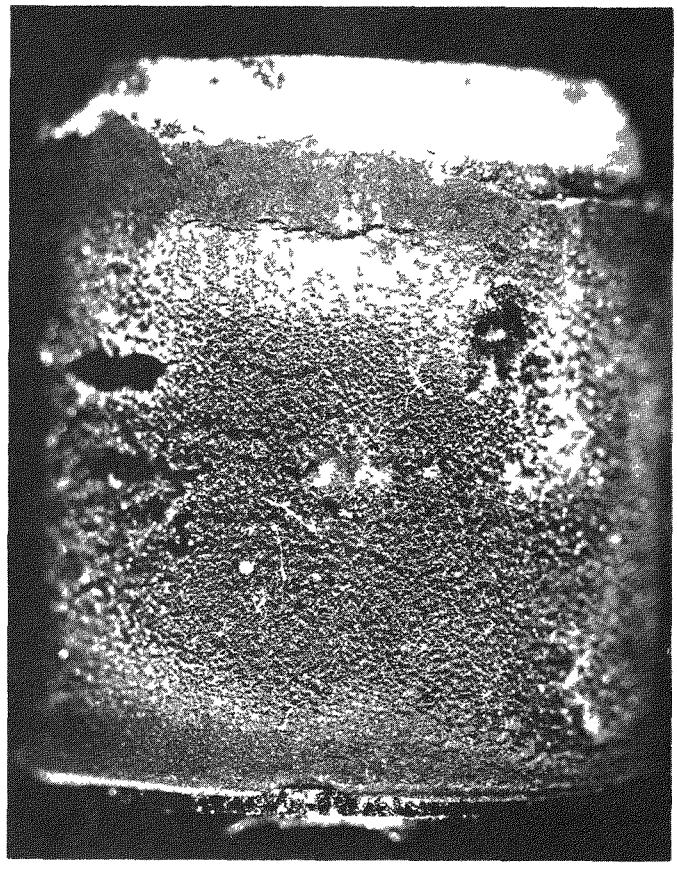

Fig. 38--Cell J emitter (after 1427 hr of operation)

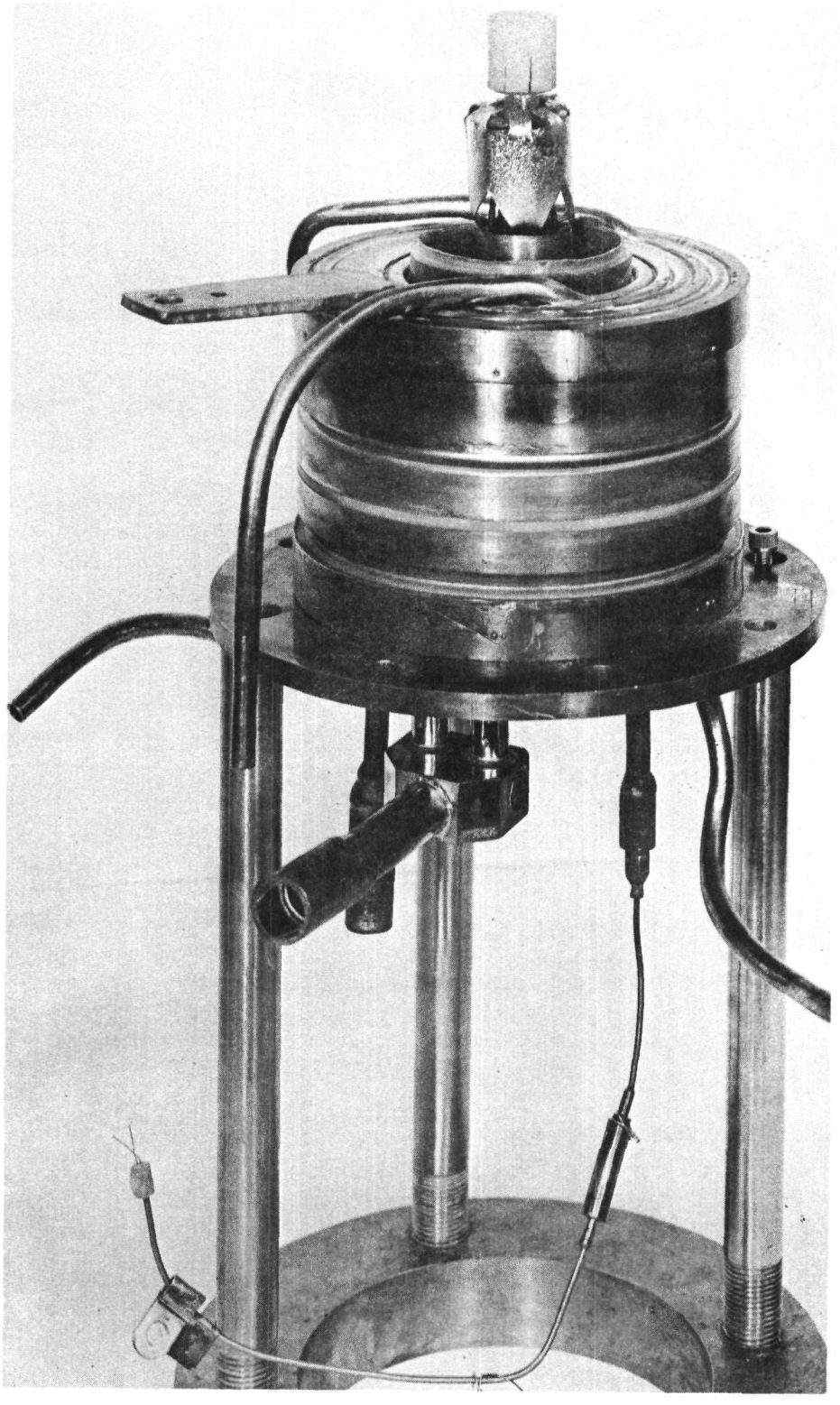

Fig. 39--Cell K after 700 hr of operation with collector removed; note cracks in emitter, and titanium getter below it

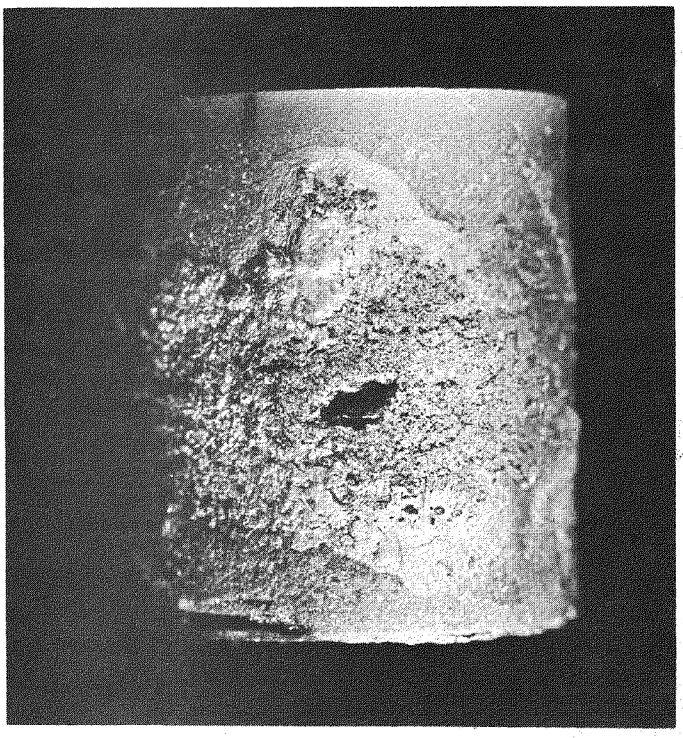

Note sharp edge on top of emitter

Note heavily eroded area and low-density material

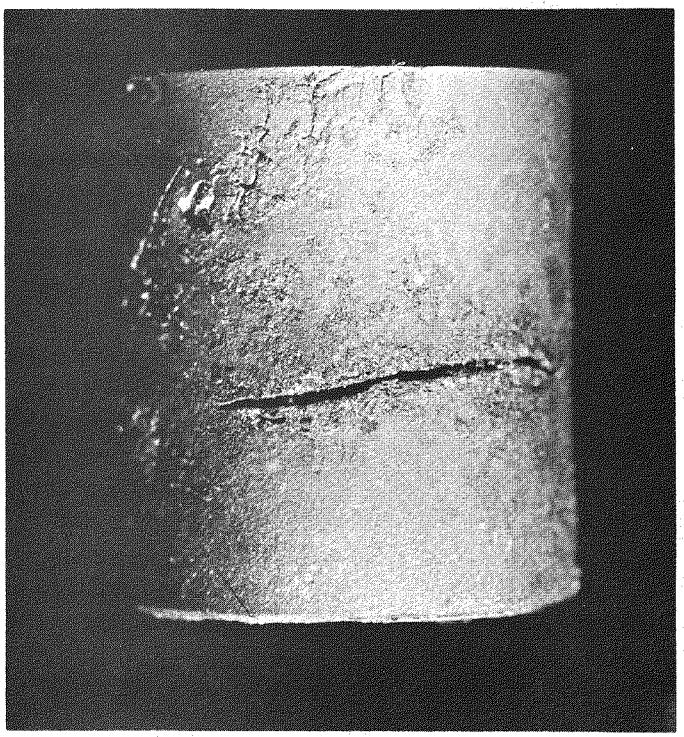

Note clear areas showing no effects of operation at elevated temperature

Fig. 40. Cell G emitter after 1753 hr of operation

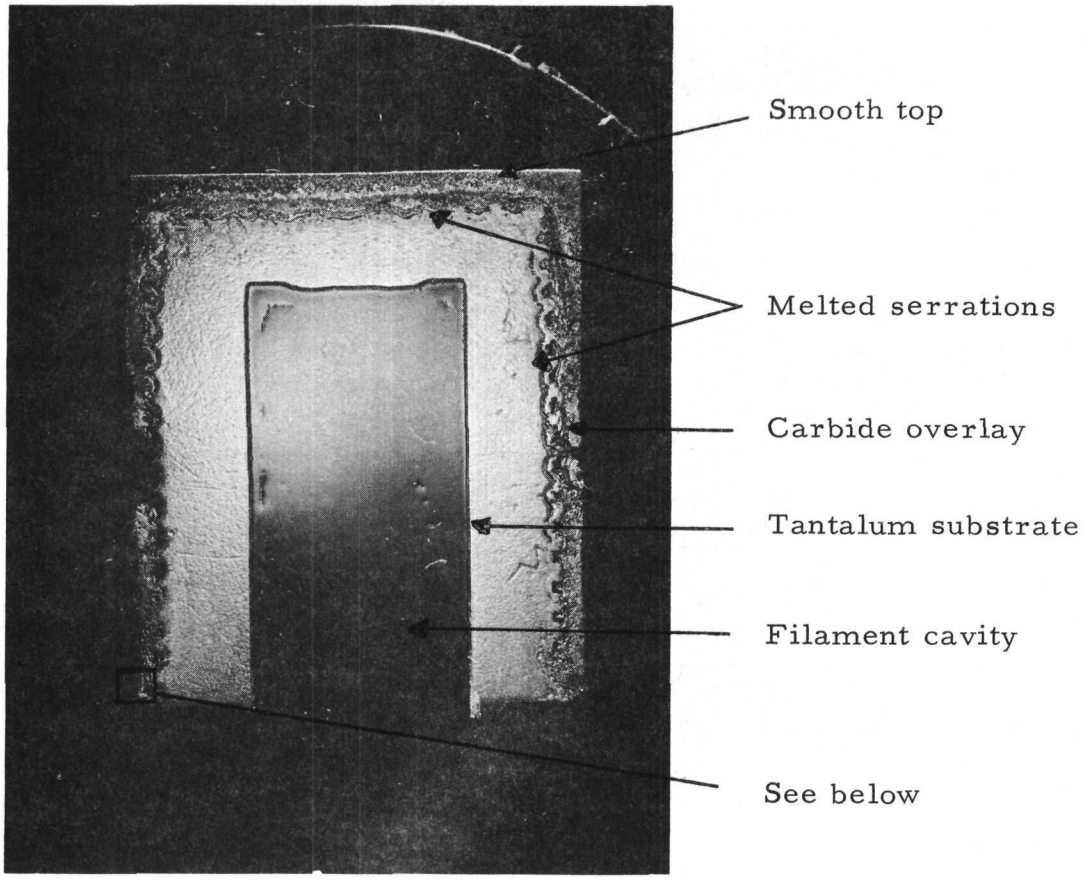

Fig. 41--Section of Cell G emitter

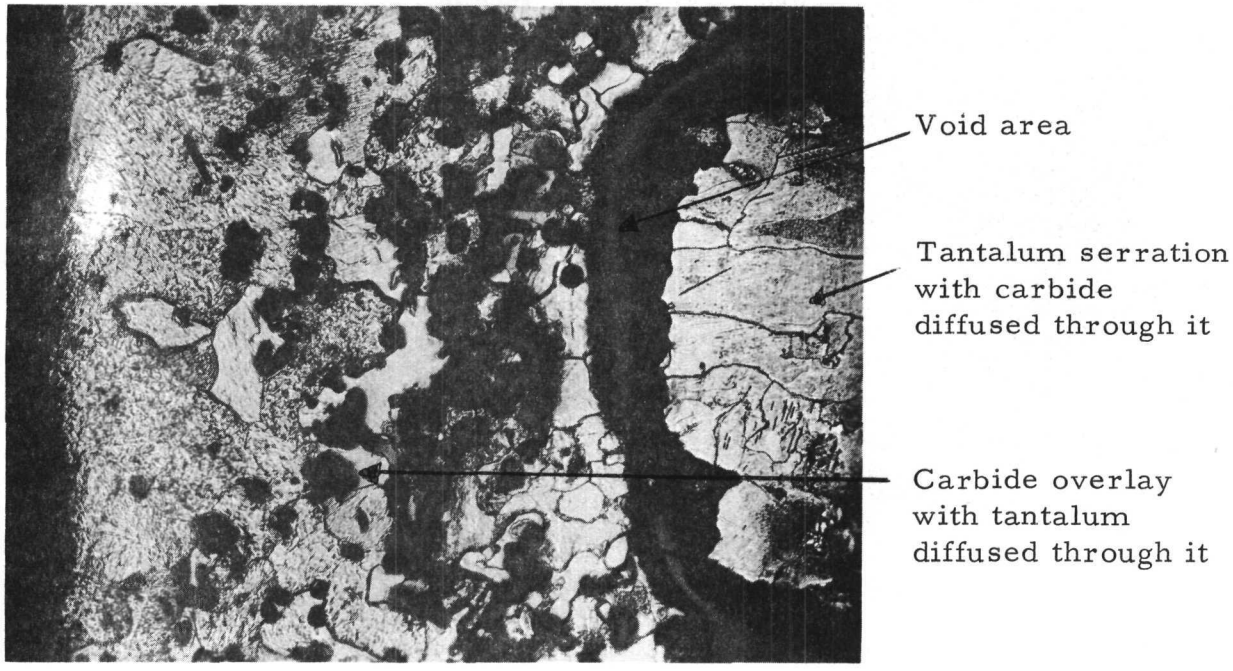

Fig. 42--Photomicrograph of Cell G emitter

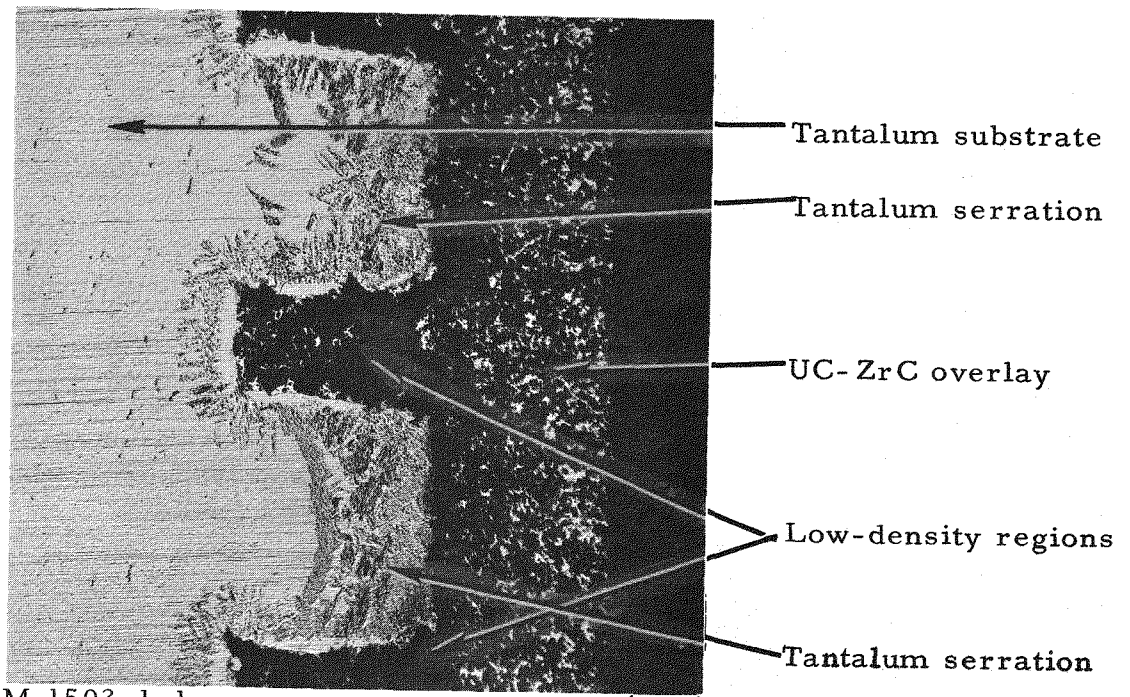

M 1503-1-1 (50×)

(a) Enlarged section of emitter showing tantalum substrate and carbide

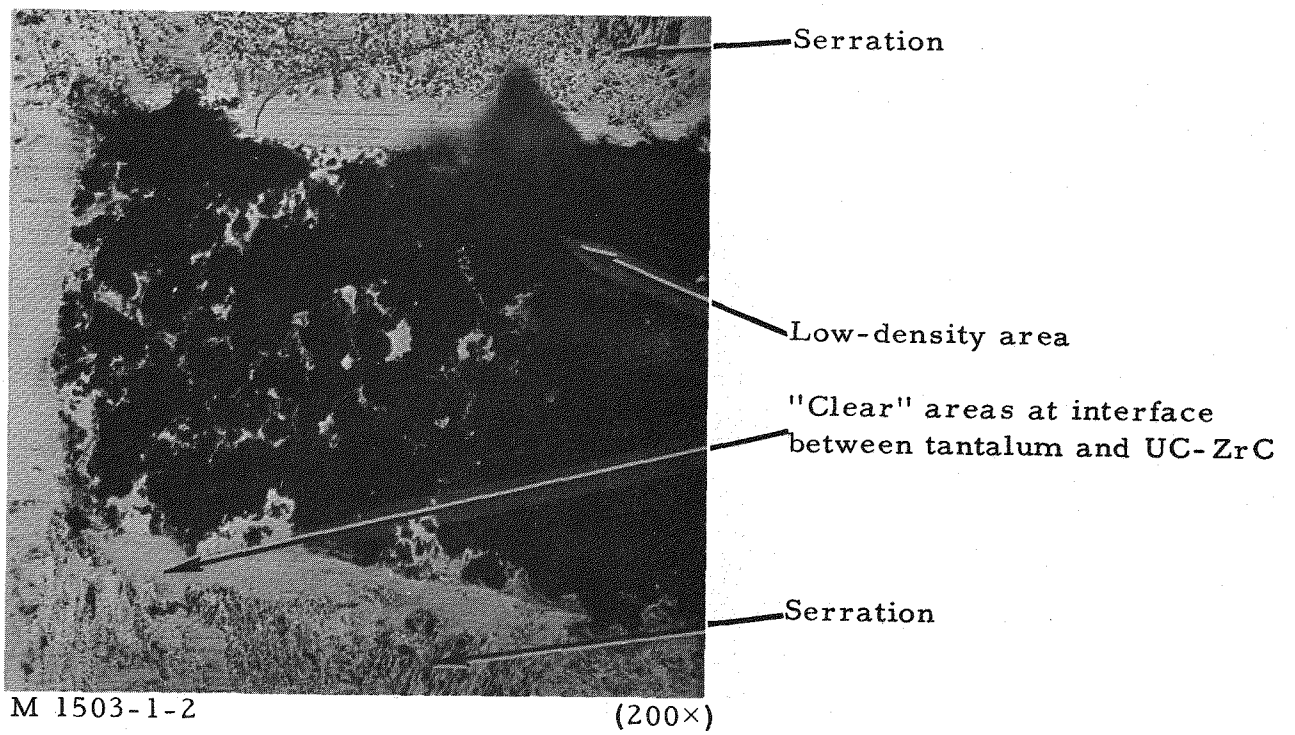

M 1503-1-2 (200×)

(b) Enlarged view of section between two serrations

Fig. 43--Enlarged view of section of emitter

varied slightly from emitter to emitter and at different locations on the emitter.

Table 8

EMITTER DIAMETERS AFTER LIFE TEST
(In inches)

Diameter	Cell F	Cell G	Cell H	Cell J	Cell K
Original	0.647	0.677	0.675	0.675	0.709 ±0.0003
Post-test					
A	0.651	0.676	0.665	0.667	0.704
B	0.645	0.679	0.665	0.658	0.699
C	0.637	0.693	0.661	0.652	0.698
D	0.639	0.687	0.656	0.652	0.697
E	0.645	0.673	0.675	0.682	0.704
Max. change	-0.010	+0.016	-0.019	-0.023	-0.012
Avg. change	-0.004	+0.005	-0.011	-0.013	-0.009

The most apparent features observed from the photomicrographs were:

1. A strong tantalum-carbon interaction. The TaC formation was particularly heavy in the serrations, and in some cases extended through the entire tantalum substrate. Some tantalum also diffused into the carbide, which was apparent from the chemical analysis presented above. The formation of TaC released free uranium, which in turn migrated to the emitter surface and evaporated.

2. A very low-density structure existed in the region between the tantalum serrations and in their immediate vicinity (Fig. 43). Studies of photomicrographs of emitters not subjected to extended thermal treatment did not reveal such low-density structures. If not all of the components of the carbide reacted uniformly with the tantalum as postulated above, a skeleton structure composed mainly of the less-reactive components must have been left behind.

3. In many cases, a narrow, "clear"-appearing region was noted at the interface between the carbide and the tantalum.

To verify the selective interaction with tantalum and to analyze the "clear" areas, a microprobe examination was conducted. The results were as follows (see Fig. 43):

1. The "clear" areas in the tantalum serrations immediately adjacent to the carbide were tantalum-uranium solid solutions containing about 3 wt-% uranium.

2. Neither uranium nor zirconium penetrated into the tantalum beyond these "clear" areas.

3. The uranium content in the carbide was non-uniform, the maximum value being 15 wt-% and the average value being 3 to 4 wt-%.

4. Tantalum penetrated fairly uniformly throughout the carbide at a level of about 6 wt-%.

5. A very fine dispersion of small particles observed in the carbide was primarily tungsten, or possibly WC.

ANALYSIS OF COLLECTORS

Visual and Metallurgical Analysis

A dark, sometimes pitch-black, deposit was found unevenly distributed in the collector cavity. The deposit was brittle and portions of it could be broken loose. However, some of it had also entered into an extensive metallurgical reaction with the nickel substrate, particularly in the case of Cell G. The resultant alloy was extremely hard and was difficult to machine off even with a carbide tool. Microhardness measurements indicated hardness values characteristic of carbides or intermetallics. The metallurgical reaction of the deposit with the nickel substrate is attributed to the high collector temperature, which at times reached 1250°K. The fact that the emitters from both Cell G and Cell J could not be extracted from the collector cavities pointed to a dimensional change of either one or both electrodes.

The dimensional changes recorded in some of the collectors are given in Table 9. Diameters A through E were measured at five different depths

(in even increments) in the collector cavity, starting with the bottom of the cavity.

Table 9

COLLECTOR DIAMETER
(In inches)

Diameter	Cell H	Cell J	Cell K
Original	0.698	0.700	0.735
Post-test			
A	0.690	0.678	0.740
B	0.689	0.674	0.733
C	0.687	0.679	0.722
D	0.692	0.679	0.723
E	0.686	0.702	0.730

From Table 9 it is apparent that the largest decrease in diameter occurred at the middle section of the collector cavity, which faces the highest temperature region of the emitter. In this section, where the highest evaporation rate of UC-ZrC was expected to occur, a reduction in diameter of 0.012 in. was measured. This was equivalent to the interelectrode spacing of Cells G through K. In the upper and lower sections, a change of only 0.002 to 0.005 in. was recorded. Since the emitters experienced a reduction in diameter in the same regions, no interelectrode shorting was experienced in two cells. In Cell H, a sudden short occurred at 700 hr which was attributed to a loss of alignment of collector and emitter; and in Cell G, the interelectrode gap had decreased to the point where contact was made.

Figure 44 is a section of the collector of Cell G, showing the heavy and very uneven deposit in the collector cavity. The width of this reaction zone, which was measured from the new boundary of the nickel substrate

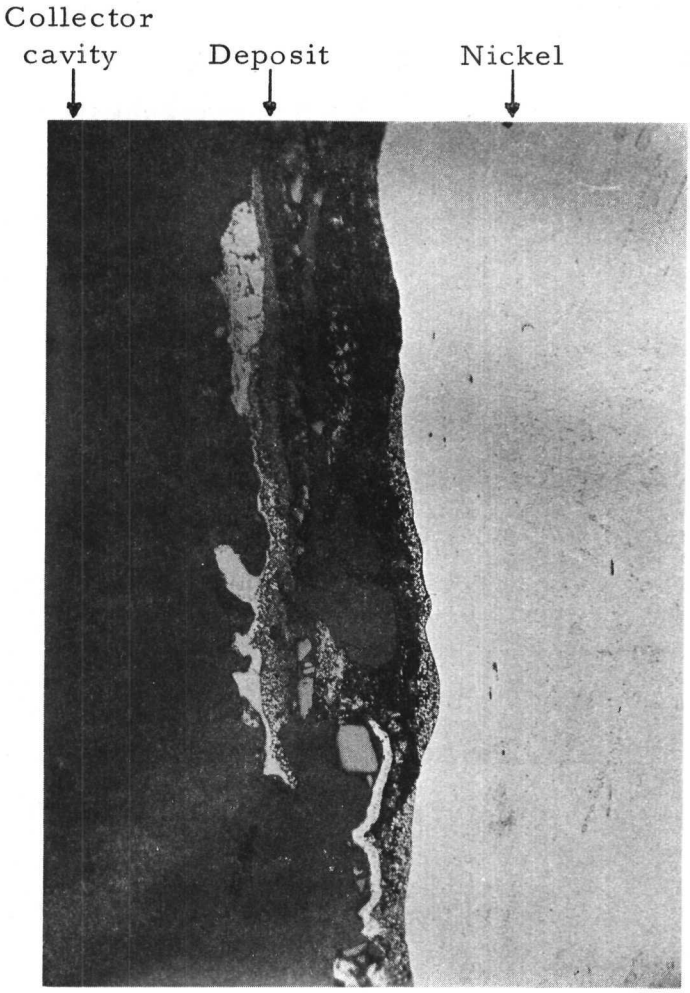

Fig. 44--Cell G collector with deposit
(50×)

to the extreme surface of the deposit, was 0.020 in. The original nickel surface was somewhere in this reaction zone. A larger magnification of a section of the collector cavity of Cell E is shown in Fig. 45. In this case, the reaction was much more uniform, and two zones could be distinguished lying on the nearly undisturbed nickel substrate. The outermost condensate had a diamond-pyramid-hardness value of 483, while the second layer had a value of 340.

Chemical Analysis

To conduct a chemical analysis of the deposit in the collector, the loose portions were removed first and the remainder was either leached out with a combination of HCl, HF, and HNO_3 or was machined out and then dissolved. The nickel content revealed by the analysis was not recorded because it was only a function of leaching time or machining depth. A summary of the results obtained is present in Table 10.

The amount of uranium deposited is quite large in view of the original uranium concentration in the emitter. Very little carbon was deposited. The maximum total deposit collected was 0.952 g (Cell G). Assuming a 12-cm^2 area and a density of 10 g/cm^3 for the emitter material, a loss from the surface of 0.008 cm (0.003 in.) was computed for a total of 1700 hr. This loss was averaged over the entire emitting area, while in actuality, owing to uneven heating, a much larger loss was observed in the center portion of the emitter.

By normalizing the amount of deposit by dividing it by the number of hours of operation, a reasonably good agreement is obtained for the five cells analyzed. All figures except that for Cell F are of the same order of magnitude, and even the deposit for Cell F is only twice as large as the average value of 5×10^{-4} g/hr.

CELL INSULATOR

Metallographical studies of various sections of the insulator were conducted. The ceramic as well as the brazed section were examined for

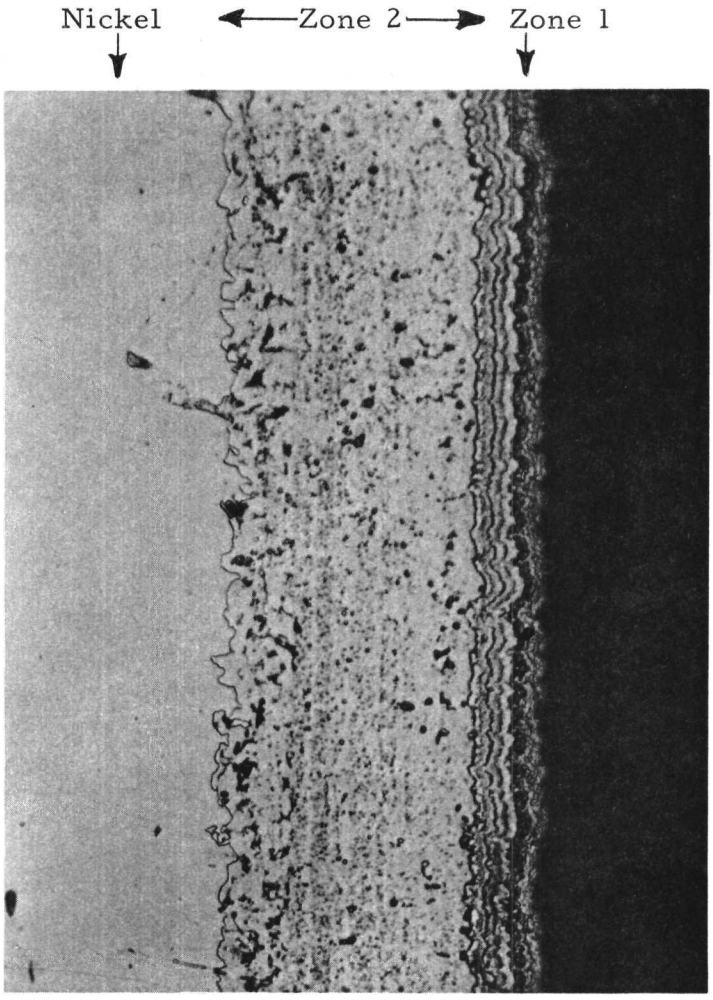

M 1457-1-1 (300×)

Fig. 45--Interior surface of collector
(Cell E)

Table 10

CHEMICAL ANALYSIS OF DEPOSIT IN COLLECTOR

Cell	Hours of Operation	Amount of Residue[a]		Composition (%)								Method of Analysis
				Top Layer				Bottom Layer				
		Total Grams	Grams/Hour	U	Zr	C	Ta	U	Zr	C	Ta	
E	1034	0.1254	1.215×10^{-4}	94.1	3.19	1.44	(b)					Wet chemistry
F	600	0.754	12.5×10^{-4}	41.2	55.9	2.9	---	90.2	9.8	---	---	Wet chemistry
G	1750	0.952	5.44×10^{-4}	55.5	41	1.8	1.7					Spectroscopy
H	700	0.40	5.72×10^{-4}	80.5	17	---	2.5					Spectroscopy
J	1430	0.304	2.13×10^{-4}	45.5	50.6	2.2	1.7					Spectroscopy

[a] Ignoring all nickel.
[b] 1.44 wt-% iron.

corrosion effects from the cesium. There was no evidence of attack on any of the insulator materials for the 1000-hr operation. Since the insulator was maintained 50° to 150°K higher than the cesium well, it was not expected that sufficient cesium would deposit on the insulator to constitute a serious attack.

VII. FISSION PRODUCTS

In the absence of data on the effect of various fission products on cell performance, an analysis of the fate of the fission products in a thermionic-cell environment was performed purely from a chemical standpoint. It was assumed that

1. Bare UC-ZrC emitters operated at 1900°C.
2. Collectors operated at 900°C.
3. Cesium pressure was 10 mm Hg at a reservoir temperature of 370°C.
4. A 15-cm^3 void volume existed in the cell.

The fission-product elements most likely to remain in the cathode are zirconium, molybdenum, technetium, ruthenium, and rhodium. Yttrium and the less volatile rare-earth elements (lanthanum, cerium, praseodymium, neodymium, and gadolinium), even though they tend to form stable carbides, will be somewhat volatile at 1900°C, while samarium and europium will be quite volatile. Release of the fission products will be determined by their rate of diffusion from the UC-ZrC matrix in which they are born, as well as by their volatility; but diffusion at 1900°C will probably be too fast to hold down release of fission products over periods of hundreds to thousands of hours.

The noble-gas fission products of krypton and xenon will not affect the converter as long as the thermionic-converter cells are vented to prevent undue pressure buildup.

The electronegative fission products selenium, bromine, tellurium, and iodine will tend to combine with cesium and thereby have their effects greatly reduced. Of the halogen fission products, iodine is the most important because of its higher fission yield; but it will tend to form cesium iodide (the most stable iodide known from the standpoint of heat of formation per iodine atom) and condense in the cesium reservoir. At a reservoir

temperature of 370°C, the vapor pressure of cesium iodide is estimated to be 2×10^{-8} atm. In the presence of cesium, the vapor pressure of selenium and tellurium will be still lower. The electronegative fission products will also show a tendency to combine with alkaline-earth and rare-earth fission-product elements and accumulate in the cesium reservoir as salts of these elements.

There is a great excess of electropositive elements formed in fission. As is indicated in Table 11, the yield of cesium itself is high (18% of fission) and that of rubidium is lower (3.5%). The relatively volatile alkaline-earth elements strontium and barium are yielded in substantial amounts (9.4% and 5.7%, respectively). The rare-earth elements are formed to an even greater extent, the yields of yttrium, lanthanum, cerium, praseodymium, neodymium, promethium, and samarium adding up to 54.9%.

If a converter cell runs for the order of 10,000 hr and a volatile fission product is not subject to condensation or dissolution in the cesium of the reservoir, enough products are formed to increase the pressure up to 1 atm at 900°C for 1% of fission yield. Thus, ample quantities of the elements would be formed to lead to condensation on the anode (at 900°C) if it were not for the lower temperature of the cesium reservoir. Actually, about half of the fission products, comprising the more volatile electropositive and the electronegative elements (the order of 20 millimoles in 10,000 hr in a cell with 15 cm^3 of free volume), will tend to condense in the cesium reservoir. However, they will also tend, to an undetermined degree, to contaminate (sorb on) the anode and to be present in the vapor or plasma phase.

Table 11

PERCENTAGE YIELD OF VARIOUS ELEMENTS
AS FISSION PRODUCTS

Element	Fission Yield of Element ΣY (%)	b.p. (^{o}K) of Element
Ge	0.00232	3,100
As	0.0008	866
Se	0.485	958
Br	0.14	331.4
Kr	3.86	119.75
Rb	3.5	974
Sr	9.4	1,640
Y	4.8	(3,500)
Zr	31.0	4,650
Nb	0	5,200
Mo	24.5	5,100
Tc	6.1	4,900
Ru	11.3	(4,000)
Rh	3.0	(4,000)
Pd	1.17	3,400
Ag	0.03	2,450
Cd	0.097	1,038
In	0.011	2,320
Sn	0.095	2,960
Sb	0.058	1,910
Te	2.42	1,260
I	1.03	456
Xe	22.3	165.04
Cs	18.0	958
Ba	5.7	1,910
La	6.2	3,640
Ce	12.4	3,200
Pr	6.0	3,290
Nd	21.2	3,360
Pm	2.4	(3,000)
Sm	1.92	(1,860)
Eu	0.183	(1,700)
Gd	0.015	(3,000)
Tb	0.0011	(2,800)
Dy	0.00005	2,600

REFERENCES

1. Campbell, A. E., F. D. Carpenter, J. B. Dunlay, and R. W. Pidd, High-Temperature, Vapor-Filled Thermionic Converter. Technical Report II, General Atomic Report GA-2911, April 4, 1962.
2. Carpenter, F.,J. Dunlay, R. Howard, and L. Yang, High-Temperature Vapor-Filled Thermionic Converter. Technical Report II, General Atomic Report GA-2530, August 31, 1961.
3. Weinberg, A., et. al., Investigation of Carbides as Cathodes for Thermionic Space Reactors. Final Report. May 15, 1961-August 31, 1962, General Atomic Report GA-3523.